Charles University in Prague

Faculty of Science

Department of Biochemistry

Diploma Thesis

Mechanism of action of non-peptide inhibitors of HIV protease

Mechanismus působení nepeptidových inhibitorů HIV proteasy

Bc. Jakub Began

Supervisor: **Doc. RNDr. Jan Konvalinka CSc.**

Prague 2011

Prohlášení

Prohlašuji, že jsem závěrečnou práci zpracoval samostatně a že jsem uvedl všechny použité informační zdroje a literaturu. Tato práce ani její podstatná část nebyla předložena k získání jiného nebo stejného akademického titulu.

V Praze dne ....

Jakub Began

ACKNOWLEDGEMENTS

Rád by som na tomto mieste poďakoval svojmu školiteľovi doc. Janu Konvalinkovi za to, že mi umožnil pracovať na mojej diplomovej práci v jeho tíme a podporoval ma, ako sa len dalo. Tri roky, ktoré som tam strávil, boli úžasné a veľa ma naučili.

Vtedy sa ma ujali jeho dvaja usmievaví študenti, dnes už doktori, Klárka Grantz-Šašková a Milan Kožíšek. Aj vďaka nim píšem tieto riadky. Klárko, Mílo, jedno veľké Ďakujem. Azda len, bez Vás by bola moja angličtina aj naďalej medzi „mŕtvymi jazykmi".

Vďaka patrí aj Michalovi Svobodovi, s ktorým sme vždy plní optimizmu energicky súťažili o to, komu sa nepodarí viac pokusov. Za to, že ma občas nechal prehrávať.

Jane Pokornej za každodenný úsmev a šálku skvelej kávy.

„Klukům a holkám od vedle" za to, že ma vždy srdečne podporovali a dodávali mi energiu, aj keď o tom možno ani nevedeli.

V neposlednom rade mojej rodine, hlavne mojej mame a bratovi Palovi, že boli vždy blízko, keď som to potreboval.

A mojej Lucke za to, že je.

TABLE OF CONTENTS

ABSTRACT

The inhibition of HIV-1 protease plays an important role in combating HIV. Nine HIV-1 protease inhibitors have been succesfully marketed for the treatment since 1995. However, their efficiencies decrease due to the resistance development. More potent compounds with novel structural motifs and mechanisms of action are therefore still needed. Several inhibitory compounds have been reported to bind to the protease at the loci different from the active site.

Interestingly, darunavir, which is the last approved inhibitor with supposedly competitive mode of action, was also suggested to bind to the flap region of the protease. Two studies discussed this alternative binding mode based on the X-ray structural and kinetic analysis, respectively. Nevertheless, it is questionable, if such a mechanism is relevant also in physiological conditions or if it is only an artifact of crystallization. Another study provided a strong evidence for the alternative binding of darunavir to highly mutated HIV-1 protease. Based on thermodynamic analysis, it was shown that two molecules of darunavir bind to the protease dimer. Surprisingly, this observation was not confirmed by the X-ray structure analysis since the inhibitor was bound only within the active site. However, this protease variant was employed in further studies.

To study the mechanism of darunavir binding to HIV-1 protease, several alternative approaches we choose including nuclear magnetic resonance (NMR) and surface plasmon resonance (SPR) methods as well as kinetic analysis using spectrophotometric assay. For these purposes, the panel of eleven isotopically labeled or tag-extended HIV-1 PR variants was prepared and characterized within this diploma thesis. The proteins were expressed, purified and characterized. The influence of the mutations and the tag-extension on the stability and activity of HIV-1 protease was investigated. Based on the kinetic analysis using spectrophotometric assay, the mechanism of inhibition of mutated protease by darunavir was suggested as that of the mixed type.

This study represents the background for further investigation of the alternative binding of protease inhibitors.

Key words: binding site; enzyme kinetics; HIV protease; protein structure; affinity tag

ABSTRAKT

Inhibice HIV-1 proteasy hraje významnou roli v boji proti viru HIV. Od roku 1995 bylo na trh uvedeno devět inhibitorů HIV-1 proteasy, avšak jejich účinnost klesá vinou vzniku rezistence viru vůči inhibitorům. Proto je potřeba vyvíjet účinnější léčiva s novými strukturními motivy a mechanismy účinku. V nedávné době byla u několika inhibitorů pozorována jejich vazba i mimo aktivní místo proteasy.

Darunavir, jenž je posledním schváleným inhibitorem HIV-1 proteasy a vykazuje kompetitivní typ inhibice, se pravděpodobně také váže do oblasti chlopní HIV-1 proteasy. Dvě studie podporující tento alternativní způsob vazby byly založeny na kinetických měřeních a rentgenové krystalografii. Je však otázkou, zda-li dochází k této vazbě i za fyziologických podmínek anebo zda-li se jedná pouze o krystalizační artefakt. I další data podporují alternativní vazbu darunaviru s vysoce mutovanou HIV-1 proteasou: pomocí termodynamické analýzy bylo prokázano, že na dimerní HIV-1 proteasu se váží dvě molekuly darunaviru. Nicméně toto pozorování nebylo potvrzeno rentgenovou krystalografií, neboť darunavir byl v krystalové struktuře přítomen pouze v aktivním místě HIV-1 proteasy. Tato vysoce mutovaná varianta HIV-1 proteasy se proto stala předmětem dalšího zkoumání.

Pro studium mechanismu vazby darunaviru na mutovanou HIV-1 proteasu jsme zvolili bylo zvoleno několik přístupů, např. jaderná magnetická rezonance (NMR), povrchová plasmonová rezonance (SPR) či kinetická měření využívající spektrofotometrické metody. Pro tyto účely byl připraven soubor jedenácti HIV-1 proteas, které byly buď izotopicky značené či obsahovaly afinitní kotvu. Proteiny byly připraveny v bakteriích, vyčištěny a charakterizovány. Byl sledován vliv mutací a afinitní kotvy na stabilitu a enzymové vlastnosti proteasy. Pomocí N-terminální sekvenace degradačních produktů byla prokázána specifická autodegradace u některých ze čtyř C-koncově označených proteas. Ty byly následně kineticky charakterizovány. Jejich katalytická účinnost (k_{cat}/K_m) ve všech případech poklesla. Na základě spektrofotometrických dat byl dále zjištěn mechanismus inhibice mutované proteasy darunavirem odpovídající smíšenému typu.

Tato práce představuje základ pro další výzkum týkající se vazby inhibitorů do alternativních míst HIV-1 proteasy.

Klíčová slova: vazební místo; enzymová kinetika; HIV proteasa; struktura proteinu; afinitní kotva

LIST OF ABBREVIATIONS

AIDS	acquired immunodeficiency disease syndrom
AKT	ATP-dependent serine/threonine protein kinase
AMP	ampicilin
ATP	adenosinetriphosphate
AP	alkaline phosphatase
APS	amonium persuphate
APV	amprenavir
ATV	atazanavir
BCV	brecanavir
bis- THF	bis- tetrahyrdrofuran
bp	base pair
CA	capsid protein
C-Avi	Avi-tag at protein C-terminus
CCD	charge-coupled device
CCR5	C-C chemokine receptor type 5
CM	chloramphenicol
C-His	Poly Histidine tag (six Histidines) at protein C-terminus
CXCR4	C-X-C chemokine receptor type 4
DAVP	4-dimethylamino-6-vinylpyriminide derivative
DICA	2-(2,4-dichloro-phenoxy)-*N*-(2-mercapto-ethyl)-acetamide
DMSO	dimethyl sulfoxide
DNA	deoxyribonucleic acid
DRV	darunavir
E.coli	*Escherichia coli*
EDTA	ethylendiaminetetraacetic acid
Env	polyprotein encoded by *env* gene
env	gene encoding envelope proteins
FDA	U.S. Food and Drug Administration
FICA	5-fluoro-1*H*-indole-2-carboxylic acid (2-mercapto-ethyl)-amide
FPLC	fast protein liquid chromatography
FSV	fosamprenavir
Gag-Pol	polyprotein encoded by *gag* and *pol* genes
gag	gene encoding structural proteins
gp120	glycoprotein 120
HAART	highly active antiretroviral therapy
HCV	hepatitis C virus
HIV	human immunodeficiency virus
HIV-1 PR	protease of human immunodeficiency virus type 1

HIV-1 RT	reverse transcriptase of human immunodeficiency virus type 1
HPLC	high pressure liquid chromatography
HRP	horseradish peroxidase
HSQC	heteronuclear single-quantum correlation
IDV	indinavir
IgG	immunoglobulin G
IMG AS CR	Institute of Molecular Genetics of Academy of Science of Czech Republic
IN	integrase
INDOPY	indolpyridone
IOCB AS CR	Institute of Organic Chemistry and Biochemistry of Academy of Science
IPTG	isopropyl-β-D-thiogalactopyranosid
ITC	isothermal titration kalorimetry
KAN	kanamycin
k_{cat}	catalytic constant
K_D	equilibrium dissociation constant
K_i	inhibition constant
K_m	Michaelis constant
k_{off}	dissociation rate constant
k_{on}	association rate constant
LB	lysogeny broth (also known as Luria-Bertani broth)
LES	local elementary structure
MA	matrix protein
MES	2-(*N*-morpholino)ethanesulfonic acid
MMP	matrix metalloprotease
MOPS	3-morpholinopropane-1-sulfonic acid
MUT	mutated
N-Avi	Avi-tag at protein N-terminus
NC	nucleocapsid
NCBR	National Centre for Biomolecular Research
nef	gene encoding negative regulatory factor
NFV	nelfinavir
N-His	Poly Histidine tag (six Histidines) at protein N-terminus
Ni-NTA	nickel-nitrilotriacetic acid
NMR	nuclear magnetic resonance
NNRTI	non-nucleoside reverse transcriptase inhibitor
NRTI	nucleotide reverse transcriptase inhibitor
NtRTI	nucleotide reverse transcriptase inhibitor
OD_{595}	optical density at 595 nm
ORF	open reading frame
p1	spacer peptide 1

p2	spacer peptide 2
$p6^{pol}$	flanking region at the N-terminus of the protease precursor
PDB	Protein Data Bank
PI	protease inhibitor
Pol	polyprotein encoded by *pol* gene
pol	gene encoding for viral enyzmes
PolyHis	Polyhistidine tag
POM	polyoxometalate
PR	protease
PVDF	polyvinylidene fluoride
rev	gene encoding for Rev protein
RNA	ribonucleic acid
RT	reverse transcriptase
RTV	ritonavir
SDS	sodium dodecyl sulphate
SDSL-EPR	side-directed spin labeling and electron paramagnetic resonance
SDS-PAGE	sodium dodecyl sulphate polyacrylamide electrophoresis
SPR	surface plasmon resonance
SQV	saquinavir
ssRNA	single-stranded ribonucleic acid
TAE	Tris-base buffer containing EDTA and acetic acid
tat	gene coding for Trans-Activator of Transcription protein
TBS	Tris Buffered Saline
TEMED	N,N,N‘,N‘-tetramethylethylendiamin
TF	tissue factor
TFP	transframe octapeptide at the N-terminus of the protease precursor
THF	tetrahydrofuran
TPV	tipranavir
TR-FRET	time-resolved fluorescence resonance energy transfer
Tris	2-Amino-2-hydroxymethyl-propane-1,3-diol
vif	gene encoding for virion infectivity factor Vif
vpr	gene encoding for viral protein R
vpu	gene encoding for viral protein U
v/v	volume ratio
w/v	weight ratio
WB	western blotting
WT	wild-type

1. INTRODUCTION

In late 1970's, a new sexually transmitted disease started spreading among homosexually oriented men in the USA. It was later called the Acquired Immunodeficiency Syndrome (AIDS). Soon, its causative agent was isolated and identified from infected patients independently by two research groups in United States and France in 1983 [1,2]. This immune disorder evolves as the consequence of the human immunodeficiency virus (HIV) infection in organism. In 2008, Françoise Barré-Sinoussi and Luc Montagnier were awarded the Nobel Prize in Physiology or Medicine for the discovery of HIV.

The global epidemiological statistics estimated that there were 33.4 million of HIV positive people, most of them (22.4 million) living in Sub-Saharan Africa, in 2009. The estimated number of newly infected is close to 2.7 million and nearly the same number represents those who die from the infection, every year. For comparison, the total numbers have raised three or four times since 1990. However, the success of anti-HIV therapy has luckily mirrored in the stabilized growth of newly HIV infected people during recent years [3].

Hand in hand with the alarming worldwide progress of HIV infection, numerous groups of scientists tried to understand the biology and the pathogenesis of this retrovirus. It was necessary to characterize the HIV life cycle and also to find the way how to suppress the formation of new infectious viral particles. Based on this primary research, reverse transcriptase and protease, two out of three viral enzymes, became promising targets of antiretroviral therapy. Consequently, the extensive structural and biochemical studies of HIV protease led to the development of potent class of retroviral protease inhibitors (PIs).

The antiviral therapy showed quite a significant success in viral load suppression. Still, the complete eradication of the virus remains to be solved. Moreover, the increasing prevalence of resistant viral strains evolving under the drug pressure has subsequently resulted in lowering their susceptibility. The adverse short or long-term side effects limit the treatment, as well.

Nevertheless, the introduction of highly active antiretroviral therapy (HAART), which combines even three antiretrovirotics, has undoubtedly improved the quality and life expectancy of HIV-infected patients.

Design of new compounds based on the knowledge of molecular mechanisms of drug resistance developement, improvement of treatment strategies in current anti-HIV therapy, as well as the identification of new antiretroviral targets are the main goals how to maintain the suppression of replication of multidrug-resistant viruses.

2. THEORETICAL PART

2.1 HUMAN IMMUNODEFICIENCY VIRUS

The International Committee on the Taxonomy of Viruses proposed the name of the newly isolated and characterized virus as Human Immunodeficiency Virus (HIV). HIV is a member of the *Lentivirus* genus that belongs to the subfamily *Orthoretrovirinae* of the *Retrovoridae*'s family. This classification reflects the replication strategy and pathogenesis of the virus [4]

Phylogenetic studies further showed that HIV virus is quite variable and is distributed worldwide predominantly as the HIV-1 type. Whereas the second viral type, called HIV-2, occurs rather locally, mostly in the regions of Western and Central Africa. Both types cause immunodeficiency in humans (AIDS). HIV-2 is less virulent [5]. Together with the improvement of molecular techniques used for HIV detection, extensive sequence homology studies revealed that HIV-1 has spread in three distinct groups: group M (as major), O (as Outlier) and N (as non-M or non-O). M group includes 9 subgroups signed A to K [6].

2.2 HIV STRUCTURE AND REPLICATION CYCLE

The mature viral particle is coated with the glycoprotein-rich lipid bilayer, derived from the host cell plasma membrane and the viral core. Inside the viral capsid, there are two identical copies of positive single- stranded RNA molecules (ssRNA) attached to the nucleocapsid core (Fig. 1b). As many other retroviruses, these RNAs encode three major genes *gag, pol* and *env* in three open reading frames (ORF1- ORF3) that are translated into the viral polyproteins Gag, Gag-Pol and Env. Structural proteins (MA- matrix, CA- capsid, NC- nucleocapsid) and enzymes (RT- reverse transcriptase, IN- integrase and PR- protease) are generated by viral protease which is autoactivated during maturation [7]. Additionally, the replication and also interaction with host proteins are regulated by the products of six other genes *vif, vpu, vpr, nef, tat* and *rev*. The organization of the HIV genome is illustrated in Fig. 1a.

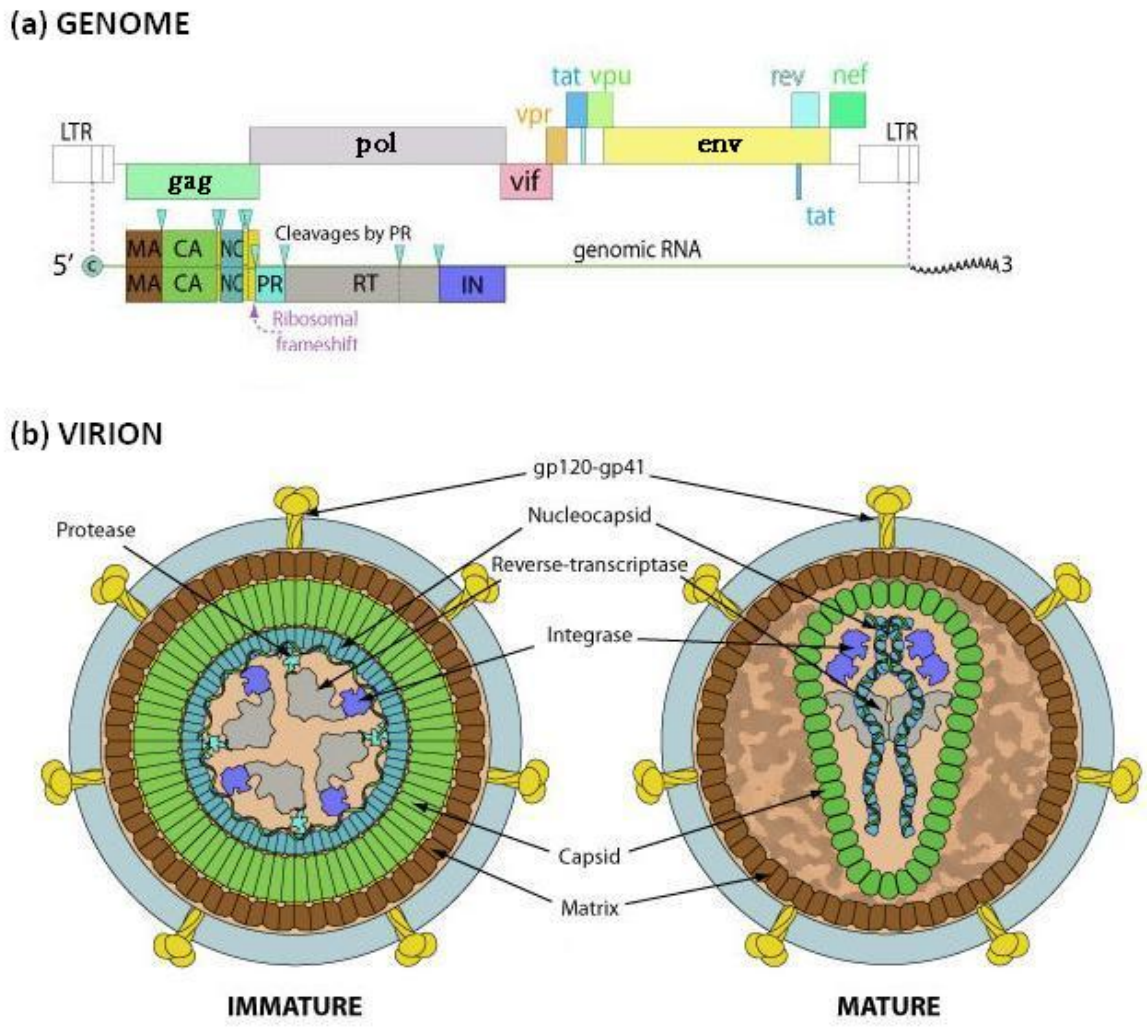

Figure 1: (a) The organization of HIV-1 genome and (b) the differences between immature and mature virion**.** Adopted from [8] and modified.

HIV replication cycle is shown in Fig. 2. It begins with the initial attachment of the viral surface glycoprotein gp120 to the host CD4 receptor of T_h-lymphocytes, promoting thus significant conformational changes. For the membrane fusion, the additional interaction of gp120 with one of the chemokine co-receptor CXCR4 or CCR5 is required. The co-receptor binding serves for the determination HIV tropism [9,10].

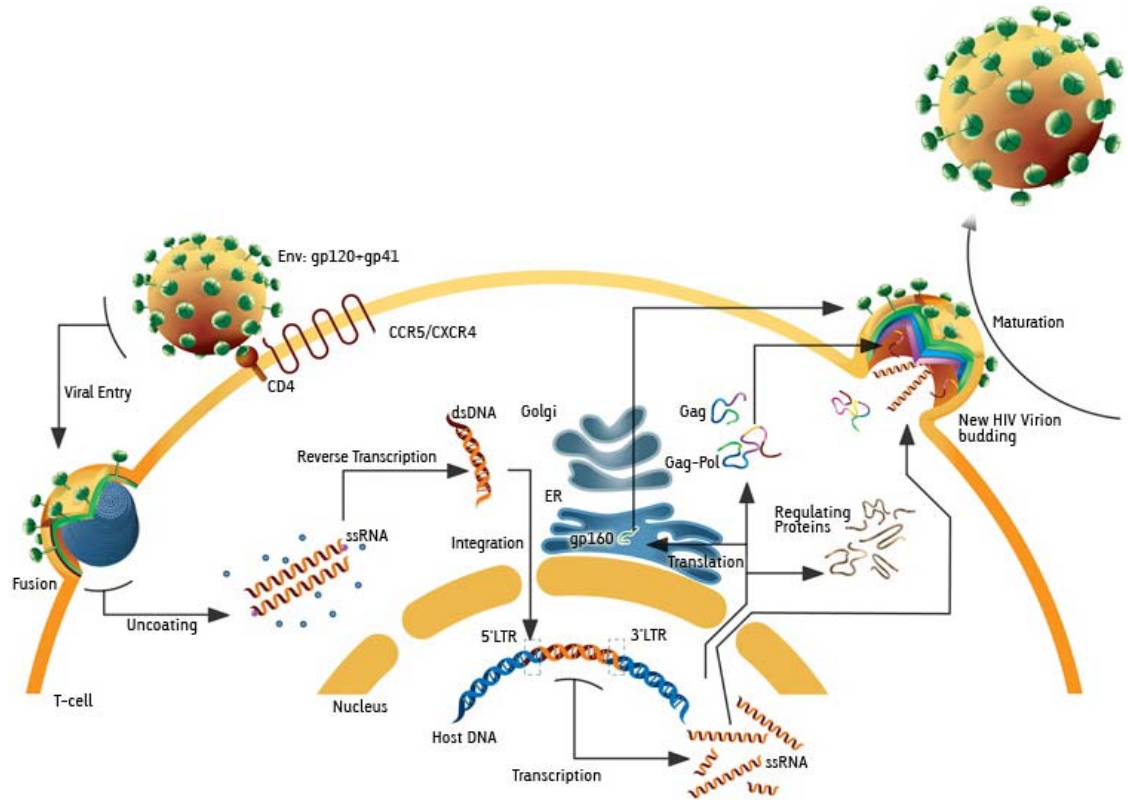

Figure 2: HIV-1 replication cycle. Adopted from [11] and modified.

After uncoating, the nucleocapsid core is released to the cytosol and viral RNA is reverse transcribed by viral reverse trancriptase into double-stranded DNA. The pre-integration complex is then formed and translocated to the nucleus, where linear form of viral DNA is incorporated into the host genome by HIV integrase. Next step involves transcription of HIV coding sequence by host RNA polymerase II. Single spliced and unspliced mRNAs are transported to the cytosol, where Gag and Gag-Pol polyprotein precursors are expressed in the ratio of 20:1. Gag-Pol is a product of -1 ribosome frameshift. Miristoylated polyproteins are targeted to the inner surface of the cell membrane where they associate with the glycosylated products of Env cleavage and form the immature viral particle [12,13]. The maturation is initiated by the action of HIV protease during and after budding. The mature viral particle contains cone-shaped core, which coats the viral enzymes- protease, reverse transcriptase and integrase [14,15].

2.3 CURRENT AND NOVEL ANTI-HIV STRATEGIES

Different classes of anti-HIV drugs have been developed throughout the last two decades. The number of those approved for therapy by the U.S. Food and Drug Administration (FDA) has increased up to 30 [16,17]. Since the introduction of zidovudine- the nucleoside analogue that blocks viral reverse-transcription (NRTI)- for treatment in 1987, subsequent progress has brought other potent nucleoside (NRTIs) non-nucleoside (NNRTIs) and nucleotide (NtRTIs) reverse transcriptase inhibitors [18]. HIV-1 protease inhibitors are another extensively studied class of compounds with anti-HIV activity and will be discussed in detail in chapter 2.4 [19]. The blocking of the binding of viral surface glycoprotein gp41 at the cell membrane is provided by the fusion inhibitor enfuvirtide [20]. The inhibitor of HIV-1 integrase (raltegravir) [21] and the antagonist of CCR5 chemokine receptor (maraviroc) [22], are the latest drugs that achieved the FDA approval for the treatment in 2007.

Despite of the undoubted success of these antiretrovirotics, there is still a persisting need of new compounds with supressory activity against HIV. The understanding of HIV biology led to the identification of novel promising drug targets. The original viral enzyme's inhibition is still being intensively studied and improved together with developing of new generations of inhibitors against resistant viruses. Screenings of chemical libraries for potential agents and rational structure-based drug design have brought several potential drug classes such as the inhibitors of viral maturation (block the CA-sp1 cleavage) [23], NC-based inhibitors (target the zinc finger motif in NC and thus abolish the RNA packaging), cyclin-dependent kinases inhibitors (play a role in HIV-1 trancription), promising CA assembly inhibitors or the compounds targeting viral accessory proteins [24,25]. Leader compounds became the candidates for further development and some of them entered pre-clinical testing or even the clinical trials.

2.4 HIV-1 PROTEASE

HIV-1 protease catalyzes the processing of Gag and Gag-Pol polyproteins in a precisely-defined order [26], at nine distinct cleavage sites (Fig. 1a). It cleaves them

with different proteolytic rates into the structural and functional proteins that form the mature viral particle [27]. Once inhibited, the maturation is disrupted. This essential enzyme therefore became the promising target of antiretroviral therapy [28].

2.4.1 Structure

HIV-1 protease is an aspartic protease that is homologous to the proteases of other phylogenetically related retroviruses (leukemia, non-human immunodeficiency and mammalian tumor viruses). Based on the importance of the conserved catalytic triad, the mechanism of action as well as their inhibition, they were classified as members of the new wide-span class of aspartic protease superfamily, where non-viral aspartic proteases pepsin and renin belong as well [29,30].

First X-ray structures of synthetic and recombinant HIV-1 protease were solved in 1989 [31,32]. It was confirmed that HIV-1 protease is catalytically active as a C2 symmetric homodimer composed of two non-covalently linked identical subunits. Each monomer consists of 99 amino acid residues with molecular mass of 11 kDa. The structure of active protease shows four duplications of β-sheet elements that give rise to the overall tertiary fold [30]. Several distinct regions can be distinguished. First, the active site catalytic triad is located at the bottom of wide loops formed by three amino acid residues: Asp25- Thr26- Gly27 of each monomer. It is stabilized by conserved hydrogen bond network called “the fireman’s grip” [33,34]. The whole substrate binding pocket consists of the residues 8, 23, 25-30, 32, 47-50, 53, 76, 80-82 and 84 of each subunit [35]. The N- and C- termini form a four-stranded β-sheet called the dimerization domain. This region is stable in solution. Interestingly, it was shown that the dimer formation occurs concomitantly with folding of both monomers [36,37]

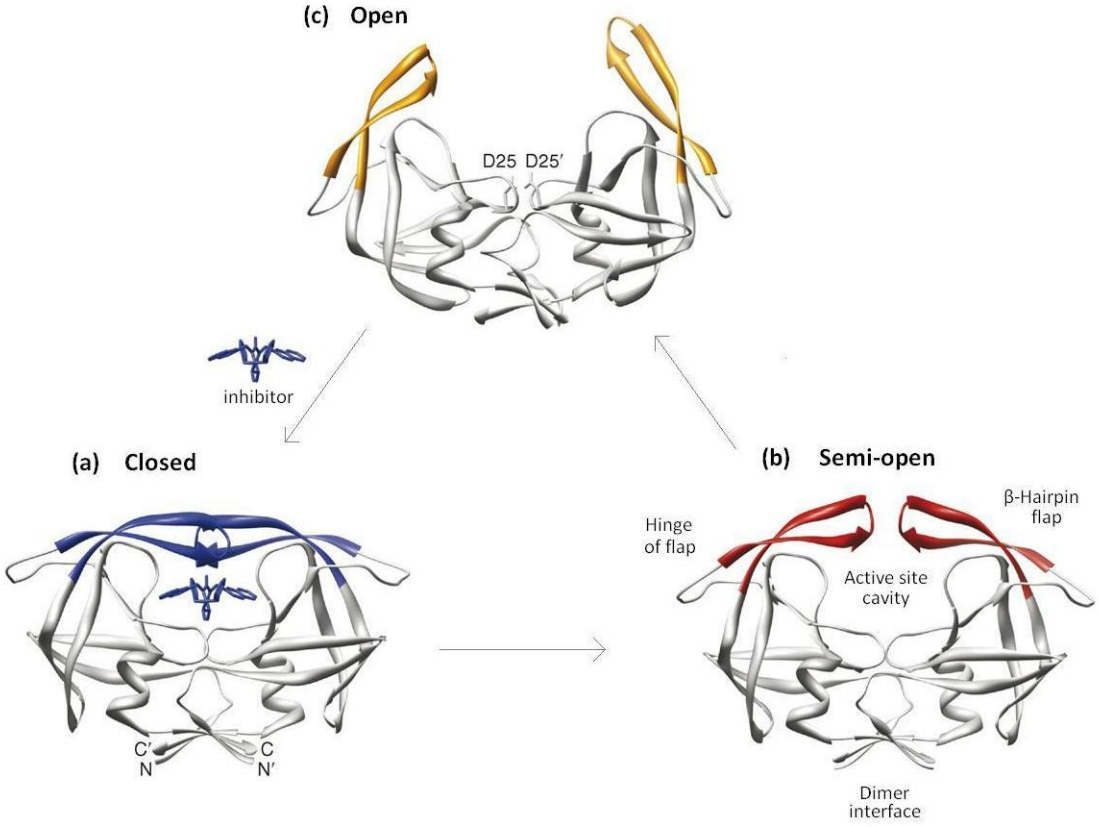

Figure 3: Three conformations of HIV-1 protease in solution: (a) closed, with an inhibitor bound (PDB code: 1HVR), (b) semi-open (PDB code: 1HHP) and (c) open. Dimer interface, active site cavity and flaps are indicated in (b). The open conformation was obtained from the molecular dymanics experiments with semi-open HIV protease, which was solved by X-ray crystallography [38]. Adopted from [39] and modified.

The role of the two flexible β-loops, also known as flaps (formed by residues 42-58) is depicted in Fig. 3. They cover the active site and allow for enhanced interaction with substrate or inhibitor. Flexibility of the flaps in the ligand-free or in the ligand-bound state of HIV-1 protease was studied by several NMR experiments and molecular dynamics simulations. Free protease exists in two largely populated states in solution: the open or the semi-open conformation, respectively. The flaps spontaneously change their conformation from one state to the other and they close upon binding the substrate or the inhibitor [40,41].

2.4.2 Activation

In the early stages of maturation, the activity of HIV protease is regulated by its self-processing from Gag-Pol polyprotein, when the protease precursor TFP-p6^{pol}-PR-RT is formed. The N-terminal transframe octapeptide (TFP) and 48-60 amino acid long

variable region $p6^{pol}$ represent the flanking region at the N-terminus of the protease precursor. The release of active protease is initiated with the N-terminal cleavage of its precursor. This step precedes the C-terminal processing and enhances the formation of the active homodimer [41,42]. *In vitro* kinetic studies of protease maturation in conditions that are optimal for catalytic activity revealed that the release of the active enzyme from the TFP-$p6^{pol}$-PR precursor occurs in two distinct steps. First, the precursor is cleaved to the $p6^{pol}$-PR. It is subsequently followed by the release of the mature protease together with the large increase of activity [42]. Moreover, Tessmer and Krausslich showed that the mutation of the N-terminal cleavage site leads to the formation of N-terminally extended $p6^{pol}$-PR. It resulted in formation of immature virus and complete loss of its infectivity, thus suggesting the essential role of this cleavage for viral replication. However, several recombinantly expressed or *in vitro*- translated miniprecursor containing $p6^{pol}$ and PR were found to be active with minor kinetic differences in cleavage compared to the wild-type protease [41,43,44]. It was explained by the possible restricted accessibility of the substrate molecule to the active site of extended PR or to the reduced processing of the Gag and Gag-Pol substrates that may have the regulatory effect on the other events during maturation [45].

2.4.3 Substrate specificity

HIV-1 protease is an endopeptidase that has certain substrate preferences. It was observed that the local secondary structure of the substrate determines the specificity and the effective binding. Substrate, which is partially unfolded, is more available for hydrolysis. For the effective and selective cleavage, the substrate requires to be at least seven amino acids long and to make sufficient amount of non-polar and water-mediated interactions with the active site residues, as illustrated in Fig. 4 [46,47]. The structural analysis of protease-substrate complexes revealed potential mechanism of substrate's recognition. It is suggested that flaps movements upon the substrate burial are asynchronous. The flap covering P1-P4 residues of substrate closes first and forms novel, probably highly conserved structural intermediate, implying the key role of this region in protease specificity [48].

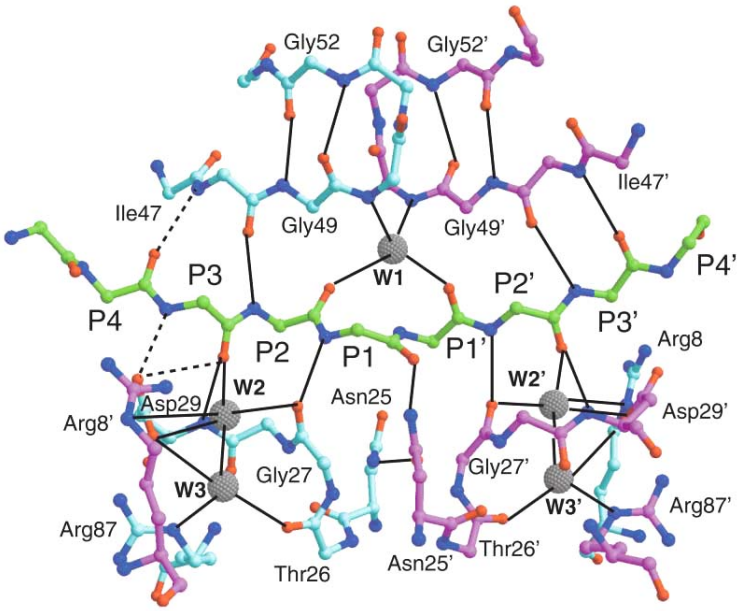

Figure 4: Conserved interactions between the substrate (green) and backbone atoms of both units in the active site (blue and magenta, respectively). Five conserved water molecules are indicated as grey spheres. W1, W2 and W2' waters contact the peptide with the inactive protease directly. W3 and W3' stabilize the peptide in its open conformation. Adapted from [47].

Although there are no strict requirements of specific amino acids, it is notable that HIV-1 protease catalyzes also the hydrolysis of the sequence containing proline at position P1', aromatic amino acid (Tyr, Phe) at P1 site and Glu or Gln at P2' site or one of the hydrophobic amino acid residues at these positions. Substrate subsites P2, P2' and P3' should contain aliphatic residues and subsite P3 some uncharged amino acid residue [49].

First class of peptidic inhibitors of HIV-1 protease was designed considering these requirements for substrate binding and with an effort to mimic the transition state with non-cleavable peptide bond isoster (Fig. 5) [37].

2.5 HIV-1 PROTEASE INHIBITORS

X-ray, NMR and kinetic studies, as well as computational modeling of HIV-1 protease complexed with substrate-derived inhibitors enabled to investigate the active site cleft on the molecular level [50,51]. It also provided researchers to prepare more selective compounds similar to the tetrahedral intermediate formed during the cleavage

[52]. This structure-based drug design has resulted in the development of so called peptidomimetic inhibitors, with non-hydrolysable hydroxyethylene or hydroxyethylamine isoster instead of the peptide bond in the cleavage site [53].

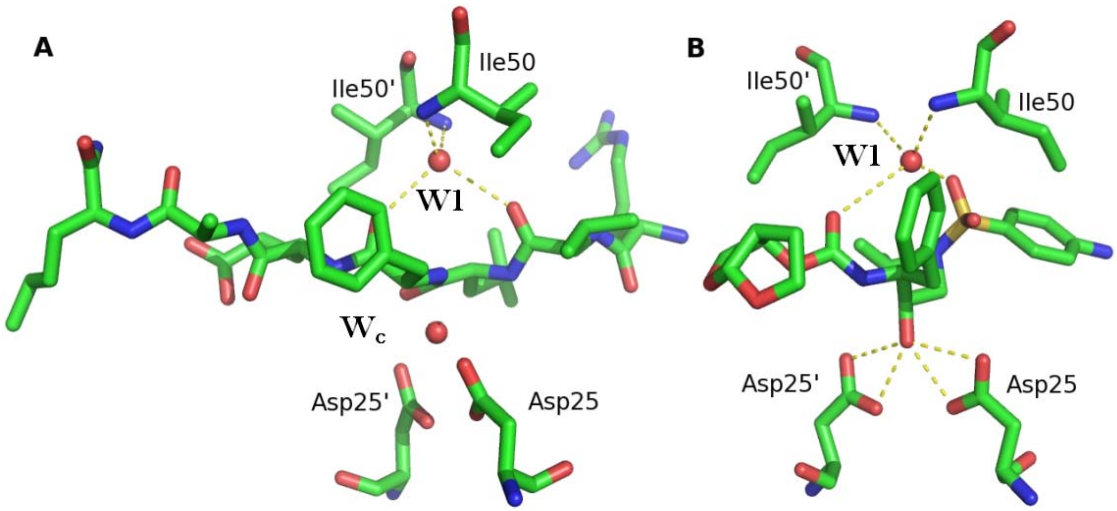

Figure 5: The model of a) substrate and b) inhibitor bound in the active site of HIV-1 protease. (a) T\he "catalytic" water molecule W_c bridges the catalytic aspartates Asp25' and Asp25 with the peptide bond of the substrate during cleavage. (b) In protease:inhibitor darunavir complex, the catalytic water is substituted with the polar group of non-hydrolysable isoster of the drug. Both complexes are stabilized by another "structural" water molecule W1. Water molecules are depicted as red spheres; particular atoms are differed by colors: carbon (green), oxygen (red), nitrogen (blue), sulphur (yellow). The figure was made by Dr. Klára Grantz-Šašková (IOCB AS CR), using programme PyMol [54].

There are currently nine inhibitors of HIV protease approved by FDA and most of them are used in clinic. With one exception, all of them are transition state analogues and they mimic the peptidic scaffold of the substrate. They are combined with other anti-HIV drugs (inhibitors of reverse transcriptase, entry inhibitors, etc.) in approach known as highly active antiretroviral therapy (HAART) [17]. It was introduced in 1996 and has dramatically decreased the HIV progression. Moreover, several other compounds are in pipeline or clinical trials.

2.5.1 First generation HIV-1 protease inhibitors

The antivirals, whose structure is analogous to that of HIV protease substrate molecule and bind to the active site of the enzyme, are often called the first generation

HIV protease inhibitors (Fig. 6). They were designed to inhibit the "wild-type" HIV-1 protease. The first one, **saquinavir** (Invirase®, Fortovase®), was licensed by FDA for therapy in 1995. One year later, more potent inhibitors **ritonavir** (Norvir®) and **indinavir** (Crixivan®) were introduced. They had better pharmacokinetic profile. All three were peptidomimetics and contained a big bulky hydrophobic moiety at the P1 position [52].

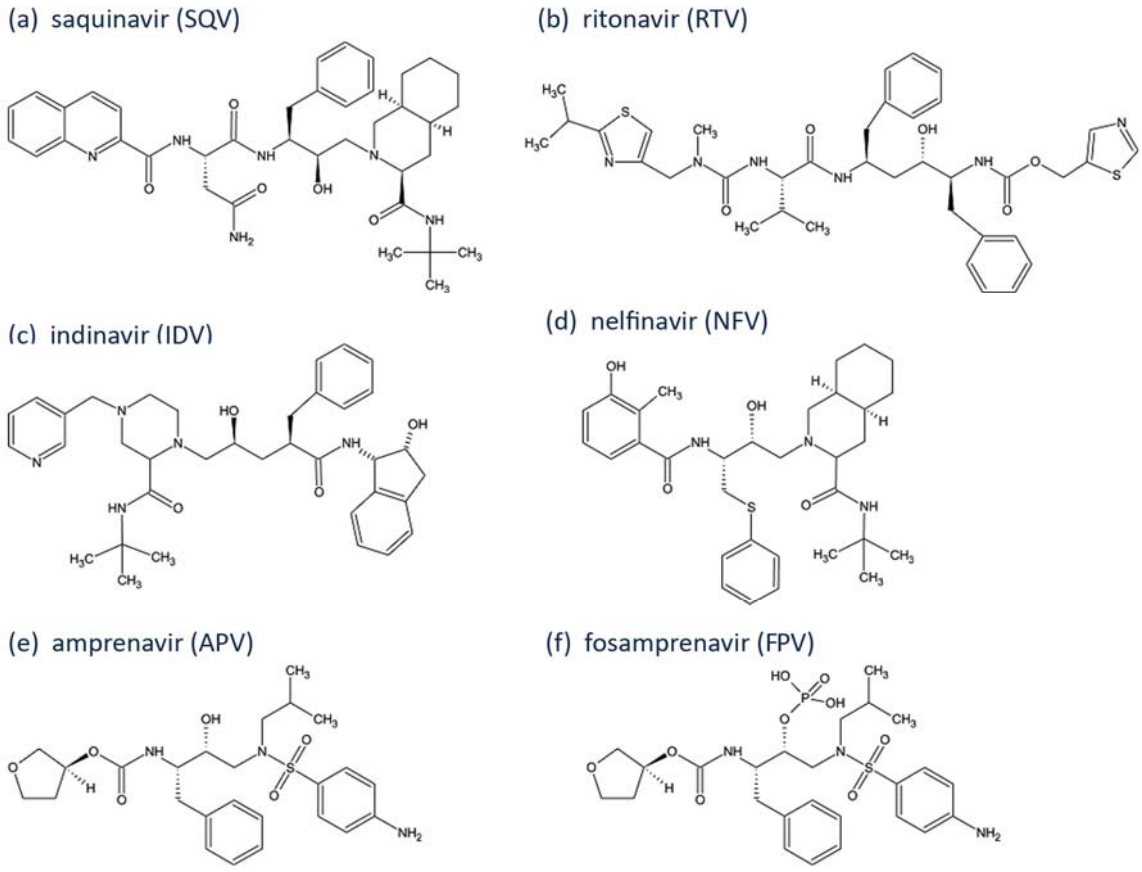

Figure 6: Chemical formulas of the first generation HIV-1 protease inhibitors.

Structural studies and molecular dynamic calculations of the enzyme-inhibitor complexes revealed other possibilities of protease inhibitor design. They led to the FDA approval of the first non-peptidic inhibitor **nelfinavir** (Viracept®) in 1997. Another inhibitor **amprenavir** (Agenerase®) was approved in 1999. It was further optimized into the prodrug **fosamprenavir,** which had better bioavailability and stability in organism. The new structural motifs were introduced at P2 and P2' position: tetrahydrofuranyl or aminophenyl sulfonamide moiety, respectively [55].

2.5.2 From the inhibition to resistance

Clinical experience showed that complications may occur even in such a successful combined drug therapy (HAART), where protease inhibitors were used. They are mostly caused by several adverse side effects (metabolic and gastrointestinal disorders) and very poor bioavailability of the first generation inhibitors [56]. Effective drug concentrations in blood plasma continuously decreased in time due to the limitations in their pharmacokinetics, such as binding to serum proteins, possible drug-drug interactions as well as their metabolism by hepatic cytochrome P450 3A4/5. This suboptimal dose exposure and quite variable patient adherence to therapy contributed to the treatment failure and to the residual replication of altered HIV variants. The fact that HIV reverse trancriptase lacks proof-reading activity enhances the generation of particular mutations in viral genome. It leads to the reduced drug susceptibility. Drug resistance may develop only in weeks during particular treatment.

The various mechanisms of drug-resistance development are intensively studied [57,58]. The resistance to HIV protease inhibitors is usually achieved through the introduction of mutations to the molecule of HIV-1 protease. These are categorized in two types. **Major mutations** occur predominantly in the active site (at positions 23, 30, 32, 47, 50, 82 and 84), could be detected also in the flap region (at positions 46, 48 and 54) or in the "interior" regions of the enzyme (76, 88 and 90). Major mutations usually lead to significant loss of direct interactions with the inhibitor thus weakening its binding. These mutations are conservative, they maintain the hydrophobic character to preserve the affinity and catalytic activity for the substrate and they preferably introduce only slight geometric shifts within the binding cleft. Another type of amino acid changes additionally appears outside of the active site. They indirectly participate on decreased susceptibility to the inhibitors when occurred together with major mutations. They are called **minor mutations.** They usually occur outside the active site (in hydrophobic pockets at more than 20 positions) and they often compensate the impaired enzyme's function in restoring its stability and activity [59,60].

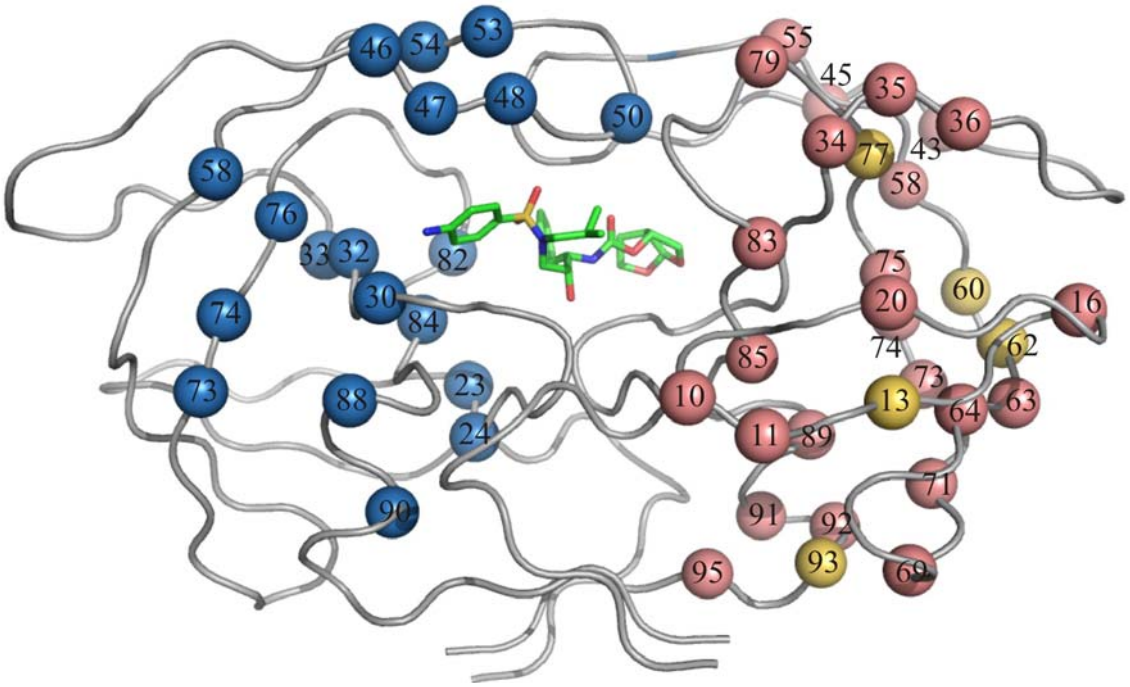

Figure 6: Structural model of HIV-1 protease: darunavir complex (PDB code: 1T3R) depicting mutations, which confer the drug resistance. Major mutations are in blue, minor in red and polymorphic mutations in yellow The figure was made by Dr. Klára Grantz-Šašková (IOCB AS CR), using programme PyMol [54].

Genotypic analysis of clinical isolates from PI treated HIV-1 positive patients confirmed more than 40 residues in one monomer of HIV-1 protease that can change. Further *in vitro* studies identified particular combinations of amino acid changes that confer resistance development. The set of mutations is referred to as the **mutational score** of an inhibitor (see Table 1). Several positions are sensitive to more than one inhibitor and they can cause **cross-resistance** [61]. Usually the combination of two or more amino acid changes has to be introduced to significantly reduce the inhibitor binding. The effect of single mutations on resistance development and their resistance pathways are studied on molecular level [62-65].

Table 1: Mutational scores of currently used inhibitors [60]:

Protease Inhibitor	Major Mutations	Minor Mutations
Saquinavir	48, 90	10, 24, 54, 62, 71, 73, 77, 82, 84
Indinavir	46, 82, 84	10, 20, 24, 32, 36, 54, 71, 73, 76, 77, 90
Nelfinavir	30, 90	10, 36, 46, 71, 77, 82, 84, 88
(Fos) Amprenavir	50, 84	10, 32, 46, 47, 54, 73, 76, 82, 90
Atazanavir	50, 84, 88	10, 16, 20, 24, 32, 33, 34, 36, 46, 48, 53, 54, 60, 62, 64, 71, 73, 82, 85, 90, 93
Lopinavir	32, 47, 82	10, 20, 24, 33, 46, 50, 53, 54, 63, 71, 73, 76, 84, 90
Tipranavir	33, 47, 58, 74, 82, 84	10, 13, 20, 35, 36, 43, 46, 54, 69, 83, 90
Darunavir	50, 54, 76, 84	11, 32, 33, 47, 74, 89, 90

There are other possible molecular mechanisms of drug resistance development. Occasional amino acid insertions to the HIV-1 protease, most prevalently between positions 32 and 42 were selected in patients treated by multiple PIs [66,67]. Furthermore, the mutations in the polyprotein cleavage sites or in their close vicinity were described. These residues contact the substrate binding pocket of the HIV-1 protease and are reported to enhance the overall processing of the Gag [68]. Some of them were shown to develop the PI resistance even without protease mutations, the other were selected in background of particular protease substitutions and they reduced response to inhibitor [69]. In addition, mutations in transframe p6 peptide [70] or substitutions affecting ribosomal frameshift, may contribute to the lowered inhibitor potency.

The knowledge of structural and thermodynamical aspects of resistance development allows the researchers both to understand and improve current treatment strategies and more importantly to design novel chemical compounds with excellent inhibitory profiles against cross-resistant viral species.

2.5.3 Second generation PIs: raising the barrier to resistance

As mentioned above, the raising prevalence of resistant HIV variants represents the major obstacle in combating HIV/AIDS. Therefore the design of novel class of

structurally different and very potent compounds that would be capable to suppress various multi- resistant viral strains is still needed [71].

Those of them that have already passed the FDA approval are known as the **second generation PIs** (Fig. 7)**.** The first one used in therapy is **lopinavir,** marketed in 2000. Due to poor pharmacokinetic profile it was subsequently formulated with a boosting agent ritonavir and the co-formulation is known as Kaletra®. In 2003 and 2005, **atazanavir** (Reyataz®) and **tipranavir** (Aptivus®), respectively, were introduced on the market as the next potent inhibitors active against resistant HIVs. Tipranavir was the first truly non-peptidic protease inhibitor with dihydropyranone ring as a central scaffold, mostly used in treatment of highly-experienced patients [55].

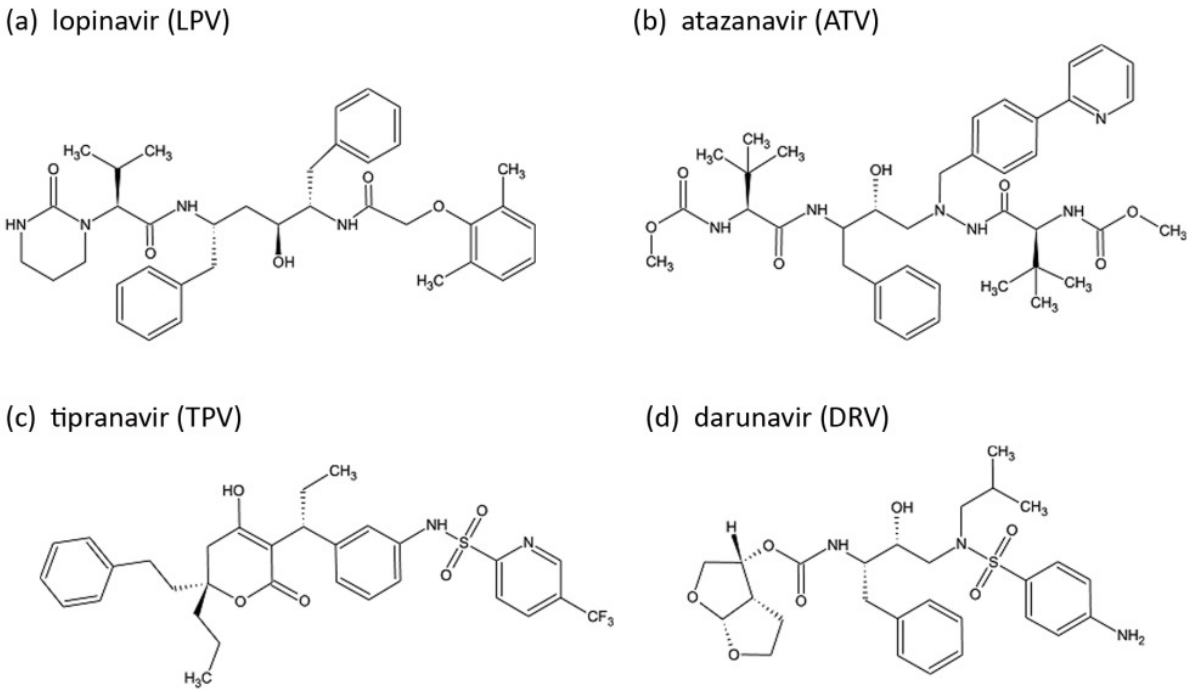

Figure 7: Chemical formulas of the second generation HIV-1 protease inhibitors.

The analyses of clinical isolates and then subsequently the laboratory-modified strains showed that HIV virus requires more mutations to accumulate for maintaining the viral fitness in the presence of second generation protease inhibitor.

The structural studies (X-ray, NMR, computational methods) of highly mutated HIV-1 proteases in complex with inhibitors allowed the chemists to introduce specific

chemical moieties that would interact directly with the backbone atoms at positions where the mutation hardly occurs [72]. The microcalorimetric analysis helped to describe the thermodynamics of binding between inhibitor and protease. Not surprisingly, the increase of number of hydrogen bonds with backbone atoms and other direct non-covalent interactions in the formation of protease-inhibitor complex leads to more favorable enthalpic contributions. Moreover, the higher structural flexibility and hydrophobic character that reflect positive enthropic changes and contribute to the overall binding energy, enables the inhibitor's molecule to adapt more effectively to the geometric alterations caused by mutations [73,74]. These findings finally led to the introduction of latest FDA approved protease inhibitor- **darunavir** for the anti-HIV treatment. Its superior features and properties will be closely discussed in the following chapters.

Although currently used protease inhibitors represent considerable success of structure-based drug design and the genetic barrier for drug resistance development increased, the virus still keep persisting in the form of the provirus.

More complex and detailed description of molecular mechanisms leading to resistance development may push the design of the next generation compounds active against the multi-drug-resistant HIV strains forward.

2.5.4 Interaction studies of HIV-1 protease and its inhibitors

To investigate the relationships between the structure and activity of HIV-1 protase and the mechanism of action of its inhibitors, it is essential to combine several approaches including conventional structural studies such X-ray, NMR and computational methods with methods that provide the information about the kinetics or thermodynamics (microcalorimetry) of the interaction between protease and inhibitor [75,76].

Since the most potent inhibitors usually reach the limit of conventional inhibition assays, little is known about the kinetics and mechanism of their action. Surface plasmon resonance (SPR)- based kinetic studies using the immobilized HIV-1 protease were previously used for screening of compounds interacting with HIV-1 protease [77]. The SPR method serves predominantly for determination of interaction

kinetic constants: the association and dissociation rate constants (k_{on} and k_{off}, respectively) and the equilibrium dissociation constant K_D ($K_D=k_{off}/k_{on}$). From the estimation of the affinities and dissociation rates of the inhibitors interacting with drug-resistant protease variants, the unique interaction profile was observed for each inhibitor/ protease variant complex. These data well correlated with those obtained from other measurements using different inhibition assays [78]

2.5.5 Darunavir (TMC-114, UIC-94017)

Darunavir is the latest HIV protease inhibitor introduced in HIV therapy. It was developed by Tibotec, Inc. The efficacy and safety studies have recommended the most effective dosing regimen of darunavir co-administered with ritonavir (DRV/r) in therapy of treatment-experienced patients to be 600/100 mg twice-daily and for -naïve patients to be 900/100mg once-daily. This combination was approved by FDA for the treatment under the commercial name Prezista®, in 2006. The clinical efficacy and pharmacodynamic as well as pharmacokinetic properties of darunavir have been intensively studied and are reviewed in details [79,80].

2.5.5.1 Discovery of darunavir

The efforts to develop the next generation inhibitors active against multi-resistant viruses resulted in design of series of potent compounds with novel structural features. The sulfonamide moiety at P2' position and *bis*- tetrahydrofuranyl (*bis*-THF) motif as P2 ligand were introduced [81-83]. TMC-114, which is chemically related to amprenavir and TMC-126 (Fig. 8), was selected as a candidate for advanced in *vitro* studies [84,85]. Darunavir showed great potency toward both "wild-type" and broad range of multi-resistant viruses, with 50% effective concentrations (EC_{50}) in low nanomolar range. It indicated low cytotoxicity at concentrations up to 100 μM and also higher genetic barrier for resistance development [86].

2.5.5.2 The structural evidence of darunavir binding in the active site

Darunavir and amprenavir slightly differ in their P2 ligand groups. Tetrahydrofuran group in amprenavir is replaced by a double-ringed *bis*-THF moiety.

King *et al.* compared the X-ray structures of both inhibitors in complexes with "wild-type" HIV-1 protease. They showed that *bis*-THF of TMC-114 binds to the active site with different binding pattern, when additional hydrogen bond is formed between the oxygen atom of the second tetrahydrofuran ring and the protease backbone nitrogen atom of Asp29 (Fig. 8d). This new interaction mimics the interaction of many of the natural substrates with protease main-chain atoms [87]. It is also hypothesized that darunavir fits within the consensus space in the PR active site as the substrates molecules do, which is called "substrate envelope" [88]. It means that it interacts only with the conserved residues in the active site, which mutate rarely. The resistance development to darunavir thus requires the accumulation of multiple mutations within the protease coding region [89].

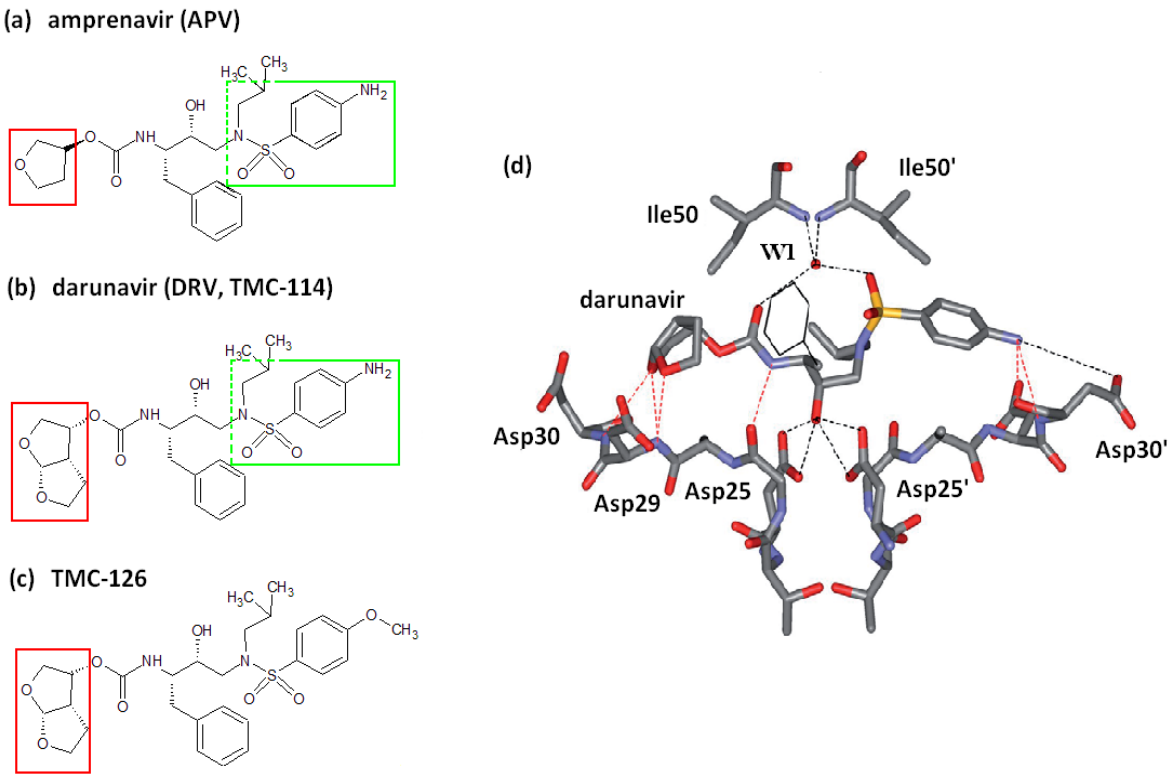

Figure 8: Comparison of chemical formulas of (a) amprenavir, (b) darunavir and (c) TMC-126. Tetrahydrofuranyl and *bis*-tetrahydrofuran moieties as P2 ligands and p-aminophenyl sulfonamide moiety as P2' ligand are highlighted in red or green squares, respectively; (d) the interaction of darunavir with the active site residues of "wild-type" HIV-1 protease. Hydrogen bonds of major position of inhibitor with protease backbone atoms are illustrated by red dashed lines and with protease side-chain atoms by black dashed lines. W1 water molecule is indicated as red sphere. (8b) adopted from [90].

The comparative study also showed stronger network of hydrogen bonds for darunavir, what was also supported with thermodynamical analysis. It revealed that it binds to the active site with the affinity approximately two orders of magnitude higher than amprenavir. Also the binding of darunavir is strongly enthalpicaly driven due to the net of hydrogen bonds formed between the bis-THF moiety and the main-chain atoms of Asp29 and Asp30. Whilst both enthalpic and enthropic contributions to the binding of APV are comparable [87]. Surface plasmon resonance (SPR)-based kinetic study performed by Dierynck and co-workers showed that even though affinity of darunavir to the wild-type protease was comparable to that of amprenavir, the dissociation rate for darunavir was about 1000-times slower [91].

The molecule of darunavir forms a network of direct or water-mediated hydrogen bonds with particular side-chains but also with the backbone atoms of residues Gly27, Ala28, Asp29, Asp30, Val32, Ile47 and Ile50. Notably, amino acids at positions 27-29 and 30 (except of nelfinavir [92]) have been detected to mutate rarely. On the other hand, substitutions V32I, I47V/A, I50V and I84V/A/C are major mutations conferring the resistance to most of the used first generation PIs [93]. Several structural studies of single- mutant HIV-1 proteases complexed with darunavir were performed to investigate the effect of these common drug-resistant mutations on the reduced susceptibility to darunavir. The mutations were located either in the active site [90,94,95] or in the flap region [96]. It was suggested, that substitutions D30N and especially I50V may be selected for resistance during the treatment. Although the introduction of particular mutations led in some cases to the local weakening of interactions with the protease, due to its structural flexibility, darunavir was able to adapt to the structural alterations of the changed residues in the active site pocket and in most cases maintained its inhibition activity. The analyses of these high-resolution crystal structures of protease- inhibitor complexes enabled the detailed description of geometrical rearrangements in the active site cavity of mutated HIV-1 proteases. This knowledge may contribute to the prediction of mechanisms involved in selection of drug-resistance mutations conferring to PIs treatment failure and also improve the genotypic as well as phenotypic resistance characterization [97,98].

2.5.5.3 The resistance development to darunavir

Koh *et al*. showed that after several passages of a mixture of multiple PI resistant viral isolates treated with darunavir, the set of 14 protease mutations was selected *in vitro*. However, the data also suggested that relatively strong genetic barrier had to be passed over for resistance development [99].

Several genotypic studies reported the protease mutations V11L, V32I, L33F, I47V, I50V, I54L/M, T74P, L76V, I84V and L89V to be associated with reduced darunavir susceptibility. They were also detected in patients who displayed anti-HIV therapy failure [100]. This set of amino acid changes represents the mutational score of darunavir. Grantz-Šašková *et al.* from the laboratory of Jan Konvalinka characterized a panel of six mutated HIV-1 variants from the database of clinical isolates that conferred the resistance to darunavir. It was confirmed that high number of these specific mutations, especially the presence of substitutions at positions 32, 47, 54, 82 and 84 increases the level of resistance to darunavir [101].

Another genotypic study of HIV-1 protease and Gag region (NC-p1/TFP-$p6^{pol}$) derived from a cohort of PI-experienced patients with darunavir regimens-failure has demonstrated the notable effect of Gag mutations A431V (nearby the NC-p1 cleavage site) and I437T/V on darunavir resistance without any amino acid changes selected in protease region [69,102].

2.5.5.4 Second binding site for darunavir

Unexpectedly, the analysis of ultra-high resolution structures of HIV-1 proteases bearing single mutations V32I or M46L, showed the second molecule of darunavir bound to the flap at the protease surface in addition to its conventional binding within the active site cavity. It was shown that darunavir binds to two distinct sites in different configurations due to the spontaneous sulfonamide nitrogen inversion. As Fig. 9 illustrates, the alternative binding of preferred S-enantiomer occurs within the groove formed by residues Glu35, Trp42, Pro44- Met46, Lys55- Arg57 and Val77- Pro79 at the surface of one protease subunit [94].

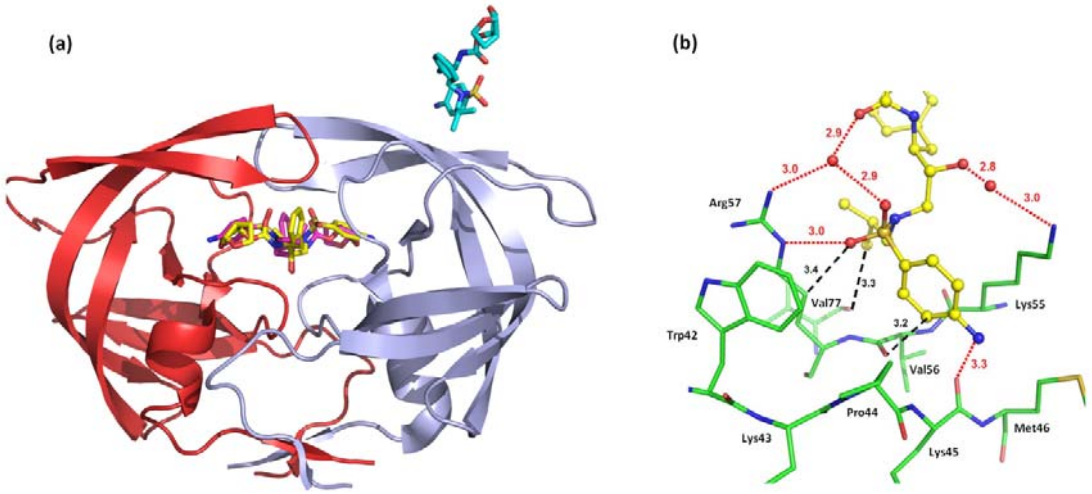

Figure 9: (a) Structure of the V32I mutated HIV-1 protease with two molecules of darunavir bound in the active site and in one flap region, respectively (PDB 1HS1). (b) The detailed view of the hydrogen bond network between the S-enantiomer of darunavir and the residues in the groove of the flap. Adopted from [94].

The kinetic measurements HIV-1 protease containing V32I mutation suggested the inhibition model for darunavir and structurally related amprenavir as well. The kinetic data have proposed the mixed-type competitive-uncompetitive mechanism for both inhibitors with the formation of ternary complex EI_2 (enzyme-inhibitor-inhibitor). It may support the existence of allosteric site for binding of darunavir as observed previously [103].

In conclusion, strong enthalpically driven binding, extra hydrogen bond with the main chain residue of the active site and possible unusual binding to the flap region of protease make darunavir very potent drug against multi-resistant HIV variants. One can argue if the alternative binding of darunavir is common mechanism of inhibition also in physiological conditions. Although the existence of HIV-1 protease allosteric sites has not been experimentally confirmed, design of inhibitors with such a mechanism of action could be an alternative to current design of competitive inhibitors.

2.6 PROTEIN EXOSITES: REGULATION OF BIOLOGICAL ACTIVITY

Biologically active proteins are usually composed of flexible domains which undergo conformational changes to achieve the proper function. The binding sites at the surface regions of many enzymes or in their core were characterized. These sites are known as allosteric sites or exosites and they influence the enzyme activity upon the modulator binding. The allosteric binding of a modulator represents quite common mechanism of regulation of many physiological processes including cell cycle control, metabolic pathways, signal transduction systems or imunne response and many others. The exosites participate on further substrate recognition and its conversion while **the allosteric activator** is bound.

The activity of enzymes involved in multistep reaction pathways is often regulated by the final product in feed-back inhibition. The final product then signifies for **the allosteric inhibitor**. It binds to a site distinct from the active site of the enzyme and thus inhibits by non-competitive mechanism.

Another example of such a non-active site inhibitor binding is represented by uncompetitive mechanism of enzyme inhibition. This type of enzyme activity regulation was, however, observed rarely in biological processes.

2.6.1 Allosteric theories

Allostery is defined as the long-distance cooperation between two or more structurally independent ligand binding sites. In **positive cooperativity**, ligand occupies the specific binding site and induces certain structural changes in its close vicinity that are transmitted to distal regions of the molecule throughout the protein scaffold. It may then result in increase of affinity of the active site for other molecule of the ligand. On the contrary, if the affinity is decreased, we talk about **negative cooperativity** [104]**.**

Several theoretical models were established to describe the allosteric behavior of protein [104,105]. Recent studies describe the allostery as the structural, energetic and dynamic property of any protein. It was shown that any structural perturbation (binding of an inhibitor, change in pH, ionic strength or temperature, etc.) can lead to the shift of

the ensemble of conformational populations, resulting in allosteric transition without obvious structural alterations [106].

2.6.2 Identification of new exosites and drug discovery

Many allosteric enzymes were identified that play important roles in many physiological events, pathological processes such as tumor cells proliferation or neurodegenerative and inflammatory diseases. Their activity is regulated by allosteric ligands. In other cases, the activity of enzymes that are formally non-allosteric may be regulated by small molecule ligands discovered to exploit the new allosteric sites by serendipity.

Different biophysical and computational strategies are used for detection of novel exosite regions and for elucidation of their roles in regulation of enzyme activity. The structural features of allosteric binding sites then serve to identify novel classes of potent and selective inhibitors or activators as the alternative to current development of the active-site drugs.

General approaches for the identification of any ligand-enzyme interaction (structure-activity relationship studies) consist in **high-throughput screening** (HTS) of large chemical libraries or more focused ***in silico* screening** for compounds with considerable inhibitory potency (hits). It is followed by kinetic characterization of target protein with leader candidates (leads) and structural studies (X-ray crystallography, multidimensional NMR spectroscopy or homology modeling). Besides these conventional methods, several structure-based strategies have been developed for the recognition of "druggable" binding sites [107].

Fragment screening method is initially used for locating the binding sites by screening libraries of small organic molecules with low binding affinities (fragments), which cannot be detected by HTS. Some guiding structural information can be deduced from analysis of either the fragment-induced changes in NMR spectra or solution of the X-ray structure of protein-fragment complexes [107,108]. Lead fragments can serve as templates for more exact optimization [109]. Another approach utilizes time resolved-fluorescence resonance energy transfer (**TR-FRET**). TR-FRET binding assays were used for focused screening of the inhibitors with novel mechanisms of action [110,111]. New allosteric sites were also discovered by **Tethering** technique. This method is based

on the formation of disulfide bonds between thiol-containing small molecules and free –SH groups of native or introduced cysteines on protein surface [112]. Allosteric binding sites for small molecule ligands can be studied by side-directed spin labeling and electron paramagnetic resonance (**SDSL- EPR**) spectroscopy. The measurement of collision frequency of spin label bound selectively to protein cystein residue and the paramagnetic metal-containing ligand bound to the exosite region can provide the information about the distances of spin-spin labeled sites [113,114]. **Surface plasmon resonance (SPR)**-based binding kinetics studies, usually supported by the X-ray structural data, were also employed in determination of the allosteric mechanism [115]. The increasing number of genomic and structural information about proteins alone or in complexes with natural and non-natural ligands enables scientists to develop **the bioinformatics approaches** for prediction of protein druggability. Many of the geometry- and energy-based algorithms were described so far to investigate possible ligand binding regions [116].

2.6.3 The examples of allosteric regulatory mechanisms

The activity of allosteric enzyme can be regulated in several ways. The conformational changes in the active site are usually induced upon small molecules or protein ligands binding to the exosites, or by the exosite phosphorylation. In some cases, allosteric modulation is achieved by changes in enzyme flexibility (reviewed in [117]). In the following chapters, several examples of the exosite-regulated enzymes and the discovery of the exosite inhibitors are discussed.

2.6.3.1 The allosteric regulation of blood clotting proteases

Blood coagulation cascade is a highly regulated process. Panel of seven specific serine proteases (also referred to as coagulation factors) is sequentially activated from their zymogens in series of proteolytic reactions. The activity of blood clotting serine proteases is regulated through their exosites formed by loops insertions mostly located at the surface of the molecule. Exosites in coagulation factors are separated from the active site region and are involved in substrate recognition [118].

Due to its critical function in final steps of the coagulation cascade, **thrombin** became the most exstensively studied allosteric protease with exosite regulation. Thrombin is activated from prothrombin by factor Xa- activator complex and prothrombinase complex. It results in processing of fibrinogen into fibrin and subsequent fibrin clot formation [119]. Numerous crystallographic and enzymology studies confirmed that thrombin has **two** surface positively charged **exosite regions**, which mediate very specific interactions with its substrates, effectors and inhibitors. Thrombin is an enzyme with quite a high level of flexibility. It exists mostly in three distinct dynamic conformations at physiological conditions. Kinetic and structural analyses revealed that thrombin activity and specificity is determined by the nature of the cofactor bound in one of the exosites or both of them simultaneously. Thrombin is inhibited by physiologic serine protease inhibitors (serpins) like antithrombin or heparin cofactor II and others. Serpins behave as natural thrombin substrates and induce irreversible unfolding of the enzyme accompanied by loss of activity and binding of other effectors. On the contrary, allosteric binding of Na^+ cation enhances the activity and specificity toward fibrinogen and it decreases the affinity for antithrombin [120-122].

Factor VIIa is trypsin-like serine protease circulating in blood as an inactive factor VII. The protease is released upon the proteolytic cleavage and fully activated after the complexation with protein called tissue factor (TF) in the presence of Ca^{2+} cations. Factor VIIa activity initiates the extrinsic pathway of blood coagulation. Thus it became another attractive target for anticoagulation drugs development. The crystal structure of the factor VIIa:TF complex showed the detail of their interaction [123]. It enabled the design of specific inhibitors that block the association, such as TF and factor VIIa antibodies. Another approach was using phage display with peptide libraries and it brought out two peptide inhibitors E-76 and A-183 specific and potent for factor VIIa. Structural analysis of their complexes with factor VIIa revealed two distinct and non overlaping exosites. Their binding induces the conformational switch from ordered conformation into the disordered zymogen structure. The reduced proteolytic activity of factor VIIa was achieved by non-competitive inhibition by E-76 and mixed type inhibition by A-183 peptide inhibitor, respectively [124,125].

2.6.3.2 Allosteric regulatory mechanisms found in other proteases

Trypsin is a serine protease that belongs to large trypsin/ chymotrypsin-like serine protease family. Like all the members, it is the endopeptidase with conserved tertiary fold and typical active site triad (His-Ser-Asp). Trypsin is synthesized as inactive zymogen trypsinogen, which has rather disordered conformation. Its proteolytic cleavage initiates the insertion of newly formed N-terminal sequence into the activation domain. That subsequently leads to structural rearrangements and formation of an ordered conformation. Interestingly, **non-proteolytic allosteric activation** was carried out by adding of dipeptide H-Ile-Val-OH resembling trypsin N-terminus to trypsinogen. It induced the conformational switch to trypsin [126]. This general mechanism of zymogen activation was confirmed by the analysis of co-crystal structure of staphylocoagulase and prothrombin-2. Prothrombin-2 was rearranged to active thrombin without any cleavage [127]. These findings can serve to design of small molecule allosteric activators that mimic the N-terminal sequences of trypin-like serine proteases.

Caspases are cysteine proteases that preferentially cleave the substrate after aspartate residue. They are proteolytically activated from their single-chain proenzymes into homodimers. For some members the allosteric regulation of caspases was described. Caspase-9 is naturally inhibited by specific multidomain endogenous inhibitor XIAP. It binds into the interface between the caspase monomers and thus blocks the process of dimerization [128]. Allosteric inhibition of caspase-3 and -7 can be also achieved by the small molecule inhibitors DICA (2-(2,4-dichloro-phenoxy)-*N*-(2-mercapto-ethyl)-acetamide) and FICA (5-fluoro-1*H*-indole-2-carboxylic acid (2-mercapto-ethyl)-amide) that were probed by tethering technique. These compounds selectively interact with cysteines located at the surface of allosteric sites of both enzymes and they subsequently induce the irreversible switch of the active caspase into the zymogen-like conformation [129].

Matrix metalloproteinases (MMPs) belong to the subfamily of zinc- and calcium-dependent endopeptidases that process extracellular proteins (collagen, elastin, etc.) and also membrane anchored proteins. They are secreted as proenzymes to the extracellular matrix and activated by the delocalization of the prodomain located in the active site. The activation is achieved by proteolytic cleavage of the prodomain or conformational change mediated by allosteric binding of the activator molecule [130].

MMP13 is one of the most studied enzymes of this family. The overexpression of MMP13 was detected in osteoarthritis and thus became the target for treatment. Chemically distinct competitive inhibitors that chelate the catalytic zinc were designed, but they lacked specificity towards MMP13. Interestingly, a potent compound of the pyrimidine dicarboxamides class was reported to bind allosterically to the "specificity loop" of the exosite region that seems to be unique for each MMP [131]. Dual inhibition studies showed that it inhibits the MMP13 activity in a non-competitive manner [132].

2.6.3.3 The allosteric inhibition of non- proteolytic enzymes

PI3K/AKT pathway has regulation role in processes of cell proliferation or apoptosis. Its hyperactivation has attracted researchers as new and promising therapeutical target in cancer treatment [133]. AKT1 is ATP-dependent serine/threonine protein kinase and belongs to the protein kinase B family. AKT1 found in cytosol is in its inactive "closed" conformation with the ATP-binding and site blocked. The activation of AKT1 is a multistep process and it occurs via its phosphorylation at the plasma membrane [134]. Several small molecule kinase inhibitors were developed and they are mostly ATP-competitive and non-selective to three of AKT isoenzymes. The screening of synthesis products library resulted in discovery of the group of allosteric AKT1-selective compounds [121]. Structural analysis showed specific hydrogen bond network between AKT1 and one of these drugs Inhibitor VIII at the interface of two enzyme domains. Allosterically inhibited AKT1 is then arrested in its inactive "closed" conformation and prevented the membrane association and its activation by phosphorylation [135].

HIV-1 reverse trancriptase and **HCV NS5B polymerase** became important targets in antiviral treatment. Allosteric mechanisms of their inhibition were reported. HIV-1 RT is RNA dependent DNA polymerase. As well as other polymerases, both viral enzymes contain subdomains that we call fingers, palm and thumb and they undergo conformational changes from open-inactive to close active form during the catalytic reaction [136]. Non-nucleoside inhibitors of both polymerases were reported to interact with the sites remote to the active sites. These compounds prevent the enzyme from the conformational switch.

Two novel classes of non-nucleoside HIV-1 RT inhibitors the indolpyridones (INDOPY-1 and VRX-329747) and the 4-dimethylamino-6-vinylpyriminide derivatives (DAVP1, 2, 3) were characterized Due to the unusual mechanisms of action, they were referred to as "nucleotide-competing HIV-1 RT inhibitors (NcRTIs)" [137,138].

Wang *et al*. published in 2003 the first two crystal structures of NS5B polymerase with non-nucleoside phenylalanine derivatives inhibitors. These compounds were reported as the non-competitive inhibitors with allosteric binding mechanism that arrested NS5B polymerase in an open inactive conformation and thus block its enzymatic activity [139].

2.6.4 The alternative binding modes for HIV-1 protease inhibitors

The inhibitor binding to the active site pocket of HIV protease and its competing with the substrate molecule is not the only possible mechanism of inhibition. More unconventional modes of action were observed and possible novel classes of antiretrovirotics were suggested. The knowledge of high resolution X-ray structure of HIV-1 protease enables to design inhibitors that may form direct interaction within particular regions of enzyme, such as N- and C- terminal residues (1-9 and 94-99) that are crucial for dimerization or flap region (47-56) involved in substrate binding and products release.

2.6.4.1 Inhibition of monomer folding and dimerization

Short peptides (p-LESs) with inhibition constants in micromolar range were characterized. They may influence homodimer stability through their interaction with "local elementary structures" (LES) of HIV-1 protease [140]. It was suggested that these particular segments could comprise the residues 23-33, 74-78 and 83-92 of folded HIV-1 protease monomer. Monte Carlo simulations describing HIV protease monomer folding mechanism demonstrated the crucial role of LES in process of dimerization [141]. Subsequently, p-LES peptides have been shown to shift the equilibrium to the unfolded state. This effective inhibition of monomer folding with peptides targeting the LES motifs of protease may represent possible way of drug design. p-LESs are also

predisposed not to create resistance [142]. Other tetrapeptides- derived from the terminal sequences of the protease interact with N- or C-termini residues of folded monomers and also block the dimerization in a direct way (Fig. 10e) [143].

Koh *et al*. identified the small non-peptidyl inhibitors that block dimerization using a FRET assay. Together with two experimental HIV-protease inhibitors and two clinically used inhibitors darunavir and tipranavir, they disrupted the dimerization at micromolar concentrations. Four of these compounds contain *bis*-THF or *bis*-THF related moiety, respectively. They were suggested to act before the association of two monomers, but this statement has not been supported by any structural data [144].

In 2008, Bartoňová *et al.* reported the study of the inhibition of HIV-1 protease by the light chain fragment of monoclonal antibody 1696, which exhibits K_i values in low nanomolar range [145]. The interaction was proved by X-ray structure of the antibody 1696 in complex with HIV protease fragment corresponding to its epitope at the N-terminal region (residues 1-6) and it is shown in Fig. 10d. This interaction was suggested to restrict dimer stability [146].

2.6.4.2 Targeting the flexible flap region

As previously mentioned (see chapter 2.4.1.), the dynamics of HIV protease is essential for substrate recognition and its access to the active site. The flaps undergo structural rearrangements upon substrate binding changing the conformation from semi-open to close conformation [147]. However, the flap motions are still poorly understood and the mechanism of its participation on the substrate entry is intensively investigated utilizing NMR studies and molecular dynamics simulations. Nevertheless, targeting of this important region that plays the key role in enzyme function appears to be an attractive drug design approach.

The kinetic and computational docking study [148] suggested that some of the inorganic compounds from the group of niob-containing polyoxometalates (POMs) bind to the surface of flexible flaps or with their hinges with the stoichiometry of 2:1 (two molecules of inhibitor per one HIV-1 PR homodimer). The model of that interaction is schemed in Fig. 10a. POMs act by noncompetitive mechanism, which seems to be preferable and thus they may restrict the flexibility of that region and the proper function of HIV-1 protease. These chemical entities exhibited the effective inhibitor

concentration against HIV-1 protease, as well as anti-HIV-1 activity at micromolar range and were not cytotoxic [148]. However, these data have not been structurally confirmed and independently reported.

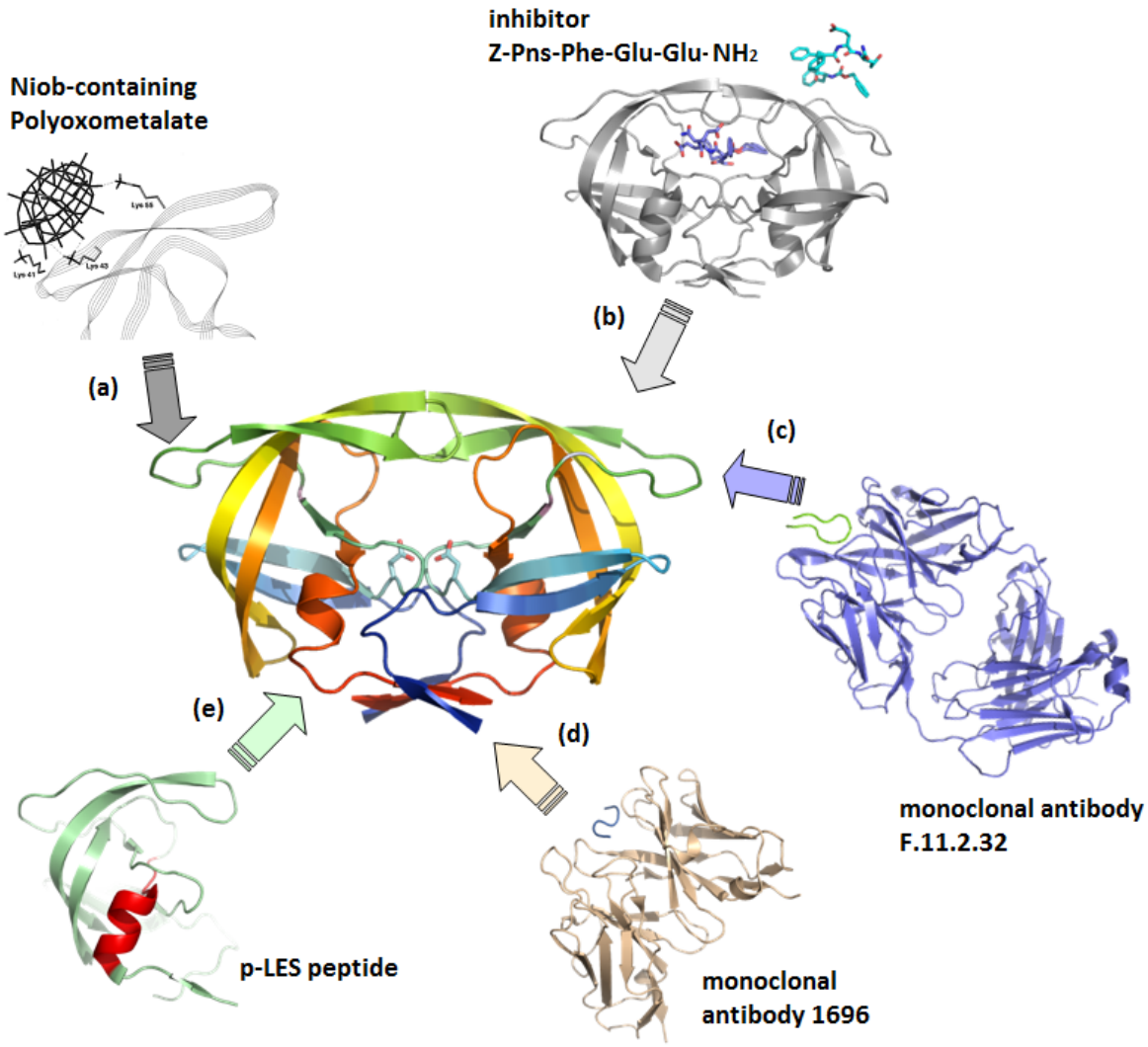

Figure 10: Scheme showing the details of interactions between the HIV-1 protease and (a) Niob-containing polyoxometalate, (b) peptidomimetic inhibitor Z-Pns-Phe-Glu-Glu.NH_2 (PDB code: 1U8G), (c) monoclonal antibody F.11.2.32 (2HRP), (d) monoclonal antibody 1696, (PDB:1JP5), (e) p-LES peptide that comprises the residues 83-92 of folded PR monomer. The figure was created by Dr. Pavlína Řezáčová (IOCB AS CR) using Pymol [54]

Bartoňová *et al.* also proved inhibitory effect of single chain fragment of monoclonal antibody F.11.2.32, when bound with the epitope at the HIV-1 protease flap region, between positions 36 and 46, as it is shown in Fig. 10c. The antibody F.11.2.32 and 1696 mentioned above were active even against the drug-resistant protease variants with K_i values in nanomolar range [145].

Brynda *et al.* identified the compounds from the phenylnorstatin group with subnanomolar inhibition activity against HIV-1 protease. They solved the crystal structure of the wild-type HIV-1 protease in complex with one of these inhibitors, Z-Pns-Phe-Glu-Glu-NH_2 (PDB code: 1U8G). The analysis showed that the asymmetric unit contained one protease dimer and two molecules of the inhibitor bound in the active site and to the protease surface, respectively. This second molecule occupied the interspace between two molecules of HIV-1 PR arranged in the crystal lattice which is quite unusual for HIV-1 protease. It interacted with the flap surface of the first and the N-terminal region of the second dimer. Its structural model is illustrated in Fig. 10b. However, its inhibitory role has to be discussed due to the unlike assembly of such a complex in solution [142].

In this sense, the secondary binding site for darunavir discussed earlier (chapter 2.5.5.4.) may represent an exosite suitable as a therapeutic target. Moreover, another study performed in our laboratory provided the strong evidence for alternative binding of darunavir. Thermodynamic analysis of the binding of darunavir into the highly mutated HIV-1 protease (L10I, L24I, L33F, M46L, I47A, I54V, L63P, A71V, V82A and I84V [93]) showed that two molecules of the inhibitor bind within the protease dimer. Unfortunately, that has not been confirmed yet by structural analysis since the inhibitor was bound only within the active site (unpublished data). To prove the existence of the alternative binding site for darunavir *in vitro* is the main goal of this thesis

3. AIMS OF THE THESIS

The main objective of this project was to study the mechanism of inhibition of highly mutated HIV-1 protease by darunavir using nuclear magnetic resonance and surface plasmon resonance. This includes the preparation of isotopically labeled and tag-extended protease variants.

- Cloning, expression and purification of ^{15}N labeled HIV-1 protease variants
- Cloning, expression and purification of His tag and Avi tag- extended HIV-1 protease variants
- Determination of the stability enzymatic activity of tag-extended protease variants
- Kinetic analyses of the mechanism of inhibition of highly mutated HIV-1 protease by darunavir using spectrophotometric assay

4. MATERIALS AND INSTRUMENTS

4.1 Chemicals

DMSO	Sigma-Aldrich, USA
ethanol	Lach-Ner., Czech Republic
methanol	Penta, Czech Republic
hydrochloric acid	Penta, Czech Republic
D-biotin	Sigma-Aldrich, USA
ammonium chloride (^{15}N labelled)	Cambridge Isotope Laboratories, Inc., USA
D-glucose	Sigma-Aldrich, USA
magnesium sulphate	Penta, Czech Republic
potasium dihydrogen phosphate	Sigma-Aldrich, USA
disodium hydrogen phosphate, dodecahydrate	Penta, Czech Republic
acetic acid	Penta, Czech Republic
sodium acetate	Penta, Czech Republic
acrylamide	USB, USA
ampicilin	Sigma-Aldrich, USA
bromphenol blue	Serva, Germany
sodium deoxycholate	Fluka, Germany
coommassie brilliant blue R-250	Fluka, Germany
ethylendiamintetraacetic acid (EDTA)	Sigma-Aldrich, USA
formaldehyde	Lachema, Czech republic
glycerol	Penta, Czech Republic
glycine	USB, USA
sodium hydroxide	Penta, Czech Republic
sodium chloride	Penta, Czech Republic
isopropyl-β-D-thiogalactopyranosid (IPTG)	Biosynth AGm, Switzerland
kanamycin sulphate	Sigma-Aldrich, USA
sodium dodecyl sulphate (SDS)	Sigma-Aldrich, USA
2-mercaptoethanol	Sigma-Aldrich, USA
isopropyl-β-D-thiogalactopyranosid (MES)	AppliChem GmbH, Germany
3-morpholinopropane-1-sulfonic acid (MOPS)	Duchefa Biochemie, Holland
2-Amino-2-hydroxymethyl-propane-1,3-diol (Tris)	Promega (USA)
N,N‘-bisacrylamide	USB, USA
amonium persulphate (APS)	Fluka, Germany
phenylmethylsulphonyl fluorid (PMSF)	Sigma-Aldrich, USA
ammonium sulphate	AppliChem GmbH, Germany
N,N,N‘,N‘-tetramethylethylendiamine (TEMED)	Sigma-Aldrich, USA

Triton X 100	Sigma-Aldrich, USA
agarose	Serva, Germany
isopropanol	Penta, Czech Republic
sucrose	Fluka, Germany
potassium acetate	Penta, Czech Republic
urea	USB, USA
imidazole	Sigma-Aldrich, USA
sodium thiosulphate, pentahydrate	Penta, Czech Republic
sodium carbonate	Penta, Czech Republic
silver nitrate	Lach-Ner., Czech Republic
deuterium oxide (D2O)	Merck, Germany
calcium chloride, dihydrate	Sigma-Aldrich, USA

4.2 Instruments

- Centrifuges: Eppendorf centrifuge 5415R, Eppendorf (Germany)
  Beckman J2-MI, Beckman Coulter (USA)
  Biofuge Pico, Hereaus Instruments (Germany)
  Megafuge 2.0R, Hereaus Instruments (Germany)
- Rotary incubator: Innova 4300, New Brunswick Scientific (USA)
- Sonicator: Soniprep 150, MSE (USA)
- Autoclave: MLS-3020U, Sanyo (Japan)
- Spectrophotometers: UV-VIS Spectrophotometer UNICAM UV500, Unicam (UK)
  UV-VIS Spectrophotometer SPECORD 210, Analytik Jena (Germany)
  NanoDrop ND-1000 spectrometer, Thermo Scientific (USA)
- Electrophoresis: Horizontal electrophoresis aparatus, Gibco (USA)
  Vertical polyacrylamide electrophoresis, Amersham Pharmacia Biotech, (Sweden)
- Blotting: Trans-Blot SD Semi-Dry Electrophoretic Transfer Cell, Bio-Rad (USA)
- Shaker: KS 260 basic shaker, IKA (Germany)
- Chromatography: FPLC ÄKTA Explorer, Amershan Pharmacia Biotech (Sweden)

- Thermal cycler: Biometra T-gradient Thermal Cycler, Labrepco (USA)
- UV Transilluminator, UltraLum (USA)
- Thermostats: Techne, Cambridge (UK)
  Thermomix BU, B. Braun (Germany)
- UV Transilluminator, UltraLum (USA)
- pH meter: Unicam 9450, Unicam (UK)
- CCD camera: LAS 3000, Fujifilm Corporation (Japan)
- Camera: DC 290 Zoom Digital camera, Kodak (USA)

4.3 Other used materials

- Enyzmes: *Pfu* DNA polymerase, Promega (USA); restriction endonucleases (*HindIII*, *XhoI*, *NdeI*, *DpnI*), T4 DNA ligase, alkaline phosphatase, New England BioLabs (USA); oligonucleotide primers, Generi Biotech (Czech republic); lysozyme, RNase A, Sigma Aldrich (USA);
- Kits and solutions:
  NEBuffer 2, NEBuffer 4, T4 DNA ligase buffer, New England BioLabs (USA);
  PPP Master Mix solution, Top-Bio (Czech Republic);
  QIAquick Gel Extraction Kit, QIAGEN (USA);
  QuickChange® Site-Directed Mutagenesis Kit, Stratagene (USA); Commassie blue G-250 solution, Bio-Rad (USA), GelRed dye, Biotium (USA)
- Standards: Protein test mixture 4+5, Serva (Germany); All Blue, Bio-Rad (USA); λ standard (8454- 702 bp), New England BioLabs (USA); 50bp ladder DNA, Quiagen (USA)
- Blotting: Neu-HRP (1 mg/ml), Casein Blocker, SuperSignal West Dura/Pico Chemoluminescence substrate, antimouse-IgG antibody conjugated with HRP (0.8 mg/ml), all Pierce (USA); Clone HIS-1, Sigma-Aldrich (USA); IgG F11.1.3.11 (7 mg/ml),

- Resins: Ni-NTA Superflow, Quiagen (USA)
  Streptavidin Mutein Matrix, ROCHE (Czech Republic)
- Columns: MonoS™ HR10/100, Superdex 75 HR 10/30 FPLC Column, Amersham Pharmacia Biotech (Sweden); plastic gravity-flow disposable columns, Pierce (USA)
- Dialysis: Dialysis membrane Spectapor, Specrrum Laboratories (USA)
  Slide-A-Lyzer® Mini Dialysis Units, Pierce (USA)

- Filtration: Sterivex™ 0.22 μm Filter Unit, Millipore
- Concentrating: Microcon® Ultra and Amicon® Centrifugal Filter Units, Millipore (USA)
- Kinetic analysis: Chromogenous substrate KARVNle*NphEANleNH$_2$ (Prepared by Mirka Blechová at IOCB AS CR), darunavir, Tibotec, BVBA, USA); brecanavir, GlaxoSmithKline plc (UK)
- Bacterial strains, vectors and media:
  E.coli BL21(DE3)RIL, Novagen (USA);
  E.coli DH5α, Novagen (USA);
  pET16b (AMP+), pET24a (KAN+), pET28b (AMP+), Novagen (USA);
  pACYC (CM+), Avidity, L.L.C. (USA)
  LB Broth, LB Agar, Sigma-Aldrich (USA)

5. METHODS

5.1 DNA manipulations

5.1.1 Amplification of HIV-1 PR coding regions

The HIV-1 PR coding regions containing either N- or C-terminal poly-His-tag (N- and C-His HIV-1 PR variants) were amplified by PCR reactions using a forward primer 5‘- ATCCTTTCATATGCCTCAGATCACTCTTTGG- 3‘ specific to the 5‘-end of the PR coding region with *NdeI* cleavage site and two reverse primers. The sequence of the first reverse primer was 5‘-ATAGACTCGAGTCATCAAAAA-TTTAAAGTGCAGCC-3‘ involving the cleavage site for *XhoI* and two stop codons, specific to N-His PR variant. The second one comprised the sequence 5‘-AGATAAAGCTTAAAATTTAAAAGTGCAGCC- 3‘ with site for *HindIII,* specific to C-His PR variant, respectively. The primers were synthetized by Generi Biotech (CZ). The PCR reaction mixture composed of 22 µl of sterile water (HPLC grade), 25 µl of PPP Master Mix solution (2x), 1 µl of 20 µM forward primer and 1 µl of 20 µM reverse primer, 0.5 µl of *Pfu* DNA polymerase (3 U/µl) and 1 µl DNA template (100 ng/µl).

All PCR reactions were performed in a thermocycler Biometra T-Gradient Thermoblock (Schoeller Instruments, Germany) as follows:

1) 95°C/ 5 min
2) (95°C/ 30 s, 55°C/ 30 s, 72°C/ 1 min), 34 cycles
3) 72°C/ 8 min, 4°C

5.1.2 DNA digestion with restriction enzymes

Purified PCR products and plasmids (pET16b, pET24a and pET28b) were digested with appropriate restriction endonucleases (New England BioLabs, USA). A typical digest reaction using *NdeI* and *XhoI* was performed under conditions recommended by the manufacturer. Digestion mixture of PCR products with restriction enzymes contained 25 µl of PCR product, 1.5 µl of *NdeI* and *XhoI* (both 20 U/µl) and 17 µl of sterile water (HPLC grade). Digest reactions proceeded at 37°C overnight. Digested plasmids were dephosphorylated using alkaline phosphatase (AP, Biotech, England). 1 µl of AP was added to a total volume of 50 µl of restriction digest reaction. The mixture was incubated at 37°C, for 10 min and the reaction mixture was loaded on the agarose gel.

5.1.3 Horizontal agarose gel electrophoresis

Buffers:

TAE buffer (50x): 242 g Tris-HCl; 57.1 ml 99 % CH_3COOH; 100 ml 0.5 M EDTA; water to 1l; pH 8.0

Sample buffer: 40 % (w/v) sucrose; 0.1 (w/v) bromphenol blue

All DNA manipulation procedures were checked by horizontal agarose gel electrophoresis as follows: 1.3 % agarose gel was prepared from 50 ml of TAE buffer (1x) and 0.65 g of agarose. The suspension was heated until agarose dissolved completely and then refilled with water to original weight. After that, 5 µl of GelRed dye (10000x diluted, Biotium) were added to the hot gel solution. Before loading to the gel, DNA samples were mixed with the sample buffer in the ratio of 5:1. Electrophoresis proceeded in a horizontal electrophoresis apparatus filled with TAE buffer (1x). Gel was run at a constant voltage of 120V for 25 min. Separated DNA molecules were detected using UV lamp (Transilluminator UVP, USA) and photographed by DC 290 Zoom Digital camera (Kodak, USA).

5.1.4 DNA isolation from agarose gel

DNA was isolated from the agarose gel using QIAquick Gel Extraction Kit (QIAGEN, USA). Gel slice containing DNA was dissolved in buffer QG (600 µl of QG for 200mg of the gel) and suspension was heated at 56°C for 10 min. 200 µl of isopropanol were added, mixture was transferred to the QIAquick Spin Column and centrifuged (10000g, 1 min, 25°C). The membrane with captured DNA was washed with 750 µl of buffer PE by centrifugation (10000g, 1 min, 25°C) and spin down again. Finally, the column was transferred into a microtube, 50 µl of sterile water were added and the DNA was eluted by following centrifugation (10000g, 1 min, 25°C).

5.1.5 Ligation of protease coding region into the expression vector

Isolated DNA was ligated into the expression vectors pET24a, pET16b or pET28b to construct the C-His or N-His PR variants constructs, respectively. A typical ligation reaction was performed according to the manufacturer's recommendations (TopBio, CZ). Ligation mixture composed of 25 µl of isolated DNA, 2 µl of plasmid, 4 µl of T4 DNA ligase buffer (10x), 1 µl of T4 DNA ligase (400 U/µl) and 8 µl of sterile water (HPLC grade). Reaction was carried out in 16°C for two hours. As a negative control 25 µl of sterile water were added instead of the DNA.

5.1.6 Transformation of bacterial cells

The host strain *E. coli* DH5α (Novagen) was transformed by the vector with ligated PR coding sequence. The transformation was proceeded as follows: 30 µl of the solution after ligation were added into 150 µl of competent cells. The mixture was left for 30 minutes on ice, followed by heat shock (42°C for 1.5 min and 2 min on ice). Cells were incubated with 850 µl of sterile medium at 37°C for one hour, followed by

spreading of the culture on the agar plates supplemented by an appropriate antibiotic. Plates were incubated at 37°C overnight.

5.1.7 Isolation of the plasmid DNA

Solutions and other material:

solution I: 25mM Tris-HCl; 50 mM glucose; 10 mM EDTA; pH 8.0

solution II: 0.2 M NaOH; 1 % (w/v) SDS

solution III: 3 M potassium acetate; 2 M CH_3COOH

3 M sodium acetate, pH 5.2; isopropanol; QIAquick Gel Extraction Kit (QUIAGEN, USA)

Single colony of transformed cells, grown on LB agar plate (chapter 5.1.6), was picked up and transferred into 12 ml of sterile LB medium supplemented by an appropriate ATB (1000x). The bacterial inoculum was then incubated in a rotary incubator (Innova 4300, New Brunswick Scientific, USA) at 220 rpm and 37°C overnight. It was then centrifuged (3300g, 10 min, 4°C) and the cell pellet was suspended in 225 µl of solution I, 12.5 µl of lysozyme (25 mg/ml) and 6 µl of RNAse (10 mg/ml). 450 µl of solution II were added and suspension was slightly stirred and left for 6 min on ice. This step was repeated with 338 µl of solution III, as well. The suspension was then centrifuged (16000g, 7 min, and 25°C) and the supernatant was mixed with 30 µl of 3 M sodium acetate (pH 5.2), 338 µl of isopropanol and 200 µl of buffer QG (QIAquick Gel Extraction Kit, QIAGEN, USA). The DNA solution was transferred into a QIAquick Spin Column and centrifuged (16000g, 1 min, and 25°C). The column membrane containing captured DNA molecules was then washed and DNA was eluted by sterile water of HPLC grade (chapter 5.1.4).

The quality and quantity of the DNA was verified by horizontal agarose gel electrophoresis (chapter 5.1.3). The concentration was determined by measuring the absorbance at 280 nm using Nanodrop® ND-1000 Spectrophotometer (Thermo Scientific, USA). The DNA coding regions for N- and C-His PR variants were sequenced and analysed in the laboratory of Dr. Felsberg (IMG AS CR).

5.1.8 Construction of inactive HIV-1 protease by site- directed mutagenesis

Mutagenesis reaction was performed following the instructions from the QuickChange® Site-Directed Mutagenesis Kit. Construction of an inactive form of HIV-1 protease (MUT) containing mutations: L10I, L24I, L33F, M46L, I47A, I54V, L63P, A71V, V82A and I84V required another single point mutation D25N . For this purpose, a pair of primers 5‘- GGAAGCTCTAATAAATACAGGAGCAGATG -3‘ and 5‘- CATCTGCTCCTGTATTTATTAGAGCTTCC -3‘ were designed. Primers were synthetized by Generi Biotech (CZ). The PCR reaction mixture composed of 22 µl of sterile water (HPLC grade), 25 µl of PPP Master Mix solution (2x), 1 µl of 10 µM forward and reverse primers, 0.5 µl of Pfu DNA polymerase (3U/µl) and 1 µl of the DNA template (100 ng/µl). PCR reaction was performed in a thermocycler Biometra T-Gradient Thermoblock (Schoeller Instruments, Germany) as follows:

1. 95°C/ 5 min
2. (95°C/ 30 s, 55°C/ 30 s, 68°C/ 5 min), 12 cycles
3. 72°C/ 8 min, 4°C

PCR reaction was followed by addition of 1 µl of *DpnI* restriction enzyme to digest the template DNA. The mixture was incubated at 37°C for 1h. Amplification was checked by horizontal agarose gel electrophoresis (chapter 5.1.3). The DNA coding region for inactive PR variant was sequenced and analysed in the laboratory of Dr. Felsberg (IMG AS CR).

5.2 Protein expression and isolation

5.2.1 Expression of HIV-1 protease variants in *E.coli*

Three ^{15}N isotope-labelled enzymes were prepared for nuclear magnetic resonance studies: wild-type HIV-1 protease (WT), mutated (MUT) variant and its inactive form with D25N mutation in the active site (inMUT).

Another eight tag fusion enzymes were prepared for surface plasmon resonance studies: N- and C- terminal Avi-tagged "wild-type" and mutated HIV-1 proteases (N-Avi and C-Avi WT, N-Avi and C-Avi MUT) and N- and C- 6x-His-tagged "wild-type" and mutated HIV-1 proteases (N-His and C-His WT, N-His and C-His MUT).

Mutated HIV-1 PR was prepared for kinetic measurements.

5.2.1.1 Expression of ^{15}N labelled HIV-1 protease

Culture medium:

M9 minimal media: 51 g $Na_2HPO_4.12H_2O$, 9 g KH_2PO_4 and 3 g NaCl were dissolved in 3 litres of sterile water and the solution was sterilized by autoclaving 121°C for 15 min. After that, 7.5g glucose, 2 g $^{15}NH_4Cl$, 1 ml of 1 M $MgSO_4$, and 1 ml 0.1 M $CaCl_2$ were added.

150 µl of *E.coli* BL21(DE3)RIL strain (Novagen) were transformed by 2 µl of the expression vector pET24a coding the relevant HIV-1 PR sequence. The transformation was carried out as described in chapter 5.1.6. The expression of ^{15}N labelled HIV-1 proteases was proceeded as follows: the culture of transformed cells was grown in 3 liters of sterile minimal media (M9) supplemented with kanamycin (40 µg/ml) in rotary incubator (Innova 4300, New Brunswick Scientific) at 37°C and 220 rpm. The growth of bacteria was checked by measuring of OD_{595}. When reaching the value of approximately 0.8, the expression was induced by the addition of IPTG to a final concentration of 0.75 mM. After 3 hours of incubation, bacterias were held at 4°C overnight. Cell suspension was then peleted by centrifugation (6000g, 10 min, 10°C).

5.2.1.2 Expression of 6xHis-tagged HIV-1 protease

Culture medium:

LB media: 60 g of LB- Broth (Sigma) were dissolved in 3 liters of distilled water. The solution was sterilized by autoclaving at 121°C for 15 min.

150 µl of *E.coli* BL21(DE3)RIL strain (Novagen) were transformed by 2 µl of expression vector pET16b or pET28b containing the relevant 6x-His-tag HIV-1 protease coding sequence and harboring resistance to ampicilin, as well. The transformation and expression were performed as described in chapters 5.1.6. and 5.2.1.1., respectively. The cell culture was grown in 3 liters of LB media supplemented with ampicilin (100 µg/ml). The MUT protease variant was expressed using the same protocol as described here.

5.2.1.3 Expression of Avi-tagged HIV-1 protease

Culture medium:

LB media: 60 g LB- Broth (Sigma) were dissolved in 3 liters of distilled water. The solution was sterilized by autoclaving at 121°C for 15 min.

150 µl of *E.coli* BL21(DE3)RIL strain (Novagen) were transformed by 2 µl of the expression vector pET24a containing the relevant Avi-tag HIV-1 protease coding sequence and by 1.5 µl of the expression vector pACYC with BirA ligase encoded (AVIDITY, L.L.C.). Expression vectors with Avi-tag HIV-1 proteases were prepared by Dr. Milan Kožíšek in laboratory of Jan Konvalinka (IOCB AS CR). The transformation was carried out as described in chapter 5.1.6., with both recombinant plasmids simultaneously.

The co-expression of both BirA ligase and relevant Avi-tagged HIV-1 protease was carried out as follows: The transformed cells were grown in 3 litres of sterile LB media supplemented with kanamycin and chloramphenicol (40 µg/ml and 34 µg/ml, respectively), in rotary incubator (Innova 4300, New Brunswick Scientific) at 37°C and 220 rpm. The growth of bacteria was checked by measuring of OD_{595}. When it reached approximately 0.5, D-biotin was added to a final concentration of 50µM and culture was grown at 20°C and 220 rpm. Temperature was lowered in order to enhance the

expession of soluble HIV PR at the expends of the inclusion bodies and thus to enable BirA ligase to biotinylate its Avi-tagged substrate). In OD_{595} value 0.8, the co-expression of Avi-tagged HIV-1 protease and BirA ligase was induced by addition of IPTG to a final concentration of 0.75 mM. After additional 3 hours of incubation, bacterias were held at 4°C overnight. Cell suspension was then peleted by centrifugation (6000g, 10 min, 10°C).

5.2.2 Isolation of inclusion bodies

Buffers:

buffer A: 50 mM Tris-HCl; 50 mM NaCl; 1 mM EDTA; pH 8.0

buffer SA: 50 mM Tris-HCl; 1 mM NaCl; 1 mM EDTA; pH 8.0

buffer TA: 50 mM Tris-HCl; 1 % (v/v) Triton X100; 1 mM EDTA; pH 8.0

Relevant HIV-1 protease variants were expressed in a form of inclusion bodies, at all cases. Their isolation and washing were carried out as follows. The bacterial pelet was suspended in 100 ml of buffer A (10 ml per 1 g of wet pellet) and the suspension was freezed and thawed three-times. To lyse the cells and to protect the expressed protein against host serine proteases, 5 ml of 1% (w/v) sodium deoxycholate and 290 µl of 10 mM phenylmethylsulfonyl fluoride were added and the mixture was stirred for 20 min at room temperature. Suspension was then sonicated on ice by 2 min pulses approximately 3 times (Soniprep 150) and centrifuged (15300g, 10 min, 4°C). The weighted pellet was resuspended in buffer SA (10 ml per 1 g) and solution was sonicated and centrifuged as previously described. The same procedure was repeated also with buffer TA and again with buffer A. The Isolation and purification procedures of the inclusion bodies were monitored by SDS PAGE (chapter 4.4.2.). The pellet of the inclusion bodies that contained mainly HIV-1 protease was used for renaturation.

5.2.3 HIV-1 PR renaturation

Buffers:

Dialysis buffer: 50 mM MES; 1mM EDTA; 10 % glycerol; 0.1% 2- mercaptoethanol; pH 5,8

The pellet of isolated and purified inclusion bodies was solubilized in 67 % (v/v) acetic acid. HIV-1 protease was then refolded by rapid dilusion into 25-fold volume excess of water. The solution was stirred at 4°C for 30 min, dialysed for 2 hours at 4°C against water and then against dialysis buffer overnight. Dialysate was further used for purification.

5.3 Purification of HIV-1 protease

5.3.1 Ion exchange chromatography

Buffers:

buffer A (pH 5.8): 50 mM MES; 10 % glycerol; 1 mM EDTA; 0.05 % 2-mercaptoethanol

buffer B (pH 6.7): 50 mM MES; 10 % glycerol; 1 mM EDTA; 0.05% 2-mercaptoethanol; 2 M NaCl

Solution containing mostly active HIV-1 protease was centrifuged (15300g, 15min, 4°C) filtered and purified on cation exchange MonoS HR10/10 column (Pharmacia) using FPLC ÄKTA Explorer (Amershan Pharmacia Biotech, Sweden). The column was equilibrated with buffer A, before use. After sample application, HIV-1 protease was eluted by linear gradient of ionic strength ranging from 0 to 40 % buffer B. Chromatography was monitored by online measurement of absorbance at 280 nm. The peak fractions were analysed for protein concentration (chapter 5.4.1) and protease activity (chapter 5.5.1) and purity by SDS-PAGE (chapter 5.4.2).

5.3.2 Gel permeation chromatography

Isolated and purified inclusion bodies that contained inactive HIV-1 protease were solubilized in 50% (v/v) acetic acid. The suspension was then centrifuged (6000g, 5min, 15°C) and filtered. Final volume of 25 ml of the supernatant was applied on Superdex 75 column (GE Healthcare) in 5 rounds of chromatography. The course of purification was monitored by measurement of absorbance at 280 nm and peak fractions were subsequently analysed by SDS PAGE (chapter 5.4.2). Fractions from all rounds that contained purified inactive HIV-1 protease were joined, protein concentration was checked (chapter 5.4.1), they were refolded (chapter 5.2.3) and used for further studies.

5.3.3 Metal-chelate affinity chromatography under denaturing conditions

Solutions and other material:

Solution A:	8 M urea; 20 mM imidazole
Solution B:	8 M urea; 250 mM imidazole
Resin:	50 % nickel- nitrilotriacetic acid resin suspension in 30% ethanol (Ni-NTA Superflow)

5 ml of Ni-NTA Superflow were added into the plastic disposable column (Pierce). Ni-NTA resin was washed and equilibrated with ml of solution A. Isolated inclusion bodies, containing denatured His-tagged HIV-1 protease were solubilized in 80 ml of solution AB, stirred overnight and then the mixture was centrifuged (6000g, 10 min, 25°C). After supernatant application, prepared Ni-NTA Superflow column was washed again with solution A. His-tagged HIV-1 protease was then eluted by 250 mM imidazole (solution B) and collected in 4 ml fractions. 400 µl of each fraction were dialysed against sterile water and were screened for protein concentration (chapter 5.4.1). The presence of His-tagged HIV-1 protease was checked by SDS PAGE (chapter 5.4.2). Fractions that contained purified PR were joined and diluted in 25-fold volume excess of sterile water. After that, HIV-1 protease was precipitated from the solution by

50 % saturation of ammonium sulphate and centrifuged (14000g, 15 min, 4°C). The pellet containing purified His-tagged HIV-1 protease was solubilized in 67 % (v/v) acetic acid and refolded (chapter 5.2.3). Active protease variant was then concentrated in centrifugal device with 10000 MWCO (Millipore, USA).

5.3.4 Small-scale purification via Avi-tag

Buffers and other material:

Buffer A:	A1: 50 mM sodium acetate; pH 4.7 A2: 50 mM sodium acetate; 150 mM NaCl; pH 4.7 A3: 50 mM MES; pH 5.8 A4: 50 mM MES; 150 mM NaCl; pH 5.8 A5: 50 mM MOPS; pH 7.0 A6: 50 mM MOPS; 150 mM NaCl; pH 7.0
Buffer B:	100mM MES; 150mM NaCl; 2mM D-biotin; pH 5.8
Buffer C:	50 mM MES, pH 5.8
Resin:	Streptavidin Mutein Matrix (ROCHE)

15 ml of renatured Avi-tagged HIV-1 PR (Avi PR) was dialysed against appropriate buffer A at 4°C, overnight. Afterwards, 100 µl of resin slurry (50% suspension in ethanol) was cleared with 500 µl of buffer A. The mixture was centrifuged (470g, 3 min, 4°C, Megafuge 2.0R, Hereaus Instruments), the supernatant was removed and resin was suspended in another 500 µl of buffer A. The pre-cleaning procedure was repeated three times.

Avi PR was then slowly mixed with pre-cleared resin and incubated for 4 hours, at 4°C, while stirring. Then, suspension was poured to the disposable gravity-flow column and flow-through fraction was collected. Sample before incubation (F0) and flow-through sample (FT) were taken for SDS-PAGE. After that, mutein matrix with bound Avi PR was washed three times by two, three and again three column volumes of buffer A. Samples (W1-W3) were taken for SDS-PAGE.

Biotinylated Avi-tagged HIV-1 PR (b-Avi PR) was eluted by 2 mM D-biotin. The elution proceeded as follows: First, one column volume of buffer B was applied

and the flow was stopped for one-hour incubation (F1 elution fraction). Then, two, another two and three column volumes of buffer B were applied to get elution fractions (F2-F4 elution fractions). Elution fractions were checked for protein concentration (chapter 4.4.1.) and protease activity was measured using spectrophotometric assay (chapter 4.5.). Fractions containing active b-Avi PR were dialysed against buffer C at 4°C, overnight to remove D-biotin. The progress of purification was analysed by SDS-PAGE (chapter 4.4.2.) and by western blotting (chapter 4.4.5.).

5.4 Protein manipulation

5.4.1 Bio-Rad assay- determination of protein concentration

Commassie blue G-250 solution (Bio-Rad): 100 mg Commassie brilliant blue G-250; 50 ml of 96 % ethanol; 100 ml of 85 % phosphoric acid; 850 ml of sterile water.

Concentration of proteins in particular fractions was determined according to Bradford [149] by measuring absorbance at 595 nm of a complex of proteins with Coomassie Brilliant Blue G-250 solution. Human serum albumine was used as a standard.

5.4.2 Sodium dodecyl sulfate- polyacrylamide gel electrophpresis (SDS-PAGE)

Solutions:

Sample buffer (6x):	0.42 g Tris; 3 ml glycerol; 1 g SDS; 600 µl 2-merkaptoethanol; 1.2 mg bromfenol blue; water to 10 ml; pH 6.8
Electrode buffer:	25 mM Tris, 250 mM glycin, 0.1% (w/v) SDS
44 % acrylamide solution:	42.8 g acrylamide; 1.2 g N,N´- methylenbisacrylamide; water to 100 ml

Table 2: The composition of 5 % stacking and 18 % resolving gels:

	1 8% resolving gel	**5 % stacking gel**
Component	Volume	
Water	*2.21 ml*	*2.6 ml*
1.5 M Tris-HCl	*2.5 ml (pH 8.8)*	*1.25 ml (pH 6.8)*
44 % acrylamide	*4.09 ml*	*570 µl*
50 % (v/v) ethanol	*1 ml*	*500 µl*
0.2 M EDTA	*70 µl*	*35 µl*
10 % (w/v) SDS	*100 µl*	*50 µl*
TEMED	*10 µl*	*10 µl*
10 % (w/v) APS	*90 µl*	*100 µl*

The analysis of the sample protein composition was carried out by vertical protein (Amersham Bioscience). Samples were mixed with sample buffer in the ratio of 5:1 and were denaturated by boiling for 5 min. Electrophoresis proceeded in a constant voltage of 140 V for 1.5 hour. To determine molecular weight of separated proteins, commercial standards Protein test mixture 4+5 (Serva) and All blue (BIO-RAD) and HIV-1 protease standard were used. The separated proteins in the gel were then visualised by silver (chapter 5.4.3) or Coomassie (chapter 5.4.4) staining. Western blotting (chapter 5.4.5) was carried out to detect the relevant tag fused to the protease.

5.4.3 Silver staining of proteins on polyacrylamide gel

Separated proteins were silver stained as described in Table 3:

Table 3:

step	**solution**	**time**
1	12 % (v/v) acetic acid, 50 % (v/v) methanol, 0.02 % (v/v) formaledehyde	*At least 30 min*
2	50 % (v/v) methanol	*3 x 15 min*
3	$Na_2S_2O_3$. $5H_2O$ (0.2 g/l)	*1 min*
4	sterile water	*3 x 20 s*
5	$AgNO_3$ (2 g/l), 0.02 % (v/v) formaldehyde	*20 min*
6	sterile water	*3 x 20 s*
7	Na_2CO_3 (60 g/l), $Na_2S_2O_3.5H_2O$ (4 mg/l), 0.02 % (v/v) formaldehyde	*Until elfogram is developed*
8	sterile water	*3 x 20 s*
9	12 % (v/v) acetic acid, 50 % (v/v) methanol	*10 min*
10	10 % (v/v) acetic acid	*overnight*

5.4.4 Coomassie staining of proteins on polyacrylamide gel

Solutions:

CBB-R 250 staining solution: 0.5 % (w/v) Coomassie Brilliant Blue-R 250, 50 % (v/v) methanol; 10 % (v/v) acetic acid

10% (v/v) acetic acid

Separated proteins were stained with CBB-R 250 staining solution for 10 min and destained by washing the gel in 10 % (v/v) acetic acid for several times. All gels were scanned.

5.4.5 Western blotting using chemoluminiscence substrates

Solutions:

Blotting concentrate: 72.1 g glycine, 15.1 g Tris, water to the final volume of 500 ml

Blotting buffer: 10 ml blotting concentrate, 1 ml of 10 % (w/v) SDS, water to the final volume of 80 ml, and afterwards, 20 ml of methanol were added

Polyacrylamide gel with separated proteins and nitrocelulose/ PVDF membrane were equilibrated in blotting buffer for 2 min (PVDF membrane in methanol and distilled water, at first) and together with pre-wetted filter paper sheets were placed on the anode of the transfer apparatus in following order (from anode to catode): 2 filter paper sheets, nitrocelulose membrane, polyacrylamide gel and 2 filter paper sheets at the top. The transfer apparatus was then assembled and connected to power supply (Bio-Rad). Proteins were electroblotted at constant voltage of 13V for 20 to 25 min. Afterwards, membrane was blocked in Blocker™ Casein in TBS, Thermo Scientific) for at least 1 hour at 4°C.

To visualise HIV-1 protease, the membrane was incubated with mouse monoclonal antibody IgG F11.1.3.11 (7 mg/ml) (2500x diluted in Blocker™ Casein in TBS, Thermo Scientific) at least 1 hour at 4°C and subsequently, secondary anti-mouse antibody conjugated with HRP (Thermo Scientific) was added (4000x diluted in Casein

blocker). Monoclonal anti-polyhistidine peroxidase conjugate (5000x, Clone HIS-1, Sigma-Aldrich) and Neutravidin HRP conjugate (2500x, Thermo Scientific) were used for visualization of His-tagged HIV-1 PR fraction and biotinylated fraction in case of Avi-tagged HIV-1 protease, respectively. In both cases, no secondary antibody was required.

Stable Peroxide Solution was mixed with Luminol/Enhancer Solution in 1:1 volume ratio (SuperSignal West Dura Chemoluminiscence Substrate, Pierce). Membrane was incubated in this mixture for 5 min and then dried between two filter paper sheets. The chemoluminiscence signal was detected using CCD camera LAS-3000 (Fujifilm).

5.4.6 Stability of prepared HIV-1 PR variants

5.4.6.1 N-terminal sequencing by Edman degradation

The sequences of degradation products of His- and Avi-tagged HIV-1 PR variants were analysed by protein microsequencing. Proteins (app. 1 μg per lane) were separated on SDS PAGE (chapter 5.4.2.), blotted to PVDF membrane (chapter 5.4.5.), stained with Coomassie and destained with the solution of 12% (v/v) acetic acid and 50% (v/v) methanol. The sequence of chosen bands was determined using Edman degradation at the N-terminus of the protein. All sequencing experiments were carried out by Zdeněk Voburka (IOCB AS CR).

5.4.6.2 Heteronuclear single-quantum correlation experiments (HSQC)

The proper fold of ^{15}N- labeled PR variants was determined from H, N-HSQC spectra. Proteases were concentrated using Amicon® Ultra Centrifugal Filter Units (10000 MWCO, Millipore) before measurement. NMR experiments were carried out by Dr. Lukáš Žídek (NCBR, Masaryk University in Brno) and by Dr. Miloš Buděšinský (IOCB AS CR).

5.5 Kinetic analyses

All kinetic parameters, as well as the activity of fractions after purification, were determined using a spectrophotometric assay with the chromogenic peptide substrate KARVNle*NphEANle-NH_2. The peptide was derived from CA-p2 cleavage site in Gag and Gag-Pol polyproteins. The decrease in absorbance at 305 nm was monitored upon the substrate cleavage of the scissile bond in 1 ml of the reaction mixture in 1 cm cuvettes using an UV/VIS spectrophotometer UNICAM UV 500 (Unicam, UK). Measurements were performed at 37°C in buffer containing 0,1M sodium acetate (pH 4.7), 4mM EDTA and 0.3M or 1M NaCl, respectively.

5.5.1 Determination of Michaelis-Menten constants

Buffers:

Buffer 1 for kinetics: 0.1 M sodium acetate; 1 M NaCl; 4 mM EDTA; pH 4.7

Buffer 2 for kinetics: 0.1 M sodium acetate; 0.3 M NaCl; 4 mM EDTA; pH 4.7

Michaelis constant K_m and catalytic efficiency k_{cat} of relevant HIV-1 PR variant were determined from the measurements of the initial rates (v_0) of substrate cleavage, in the presence of increasing substrate concentrations and constant enzyme concentration. The data were analyzed using the program Grafit 5.0.4 (Erithacus Software Limited) [150], which operates with Michaelis-Menten equation:

$$v_0 = \frac{V_{\max} \cdot [S]}{K_m + [S]}$$

where v_0 is the initial rate of the reaction, K_m is Michaelis constant, [S] is concentration of the substrate and V_{max} is limit reaction rate.

Catalytic efficiency k_{cat} is characterized as the rate of the substrate cleavage. It was calculated from the following equation:

$$k_{cat} = \frac{V_{\max}}{\varepsilon.[E]_0}$$

Concentration of the active enzyme $[E]_0$ was determined by titration of its active site by tight-binding inhibitor brecanavir [151]. The molar absorption coefficient ε was calculated from the change of the absorbance after total cleavage of the substrate for particular reaction condition at 305 nm.

5.5.2 Determination of the inhibition mode

Buffers:

Buffer 2 for kinetics: 0.1 M sodium acetate; 0.3 M NaCl; 4 mM EDTA; pH 4.7

The binding kinetics between mutated HIV-1 PR, its substrate and inbihitor darunavir in solution was determined by measurement of the initial reaction rates ($v_{0,i}$). The initial reaction rates were measured at different substrate concentrations and constant protease concentration. The curves were measuered at several inhibitor concentrations and visualised using double-reciprocal Lineweaver-Burk plot [152].

6. RESULTS

Recently, the thermodynamic characterization of interactions between mutated HIV-1 protease (MUT PR, for description see Table 1) and protease inhibitor darunavir performed by Dr. Milan Kožíšek (IOCB AS CR) suggested the alternative binding site for second darunavir molecule.

To study the mechanism of darunavir binding to MUT PR, several approaches were chosen including Nuclear Magnetic Resonance (NMR) and Surface Plasmon Resonance (SPR) methods as well as kinetic analysis using spectrophotometric assay. For these purposes, it was necessary to prepare isotopically labeled or tag-extended protease variants, respectively. The panel of eleven HIV-1 PR variants that were prepared within this diploma thesis is summarized in Table 7 and schematically shown in Fig. 11:

Table 7.: HIV-1 PR variants prepared within thisdiploma thesis:

HIV-1 PR variant	***Description***	***Purpose***
WT	Wild type of HIV-1 PR	DNA used for cloning
MUT	WT + L10I, L24I, L33F, M46L, I47A, I54V, L63P, A71V, V82A, I84V mutations	Kinetic analysis, HSQC experiment
inWT	WT + D25N mutation*	HSQC experiment
inMUT	MUT + D25N	HSQC experiment
C-His WT	WT + **6x-His-tag** at C-terminus	SPR kinetic studies
N-His WT	WT + 6x-His-tag at N-terminus	
C-His MUT	MUT + 6x-His-tag at C-terminus	
N-His MUT	MUT + 6x-His-tag at N-terminus	
C-Avi WT	WT + **Avi-tag** at C-terminus	
N-Avi WT	WT + Avi-tag at N-terminus	
C-Avi MUT	MUT + Avi-tag at C-terminus	
N-Avi MUT	MUT + Avi-tag at N-terminus	

** mutation in the active site, which inactivates the protease*

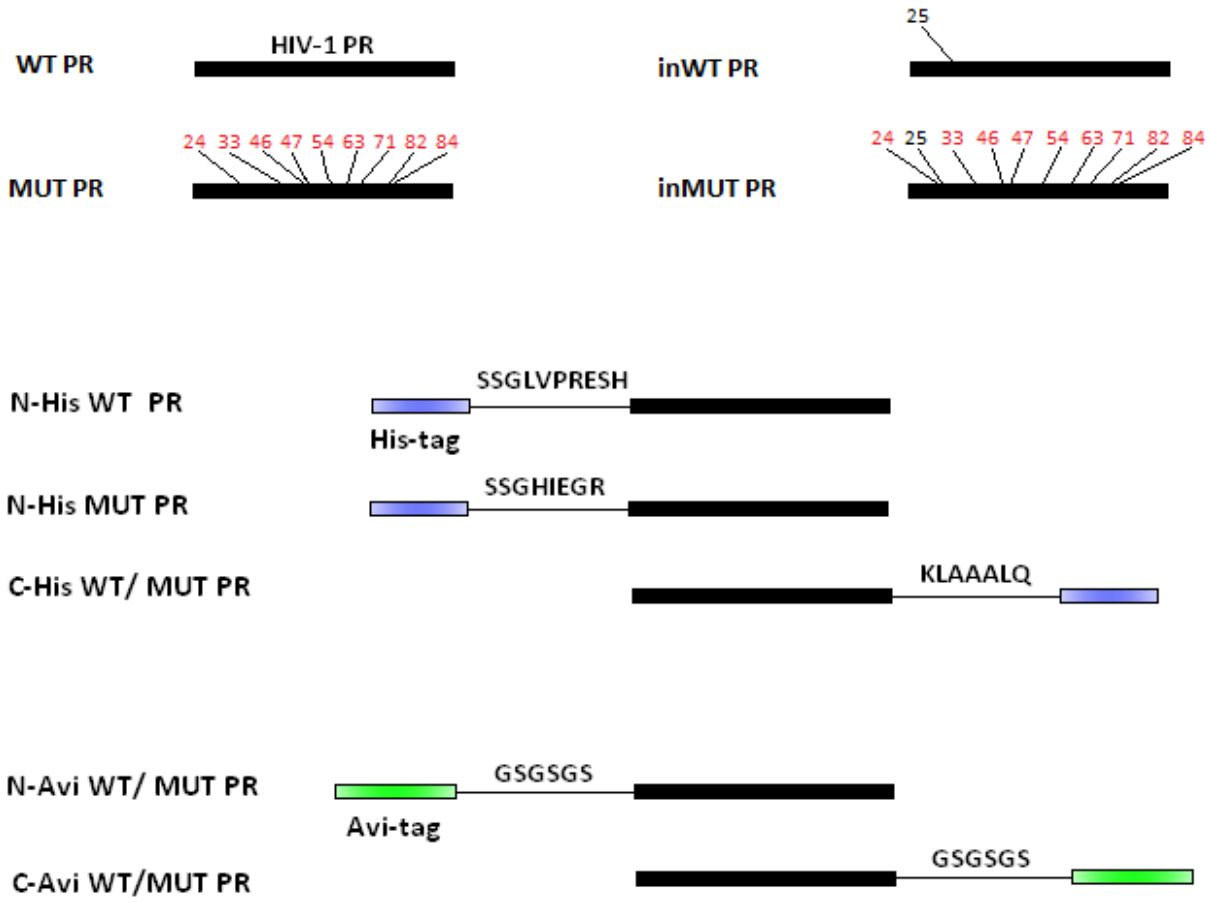

Figure 11: Scheme showing the panel of all prepared HIV-1 PR variants. Positions, where the mutations occur are indicated by numbers. His-tag (amino acid sequence: HHHHHH) and Avi-tag (GLNDIFEAQKIEWHE) are depicted in blue and green, respectively. Linker amino acid sequences are shown as black lines.

The wild-type and mutated HIV-1 proteases will be denoted **WT PR** and **MUT PR** through whole this thesis. Their tag-fused variants will be indicated, regarding the position and type of the tag, as **C-Avi**, **N-Avi**, **C-His** and **N-His WT** and **MUT PR**, respectively.

In the Results section, the preparation of DNA constructs for expression of isotopically labeled inactive MUT protease and four tag- extended (His-tag on both C- and N-termini) HIV-1 protease variants are described. Three isotopically labeled and eight tag-extended PR variants were expressed in bacteria, purified and enzymatically characterized. The influences of D25N mutation on activity of inactive PRs as well as the tag-extensions on activity and stability of tag-extended PR variants were studied.

Finally, the analysis of inhibitory mechanism measurements of MUT PR by darunavir using Michaelis- Menten kinetic model are shown.

6.1 Cloning of HIV-1 proteases

6.1.1 Preparation of inactive HIV-1 PR by site-directed mutagenesis

The DNA for expression of inactive MUT HIV-1 protease was prepared by site-directed mutagenesis. Template DNA coding for MUT PR was prepared by Klára Grantz-Šašková (IOCB AS CR). Primers for introduction of D25N mutation used for PCR reaction are described in chapter 4.1.8. PCR product was then incubated with *DpnI* restriction enzyme to digest template DNA. The result of mutagenesis was visualised by horizontal agarose gel electrophoresis (chapter 5.1.3.) and is shown in Fig. 12. Mutated DNA was verified by sequence analysis and used for bacterial expression of inMUT HIV-1 PR (chapter 5.2.1.)

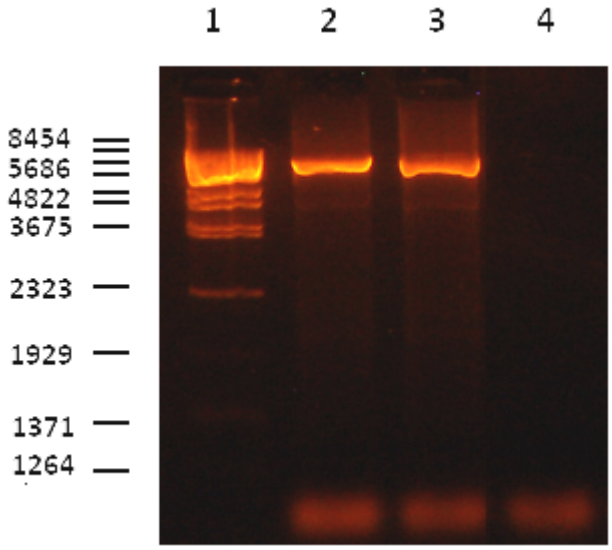

Figure 12: Horisontal agarose electrophoresis showing DNA product of site-directed mutagenesis coding for inactive MUT HIV-1 protease. *Lane 1*: λ DNA-*BstEII* Digest standard, *lane 2* and *3:* vector pET24a coding inMUT PR (two different concentrations of template DNA were used for mutagenesis reaction), *lane 4:* negative control (reaction without template DNA).

6.1.2 Cloning of His-tagged HIV-1 PRs

The expression vectors coding N- and C-His HIV-1 PR variants (WT and MUT) were prepared using the cloning procedure, which is illustrated in Fig. 13.

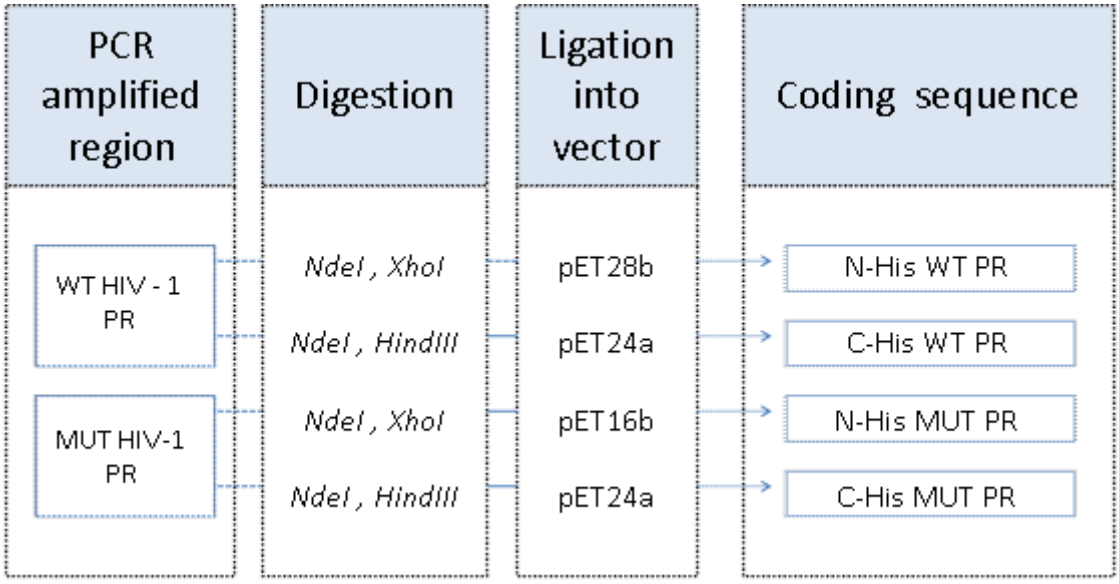

Figure 13: Scheme of the cloning procedure used for preparation of His-tagged protease variants.

Briefly, HIV-1 PR coding regions were amplified by PCR reaction, using two primers with cleavage sites for particular restriction endonucleases (chapter 5.1.1.). The results of PCR reactions were monitored on agarose gel and DNA products were isolated and purified. DNA products were ligated into the appropriate expression vectors coding 6x-His-tag to the N- or C-terminus of inserted sequence (chapters 5.1.4. and 5.1.5.). The results of ligation were controlled by horizontal agarose gel electrophoresis. Purified DNAs were used for transformation of competent bacterial cells- *E.coli* DH5α (chapter 5.1.6.) and plasmids were prepared using minipreparation protocol (chapter 5.1.7.).

The ligations were tested by control cleavage of the plasmid with restriction enzymes followed by visualization on agarose gel. Positive clones were verified by sequence analysis and used for expression of His-tag HIV-1 PR.

6.2 Expression of HIV-1 proteases

All protease variants were expressed in competent cells of *E.coli* BL21(DE3)RIL strain. Generally, the cell culture was cultivated in 3 litres of LB media or in minimal media containing $^{15}NH_4Cl$ in the presence of appropriate antibiotics, at 37°C (chapter 4.2.1.). The typical curve of bacterial growth is shown in Fig. 14. When OD_{595} reached approximately 0.8, the expression was initiated by IPTG addition to a final concentration of 0.75 mM (chapter 5.2.1). The Avi-tagged HIV-1 PRs were co-expressed with BirA ligase in LB media in the presence of 50 μM D-biotin, at 20°C as described in chapter 5.2.1.3. Expression vector coding Avi-tagged PR was prepared by Dr. Milan Kožíšek at IOCB AS CR.

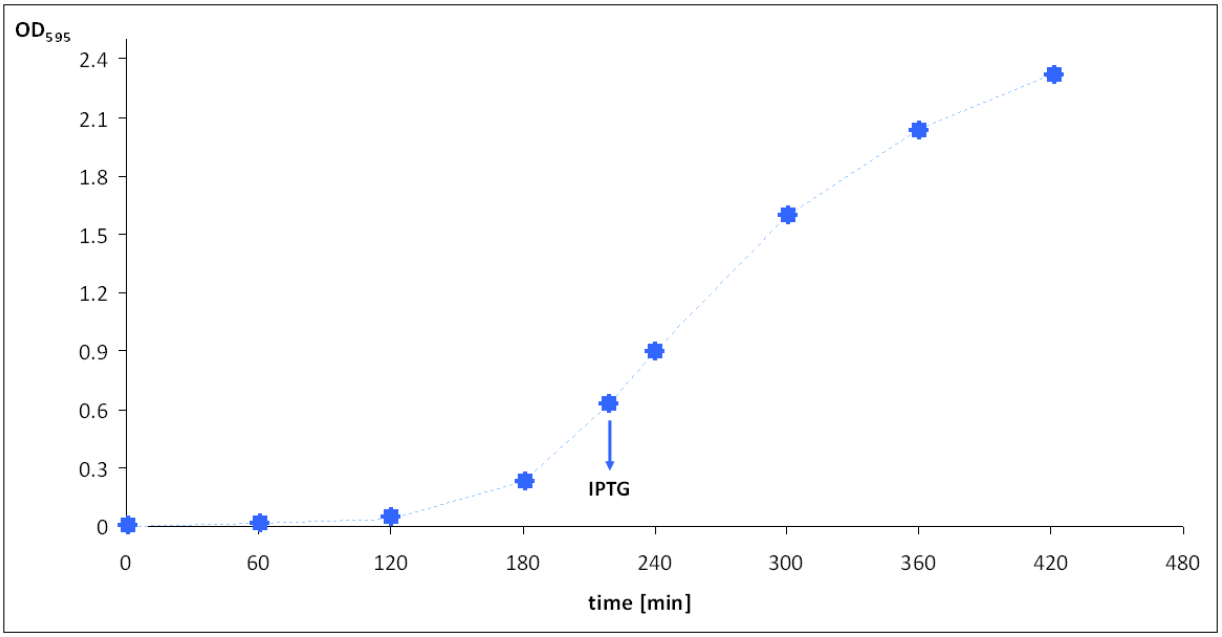

Figure 14: The typical growth curve of *E.coli* BL21(DE3)RIL transformed with HIV-1 PR expression vector. Induction with IPTG is marked.

Cells were harvested after overnight incubation at 4°C. The typical yield of wet bacterial biomass was about 3 g per liter of bacterial culture. In all cases, proteases were expressed in denatured state in inclusion bodies.

6.3 Isolation of HIV-1 proteases

Inclusion bodies containing denatured HIV-1 PR were isolated and washed in several steps using standard protocol, as described in chapter 5.2.2. Fig. 15 is showing SDS-PAGE monitoring a typical isolation and washing procedure. Moreover, the presence of tag-extended PR variants in inclusion bodies was checked also by western blotting (5.4.5). During the washing procedure, some host proteins were removed and isolated inclusion bodies contained large amount of partially purified HIV-1 PR. The yields were about 0.5 g of wet inclusion bodies per 1 liter of bacterial culture, typically.

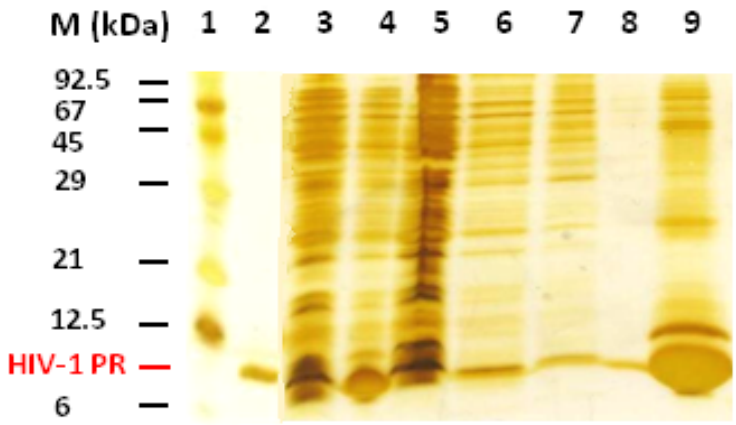

Figure 15: SDS-PAGE showing the procedure of isolation and washing of inclusion bodies containing MUT HIV-1 PR. *Lane 1*: molecular weight standard (6 µl); *lane 2:* HIV-1 PR standard (0.5 µg); *lane 3*: bacterial cells before induction (6 µl); *lane 4*: bacterial cells after induction (6 µl); *lane 5*: supernatant after cell lysis (6 µl); *lane 6*: supernatant after washing with buffer SA (6 µl); *lane 7*: supernatant after washing with buffer TA (6 µl); *lane 8*: supernatant after washing with buffer A (6 µl); *lane 9*: isolated inclusion bodies (6 µl). Proteins were separated on 18% polyacrylamide gel and silver stained (chapters 5.4.2 and 5.4.3).

Isolated inclusion bodies were then dissolved in 67% (v/v) acetic acid and HIV-1 protease was refolded by renaturation protocol described in chapter 5.2.3.

6.4 Purification of HIV-1 proteases

Mutated HIV-1 protease and its isotopically labelled form were purified by cation exchange chromatography. Inactive isotopically labelled HIV-1 proteases were purified by size-exclusion gel chromatography. Metal-chelate afinity chromatography and cation exchange chromagraphy were used for purification of His-tagged protease variants. Affinity chromatography via Streptavidin Mutein Matrix was employed in purification of Avi-tagged proteases.

Purification results for MUT PR (unlabeled form) and its inactive ^{15}N labelled variant (inMUT PR) are described in chapters 6.4.1 and 6.4.2. Since His- and Avi-tag extended HIV-1 PR variants have not been prepared before, it was necessary to optimize the conditions of purification. Therefore, the isolation and purification of C-His and C-Avi WT PRs are described in detail in chapters 6.4.3.1 and 6.4.3.2, respectively.

Finally, the purification results for all prepared HIV-1 protease variants (see Table 7) are summarized in chapter 6.4.4.

6.4.1 Mutated HIV-1 protease

Inclusion bodies containing mostly MUT PR were dissolved in 67% (v/v) acetic acid and HIV-1 protease was refolded by renaturation protocol described in chapter 5.2.3. Dialysate containing active protease was centrifuged (15000 g, 20 min, 4°C) and filtered through the 0.22 μm filter unit (Millipore) before it was loaded on MonoS HR10/100 column (Pharmacia) and purified by cation exchange FPLC. Protease was eluted by linear salt gradient from 0 to 40 % of buffer B (chapter 5.3.1.). The course of purification was detected by measurement of absorbance at 280 nm and is shown on chromatogram in Fig. 16. The presence and purity of HIV-1 protease in eluted fractions were analysed on SDS-PAGE (Fig. 17).

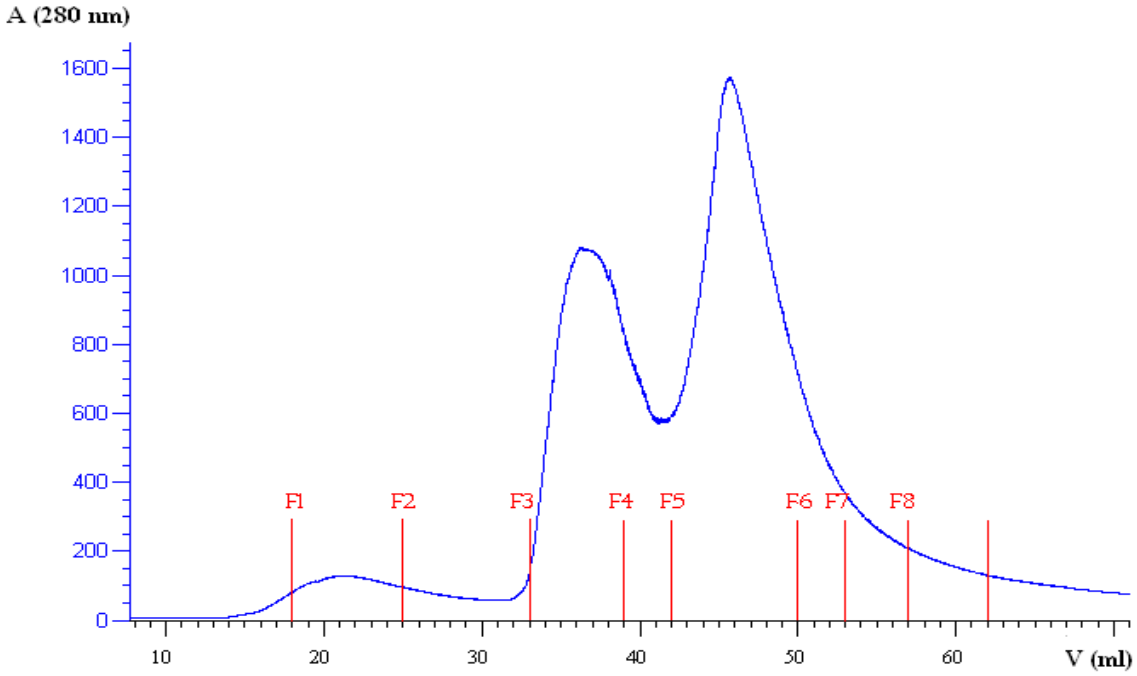

Figure 16: Purification of MUT PR by FPLC catex chromatography on MonoS HR10/100 column. Red lines indicate collected fractions.

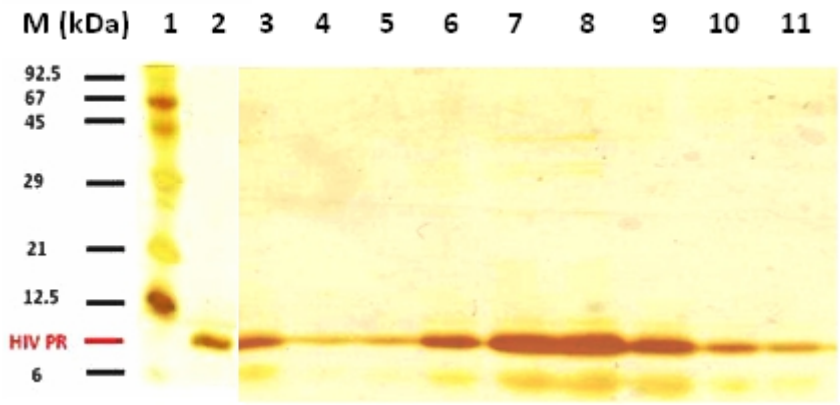

Figure 17: SDS-PAGE showing the purity of MUT HIV-1 PR in elution fractions collected during MUT PR purification. *Lane 1:* molecular weight standard (5 µl), lane 2: HIV-1 PR standard (5 µl), lane 3: Sample before cation exchange purification (2 µl), lane 4- 11: fractions F1- F8 (1 µl of each fraction).

Elution fractions were screened for protein concentration (according to Bradford, chapter 5.4.1.) and HIV-1 protease activity (chapter 5.5.). Very low activity was detected in fractions F1, F2 and F8. They were not included into evaluation of purification and overall yield. Fractions F3- F5 contained the most active and purest protein relatively to fraction before purification and they were used for further studies (kinetic analysis). The specific activities and purification coefficients as well as the

partial yields of active protease were calculated for each fraction. Relative activity unit (ru) was calculated for better illustration of PR activities on fractions. It was defined as the activity of protease that causes the decrease in absorbance of 10^{-4} AU. S^{-1} during the cleavage of chromogenic substrate (measured at standard conditions of 15 μM substrate, 37°C, pH 4.7). All of these results are summarized in Table 8.

Table 8: Table summarizing the purification of mutated HIV-1 PR by catex chromatography:

MUT HIV-1 PR	**purification table**						
	volume [ml]	**activity [AU.s^{-1}.μl^{-1}]**	**relative activity [ru]**	**yield [%]**	**protein conc. [μg.ml^{-1}]**	**specific activity [ru.μg^{-1}]**	**purification coefficient**
Prior purification	177	0.45 .10^{-5}	8000		520	0.09	1
F3	4	3.8 .10^{-5}	1500	19	2000	0.19	2.2
F4	2	3.5 .10^{-5}	700	9	2000	0.17	2.0
F5	5	6.5 .10^{-5}	3200	40	3000	0.22	2.5
F6	2.5	3.4 .10^{-5}	800	10	2400	0.14	1.6
F7	4	0.8 . 10^{-5}	300	4	1000	0.08	0.9
pooled	**17.5**			**82**			

The overall yield of pure and active MUT PR was 16 mg per 1 liter of bacterial culture. The purified protease preserved 82 % activity in comparison with the sample prior purification.

6.4.2 Inactive HIV-1 protease

1.3 g of isolated and washed inclusion bodies containing isotopically labelled inMUT PR were dissolved in 30 ml of 50 % (v/v) acetic acid. 25 ml of centrifuged and filtered solution was stepwised injected into the Superdex 75 column and purified under denaturing conditions (50 % (v/v) acetic acid, chapter 5.3.2). Fig. 18 shows the chromatogram (detection at 280 nm) and SDS-PAGE monitoring the purification process.

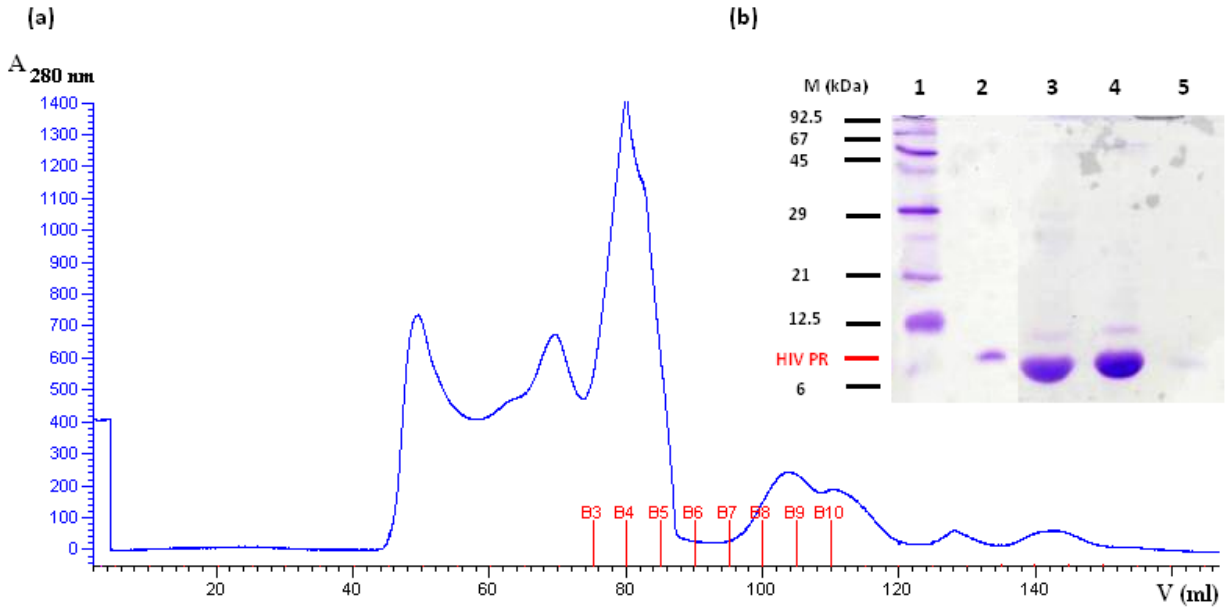

Figure 18: The purification of inactive mutated HIV-1 protease under denaturing conditions by gel permeation chromatography on FPLC using Superdex 75 column visualized by (a) chromatogram with fractions indicated by red lines and (b) electrophoretogram of fractions. (b) Lane 1: molecular weight standard (3.5 µl), lane 2: HIV-1 PR standard (3.5 µl), lane 3: fraction B3 (15 µl), lane 4: fraction B4 (15 µl), lane 5: fraction B5 (15 µl).

Collected fractions containing inMUT PR were joined and refolded using standard renaturation protocol and dialysed against 20 mM sodium acetate buffer, pH 4.7. Renatured inMUT PR was concentrated using Amicon Ultra-4 devices (10000 MWCO, Millipore) and stored for further NMR experiments. The overall yield of pure inactive protease after purification and renaturation was 10 mg per liter of bacterial culture.

The stability in solution at higher concentration that is required for protein NMR studies was tested. Protease was concentrated to a final concentration of 4.7 mg/ml (190 µM). Protein solubility was not changed even after four days at 25°C (data not shown).

6.4.3 Tagged HIV-1 proteases

Affinity tags are widely employed in biochemistry and molecular biology. Many different peptides or proteins of different sizes can be fused with the protein of interest, depending on the purpose for which this is used. Usually, the affinity tags are used to facilitate the detection, purification and also immobilization of the target protein

[153,154]. To study the mechanism of inhibitor binding to HIV-1 protease using surface plasmon resonance (SPR) technique, the panel of eight tag-fused HIV-1 PR variants was expressed and purified under this study, since the tag-extensions were important for oriented immobilization of the enzyme on the surface used for SPR. That would enable the access of ligands and inhibitors to the corresponding binding site(s). Either N- or C-terminal polyhistidine-tag (His-tag, comprising the amino acid sequence HHHHHH) or Avi-tag (comprising the sequence GLNDIFEAQKIEWHE), which are the two commonly used affinity tags, were fused to the monomer of HIV-1 protease. The sequence organization of all prepared tag-extended PR variants is schematically shown in Fig. 11.

6.4.3.1 Isolation and purification of C-His WT PR

Inclusion bodies were isolated using the standard protocol (chapter 5.2.2.). Washing procedure was monitored by SDS-PAGE and by western blotting (Fig. 20).

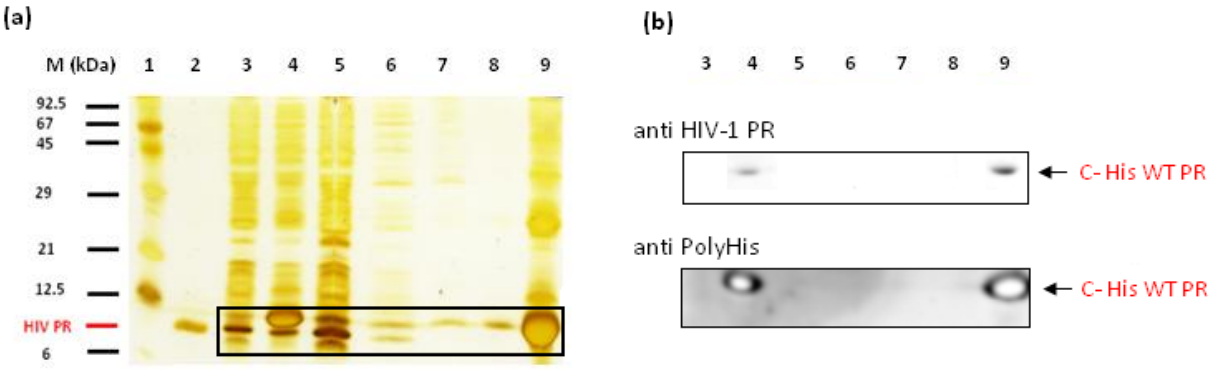

Figure 20: Isolation of inclusion bodies containing C-His WT PR. (a) SDS-PAGE and (b) Western blotting with using specific antibodies anti HIV-1 PR and 6xHis-tag. *Lane 1*: molecular weight standard (4 µl), *lane 2*: HIV-1 PR standard (5 µl), *lane 3*: bacterial cells before induction (8 µl); *lane 4*: bacterial cells after induction (6 µl); *lane 5*: supernatant after cell lysis (6 µl); *lane 6*: washing with buffer SA (6 µl); *lane 7*: washing with buffer TA (6 µl); *lane 8*: washing with buffer A (6 µl); *lane 9*: isolated inclusion bodies (6 µl). Proteins were separated on 18% polyacrylamide gel and (a) silver stained (chapters 4.4.2 and 4.4.3) or (b) electroblotted, respectively (chapter 4.4.5), using antibodies against Polyhistidine tag and HIV-1 protease.

Inclusion bodies were dissolved in 8M urea containing 20mM imidazole and applied onto disposable gravity-flow column filled with Ni-NTA resin. (chapter 5.3.3).

C-His WT PR was eluted by 250 mM imidazole. 0.5 ml samples of elution fractions were dialysed overnight against water using Slide-A-Lyzer® MINI Dialysis Units (MWCO 7000, Thermo Scinetific) to remove 8M urea. Protein concentration was then determined (chapter 5.4.1). The course of purification and purity of collected fractions were monitored by SDS-PAGE and western blotting (Fig. 21). Elution fractions containing C-His MUT PR (F1- F3, Fig. 20a) were joined, diluted in 25-fold excess of distilled water and precipitated by 50% saturated ammonium sulphate. The pellet was then solubilized in 67% (v/v) acetic acid and refolded by standard protocol (chapter 5.2.3). Renatured C-His MUT PR had very low proteolytic activity, probably due to ineffective refolding protocol.

Therefore, we decided to modify the purification and renaturation procedure. Protease was refolded from inclusion bodies (chapter 5.2.3.), dialysed against buffer A (see chapter 5.3.1, buffer without 10% glycerol and 1mM EDTA) and purified by cation exchange FPLC chromatography using MonoS HR10/10 column. PR was eluted by linear salt and pH gradient (chapter 5.3.1). The course of C-His WT PR purification was analysed by SDS-PAGE and by western blotting. Fig 20b is showing that the C-terminal His-tag is cleaved out during purification, since the intensities of anti-PolyHis antibody response decrease in each following fraction while the response of specific anti-(HIV-1 PR) antibody continually increase. The identity of the degradation products observed around 10 kDa were analysed by protein microsequencing (for results see chapter 6.6.3.). The protein concentrations, activities, specific activities and purification coefficients for eluted fractions are summarized in Table 9.

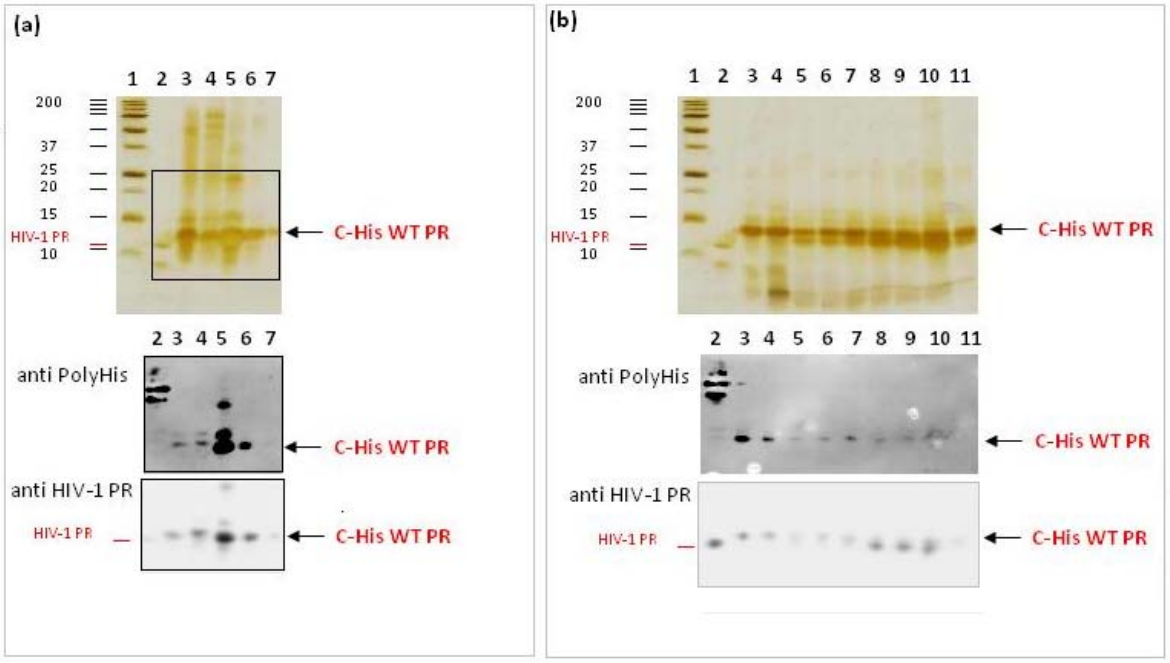

Figure 21: SDS-PAGE and western blot analysis representing the purity of C-His WT PR in fractions collected during (a) afinity purification using Ni-NTASuperflow column and (b) FPLC cation exchange chromatography using MonoS HR10/100 column. (a) *Lane 1*: Molecular Weight Standard (All blue, 4 µl), *lane 2*: 6x His-tagged standard (37 and 25 kDa) + HIV-1 PR standard (0.4 + 0.4 µg), *lane 3*: sample before purification (5 µl), *lane 4*: sample of flow-through fraction (5 µl), *lane 5-7*: fractions F1-F3 (all 10 µl). (b) *Lane 1*: molecular weight standard (All blue, 4 µl), *lane 2*: 6x His-tag standard + HIV-1 PR standard (80 +80 ng), *lane 3*: sample prior purification (10 µl), *lane 4-11*: fractions F1, F6-F12 (all 10 µl). The samples for western blotting were 5x diluted.

Table 9: Evaluation of C-His WT HIV-1 protease purification by catex chromatography:

C-His MUT HIV-1 PR	**purification table**						
	volume [ml]	**activity [AU.s^{-1}.µl^{-1}]**	**relative activity [ru]**	**yield [%]**	**protein conc. [µg.ml^{-1}]**	**specific activity [ru.µg^{-1}]**	**purification coefficient**
Sample before purification	140	0.2 .10^{-4}	30000		240	0.91	1
F1	2.0	0.2 .10^{-4}	470	2	220	1.1	1.2
F6	7.5	0.1 .10^{-4}	740	2	220	0.5	0.5
F7	7.0	0.1 .10^{-4}	630	2	240	0.4	0.4
F8	7.0	0.1 .10^{-4}	1000	3	230	0.6	0.7
F9	7.0	0.4 .10^{-4}	3100	10	230	2.0	2.2
F10	2.0	0.4 .10^{-4}	770	3	210	1.8	2.0
F11	6.5	0.8 .10^{-4}	5000	17	320	2.4	2.6
F12	6.5	0.3 .10^{-4}	1600	5	150	1.6	1.8
pooled	**31.5**			**44**			

The yield of active C-His WT PR after purification on catex column was 2 mg per liter of bacterial culture. SDS-PAGE as well as western blots in Fig. 5 show that some degradation products occurred during cation exchange purification. Their identity was analysed by protein microsequencing (for results see chapter 6.6.2.). Despite of the presence degradation product about 2-3 kDa, F1 fraction (Fig. 20b, lane 4) was further used for kinetic characterization.

6.4.3.2 Isolation and purification of C-Avi WT PR

Fig. 22 shows the SDS-PAGE and Western blotting analysis of the expression of biotinylated C-Avi WT PR and its isolation. Cells were cultivated in presence of 50 μM (Fig. 22, lane 4) and 400 μM D-biotin (lane 5), respectively. Co-expression of PR and BirA ligase was preformed as described in chapter 5.2.1.3. The western blot analysis showed that 8-fold molar access of D-biotin had no significant effect on biotinylation of C-Avi WT PR. However, the most of the biotinylated PR was expressed in inclusion bodies (lane 10), despite of the attempt to produce it in soluble form. Cell lysis supernatant contained only about 10% of biotinylated (22b, lane 5). The protease activity in cell lysis supernatant was not observed, probably due to the host protein contamination. The purification of the C-Avi WT PR from the cell lysis supernatant fraction via Streptavidin Mutein Matrix was ineffective (data not shown).

On the other hand, washed and isolated inclusion bodies contained probably both non-biotinylated and biotinylated (b) C-Avi WT PR. The yield of wet inclusion bodies was about 0.3 g per 1 liter of bacterial culture. Protease was renatured as described above (chapter 5.2.3.)

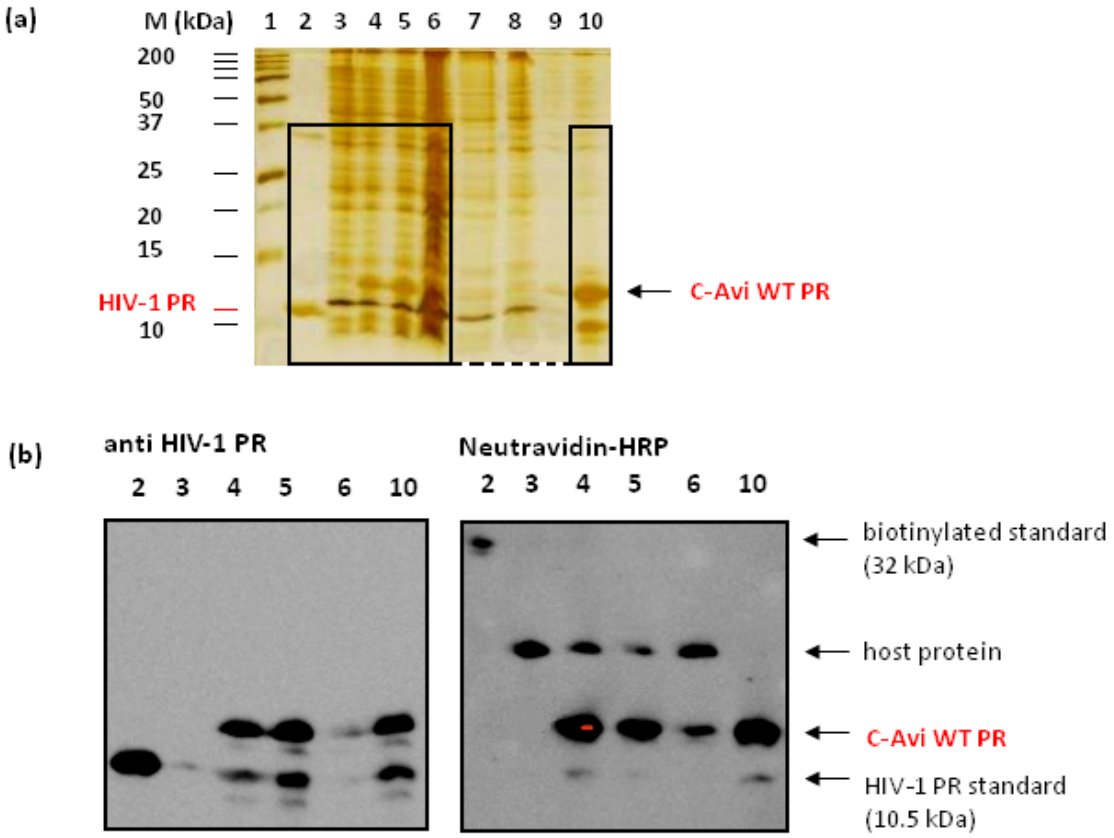

Figure 22: (a) SDS-PAGE and (b) western blotting showing the isolation and washing of inclusion bodies containing C-Avi WT PR. *Lane 1*: molecular weight standard All blue (4 µl); *lane 2*: HIV-1 PR standard + biotinylated standard (5+5 µl, 5x diluted in panel (b)), *lane 3*: bacterial cells before induction (3 µl, 20x diluted in (b)), *lane 4* and *5*: bacterial cells after induction in the presence of 50 and 400 µM D-biotin (3 µl and 3.8 µl, 10x diluted in (b)), *lane 6*: supernatant after cell lysis (6 µl, 20x diluted in (b)), *lane 7*: supernatant after washing by buffer SA (6µl), *lane 8*: supernatant after washing by buffer TA (6 µl), *lane 9*: supernatant after washing by buffer A (6 µl), *lane 10*: isolated inclusion bodies (6 µl, 20x diluted in (b)).

Commercially available Streptavidin Mutein Matrix (ROCHE) was used as a matrix for the affinity purification of C-Avi WT PR. To pull down the biotinylated fraction of the protease, it was necessary to optimize the purification protocol. The influence of ionic strength and pH of dialysis buffer on the interaction with the matrix were investigated (chapter 5.3.4.).

The course of one of the purification trials was monitored by SDS-PAGE and Western blotting and is shown in Fig. 23. Renatured protease was dialysed against buffer A2 (chapter 5.3.4.). Although the elution fractions as well as the fraction before purification and flow-through fraction were stained for protein concentration and protease activity (data not shown), none contained biotinylated C-Avi WT PR (Fig. 23b). The biotinylated PR probably precipitated during renaturation and consequent

dialysis. Almost all of the renatured protease precipitated during dialysis against buffers A5 and A6 (higher pH). The fraction before purification (Fig. 23a, lane 3) contained sufficient amount of active, non-degraded, but non-biotinylated C-Avi WT PR, which was pure enough. Moreover, some non-biotinylated PR was non-specifically on the mutein matrix after elution (Fig. 23, lane 9)

In order to increase the overall yield of WT and MUT avi-tagged proteases, but not biotinylated, the inclusion bodies were dissolved in 67% (v/v) acetic acid, proteases was renatured, dialysed against 50 mM MES buffer, pH 5.8 and kinetically characterized (see the chapter 6.6.3.). The facts that biotinylation probably does not influence protease activity and that the major part of both expressed Avi-tagged proteases (WT and MUT) is not biotinylated were taken into consideration.

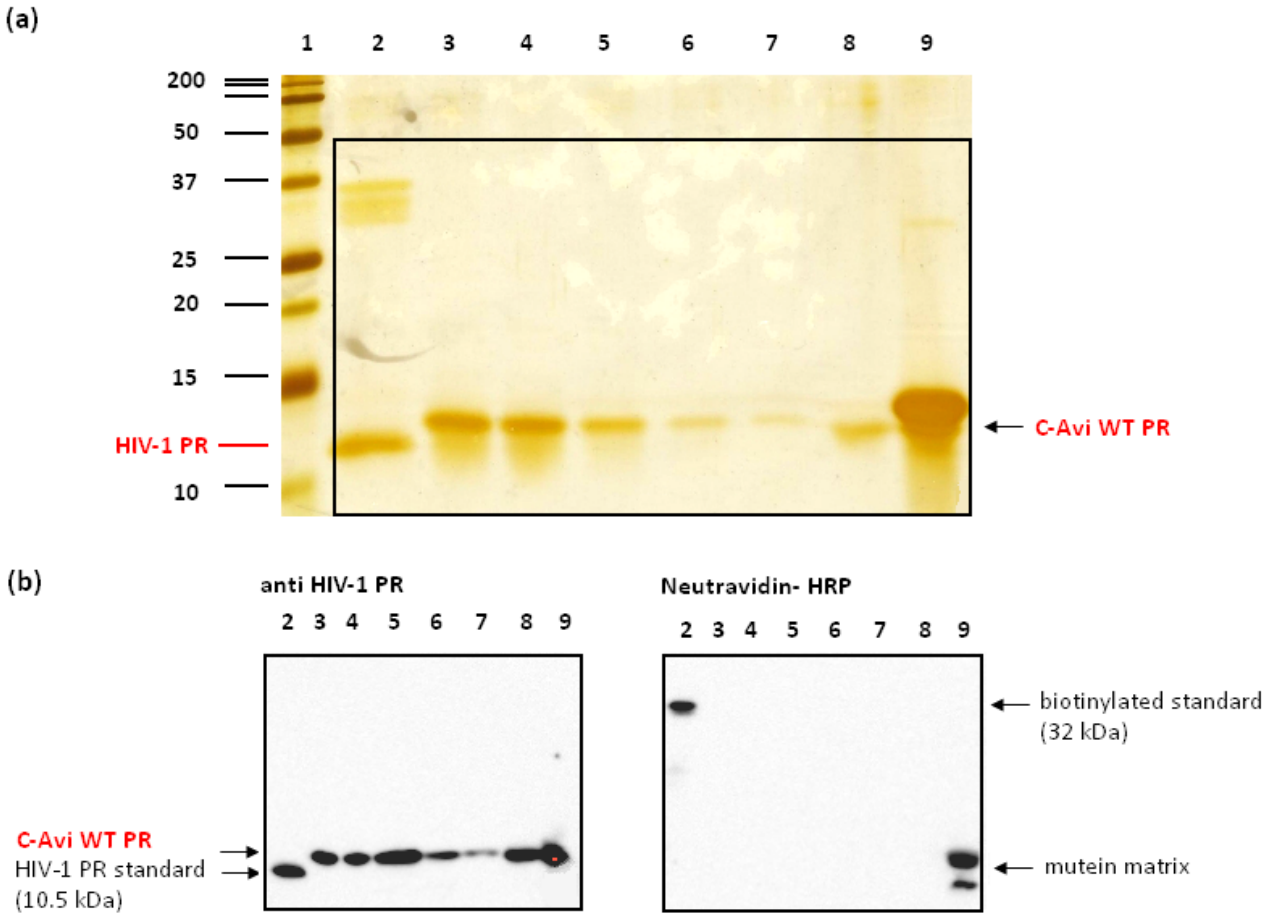

Figure 23: Small-scale purification of C-Avi WT PR via mutein. Lane 1: molecular weight standard (4 µl), lane 2: HIV-1 PR standard + biotinylated standard (5 + 5 µl, 5x and 20x diluted in panel (b)), lane 3: fraction before purification (12 µl), lane 4: flow-trough fraction (12 µl), lanes 5-7: samples after washing steps 1-3 (12 µl), lane 8: elution fraction E2 (12 µl), lane 9: sample of mutein matrix after elution and additional washing step (5 µl).

6.5 Overview of prepared HIV-1 PR variants

The purification results for all HIV-1 protease variants prepared within this thesis are summarized here. Fig. 24 represents the purity of these proteins and Table 10 shows their overall yields per liter of bacterial culture [mg] and yields of activity [%] of proteases after cation Exchange purification. Notably, all of the N-terminally extended PR variants except N-His WT, were not active (N-Avi WT, N-Avi MUT) or displayed very low proteolytic activity after purification (N-His MUT), respectively.

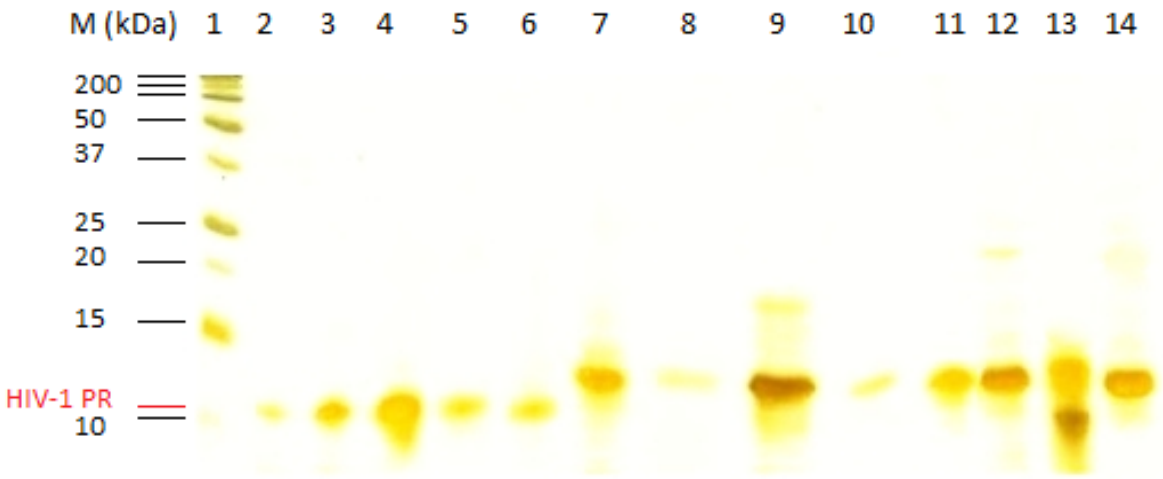

Figure 24: SDS-PAGE representing the panel of all prepared HIV-1 PR variants. *Lane 1*: molecular weight standard All blue (4 µl), *lane 2*: HIV-1 PR standard (0.5 µg), *lane 3*: MUT PR, *lane 4*: MUT PR (labelled), *lane 5*: inWT PR (labelled), *lane 6*: inMUT PR (labelled), *lane 7*: C-His WT PR, *lane 8*: N-His WT, *lane 9*: C-His MUT PR, *lane 10*: N-His MUT PR, *lane 11*: C-Avi WT PR, *lane 12*: N-Avi WT PR, *lane 13*: C-Avi MUT PR, *lane 14*: N-Avi MUT PR. 1 µg of protein was loaded in the gel, except from the N-His WT and N-His MUT PR in lanes 8 and 10 (0.5 µg).

Table 10: The overall yields of all prepared proteins:

HIV-1 PR variant	Purification method	Yield	
		[mg]	[%]
MUT	Catex (FPLC)	18	82
MUT (^{15}N labelled)	Catex (FPLC)	1.1	93
inWT (^{15}N labelled)	Gel permeation chrom.	1.5	
inMUT (^{15}N labelled)	Gel permeation chrom	2.2	
C-His WT	Catex (FPLC)	3.5	44
N-His WT	Catex (FPLC)	3.7	Low activity
C-His MUT	Catex (FPLC)	2	10
N-His MUT	Catex (FPLC)	0.2	No activity
C-Avi WT	Without purification	2.5	Not determined
N-Avi WT	Without purification	-	No activity
C-Avi MUT	Without purification	2.3	Not determined
N-Avi MUT	Without purification	-	No activity

In addition, the influences of D25N mutation and the tag extension on the stability and proteolytic activity of appropriate PR variants were investigated and are described in following chapters.

6.6 Stability of prepared HIV-1 PR variants

6.6.1 Determination of stability of isotopically labelled HIV-1 PRs

D25N mutation was introduced to the sequence of MUT and WT HIV-1 PR in order to prevent auto-proteolysis. It is the inevitable step in preparation of stable, highly- concentrated HIV-1 PR, which is to be studied by NMR techniques. However, it was necessary to determine its stability in solution.

Isotopically labelled inactive and active MUT PR variants were concentrated to 4.3 mg/ml and 3.1 mg/ml, respectively. The exact concentration of the protease in solution was calculated using molar extinction coefficient for inMUT PR (ε_{280} = 29392

$M^{-1}.cm^{-1}$) determined by quantitative amino-acid analysis performed by Radko Souček (IOCB AS CR). The active MUT PR was concentrated in presence of inhibitor saquinavir. Concentrating of inWT PR was not successful due to the rapid precipitation during that process.

To determine the stability of both MUT and inMUT PRs in solution, important for further NMR characterization, preliminary Heteronuclear single-quantum correlation (HSQC) experiments were performed by Dr. Lukáš Žídek (NCBR, Masaryk University, Brno) and by Dr. Miloš Buděšinský (IOCB AS CR), respectively. The chemical shifts in ^{1}H-^{15}N HSQC spectra indicated unfolded structures for both proteases (Fig. 25). In general, several unique regions of cross peaks that are well dispersed through whole two-dimensional map are characteristic for the typical 2D spectra of properly folded protein, denoting the interactions at the level of terciary structure. The cross peaks that were observed for both PRs indicated mostly unfolded structure. Likely explanation was probably due to the destabilizing effect of D25N on the folding process. The MUT PR containing active site Asp25 residues was auto-degraded during the concentrating step and subsequent NMR measurement (Fig. 26).

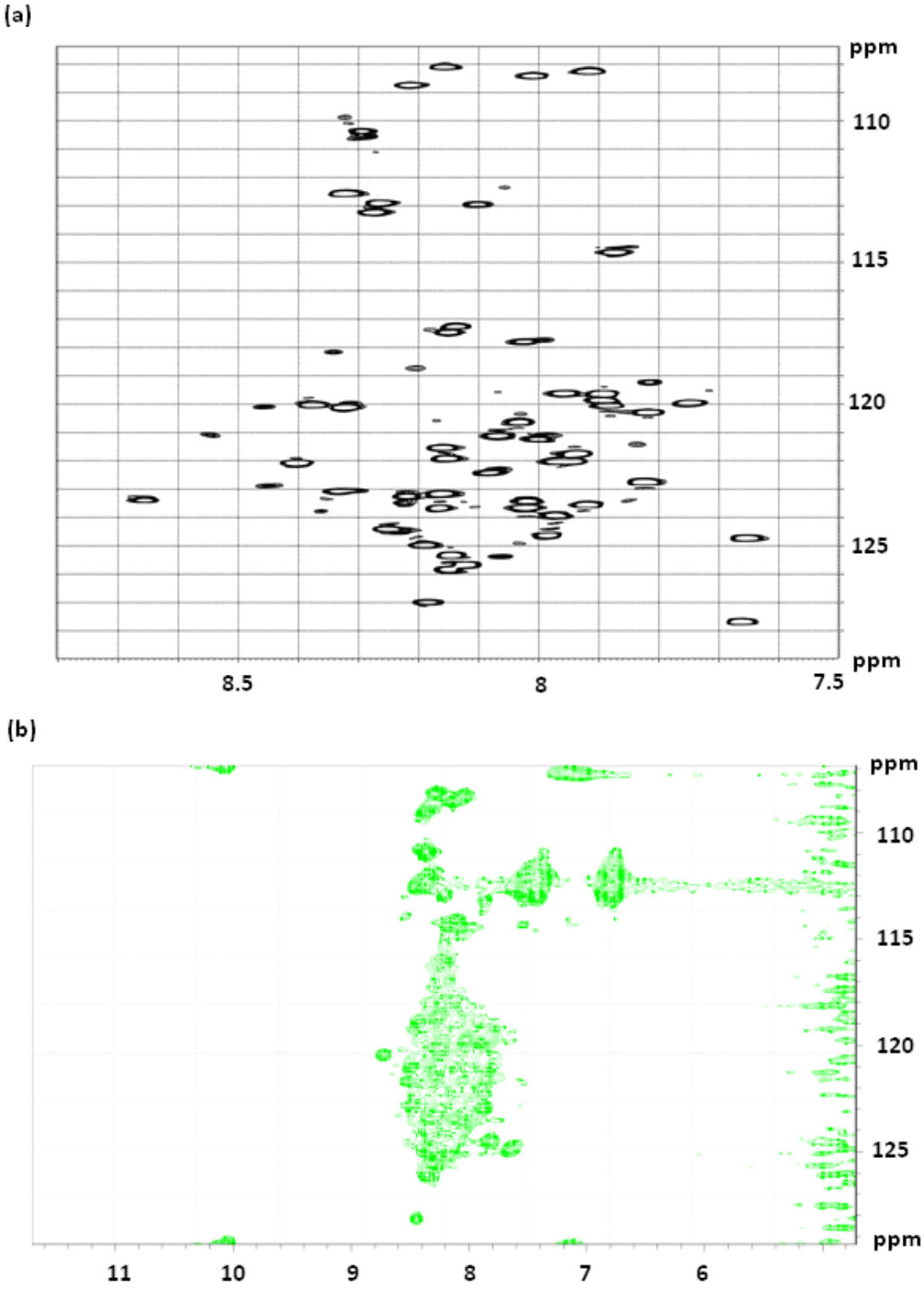

Figure 25: ^{1}H-^{15}N HSQC spectra of ^{15}N- labelled (a) inMUT and (b) MUT HIV-1 proteases in 20 mM sodium acetate buffer, pH 4.7. The cross peaks that are not well dispersed show mostly unfolded structure in both cases.

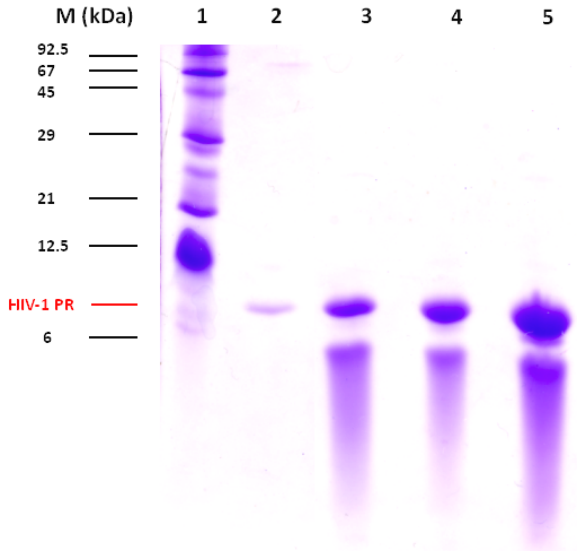

Figure 26: Auto-degradation of ^{15}N- labeled MUT PR during concentration step and NMR measurement. *Lane 1*: Molecular Weight Standard (4 µl), *lane 2*: HIV-1 PR Standard (4 µl), *lane 3*: sample taken during concentrating in presence of inhibitor (5 µl), *lane 4*: pellet of precipitated MUT PR after HSQC (5 µl), *lane 5:* MUT PR after HSQC.

6.6.2 Degradation of tagged HIV-1 PRs

Degradation products occured during purification procedures of C-His, N-His WT, C-His MUT and C-Avi MUT PR variants. Selected fractions (prior purification and/ or elution fraction) were separated on the SDS polyacrylamide gel and subsequently blotted on PVDF membrane, as described in chapter 4.4.6.1. The cleavage sites in tagged PR variants were determined by N-terminal sequencing using Edman degradation technique. All sequencing experiments were performed by Zdeněk Voburka (IOCB AS CR). The results are schematically shown in Fig. 27. The cleavage at position 33*34 (TVL*EEMNL, * denotes for scissile peptide bond) was observed for C-His and C-Avi MUT PR variants and also for N-His WT PR. The cleavage product that occurred during purification of C-His WT (Fig. 21b) comprised the N-terminal sequence of the "non-tagged" WT PR. However the cleavage site was not identified in this case.

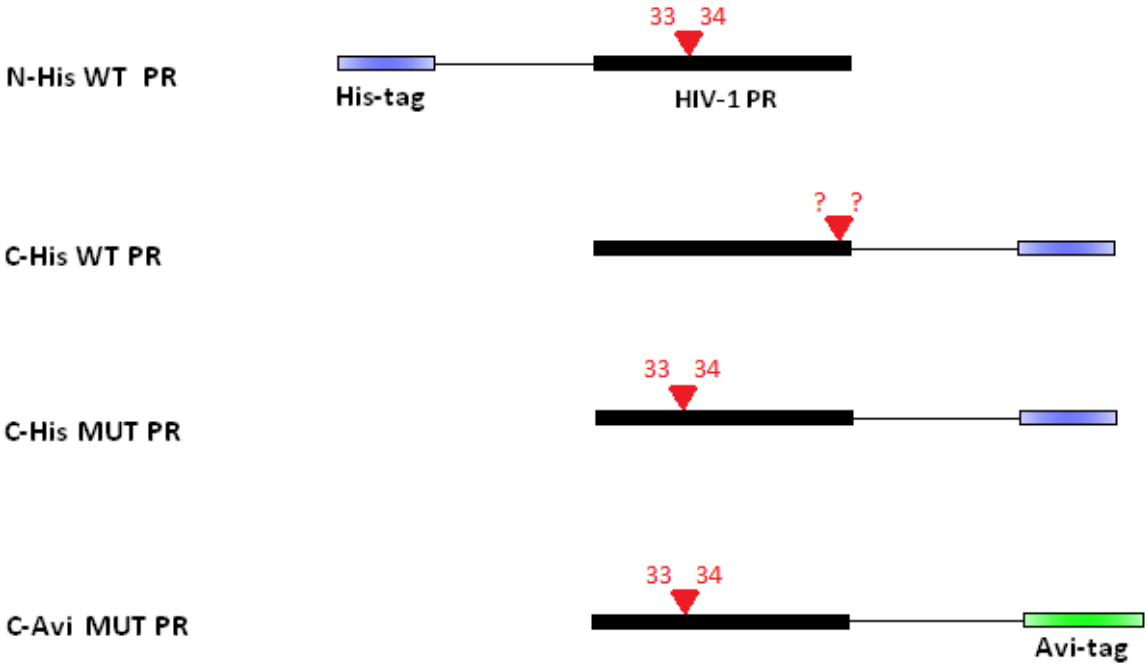

Figure 27: N-terminal sequencing of the degradation products detected during the purification of tag-extended PR variants N- and C-His WT, C-His MUT and C-Avi MUT. The positions of identified cleavage sites are indicated by red triangles. In all cases except one (C-His WT PR), the cleavage occurred between position 33 and 34 comprising the residues TVL/F*EEMNL (* denotes for scissile peptide bond). The cleavage site for C-His WT PR was not identified.

Chyba! Záložka není definována.Chyba! Záložka není definována.

6.6.3 The influence of the tag-extension on activity of HIV-1 PR

The values of Michaelis constants (K_m) and catalytic efficiencies (k_{cat}), measured for C-terminally tagged PR variants, as well as the reference values for WT and MUT proteases are summarized in Table 11. All kinetic measurements were performed using the chromogenic substrate Lys-Ala-Arg-Val-Nle~Nph-Glu-Ala-Nle-NH_2 in pH 4.7, in buffer containing higher salt concentration (chapter 5.5.)

The proteolytic activity of tagged PR variant, characterized by its affinity to the substrate molecule (K_m), as well as efficiency of the substrate‘s cleavage (k_{cat}) was influenced in negative manner in all cases, when compared to the relevant reference values (WT or MUT) and to those of the WT, respectively. The tag influences were most significant for C-Avi protease variants, since catalytic efficiencies decreased 5-times (C-Avi WT) or even 16- times (C-Avi MUT), when compared to relevant reference values. His-tag extension of WT PR caused the decrease of K_m value only slightly, and k_{cat} value to the half of that for WT reference.

Table 11: Values of Michaelis constants (K_m) and catalytic efficiencies for C-terminally tagged WT and MUT HIV-1 protease variants:

variant	K_m [µM]	k_{cat} [s^{-1}]	k_{cat}/K_m [$mM^{-1}.s^{-1}$]	$\frac{k_{cat}/K_m(\text{var})}{k_{cat}/K_m(wt)}$
WT	7 ± 1	18 ± 1	2700 ± 270	1.0
C-His WT	10 ± 1	11 ± 0.4	1100 ± 10	0.41
C-Avi WT	18 ± 2	9 ± 0.3	500 ± 50	0.19
MUT	47 ± 2	41 ± 1	900 ± 50	0.33
C-His MUT	66 ± 5	14 ± 2	200 ± 30	0.07
C-Avi MUT	83 ± 6	4 ± 0.2	50 ± 5	0.02

6.6.4 Kinetic analysis of MUT HIV-1 protease inhibition by darunavir

The mechanism of inhibition of MUT HIV-1 protease with darunavir (DRV) was determined by double reciprocal Lineweaver- Burk plot (Fig. 28). Measurements of inicial reaction rates were performed for five different concentrations of inhibitor (0; 1.7; 2.5; 3.4 and 4.2 nM) in the presence of 7 nM HIV-1 protease, at standard conditions (chapter 5.5.2.). Since the curves do not intersect at any axis, the mechanism was interpreted as that of mixed-type.

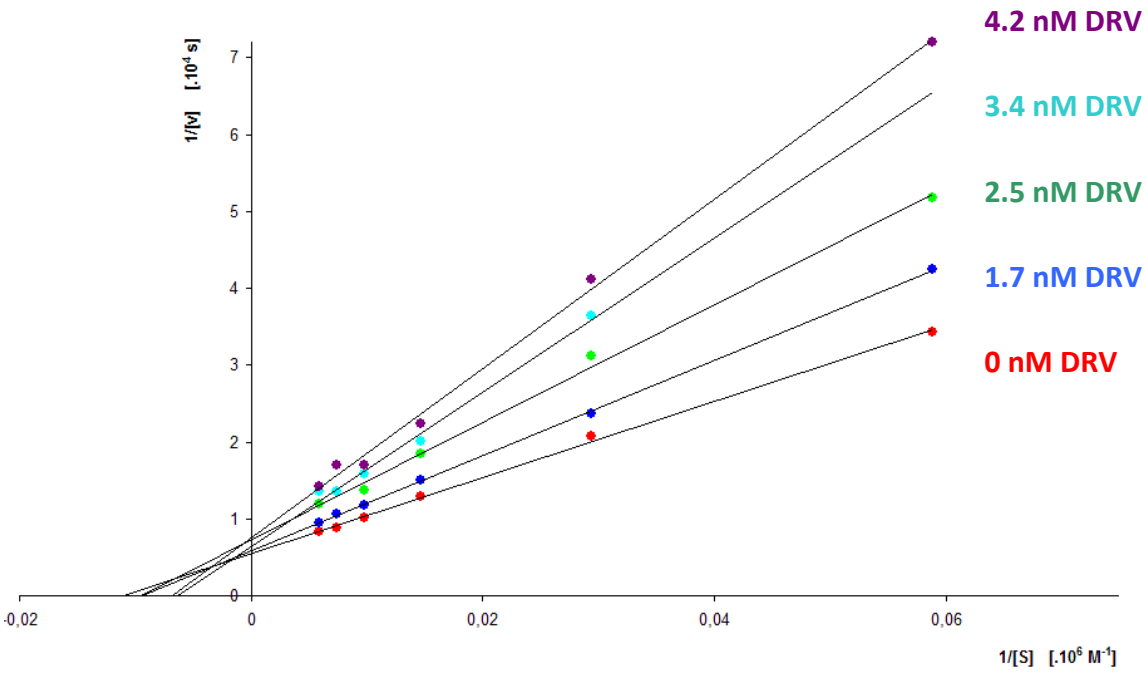

Figure 28: Double reciprocal Lineweaver- Burk plot representing the mechanism of MUT PR inhibition by darunavir.

7. DISCUSSION

The inhibition of HIV-1 protease plays an important role in combating HIV. Nine HIV-1 protease inhibitors have been succesfully marketed for the treatment since 1995. However, their efficiencies decrease due to the resistance development. More potent compounds with novel structural motifs and mechanisms of action are therefore still needed. Several inhibitory compounds have been reported to bind to the protease at the loci different from the active site.

Interestingly, darunavir, which is the last approved inhibitor with supposedly competitive mode of action, was also suggested to bind to the flap region of the protease (PR) molecule harboring single mutation V32I. Two studies discussed this alternative binding mode based on the X-ray structural and kinetic analysis, respectively. Nevertheless, it was questionable, if such a mechanism is relevant also in physiological conditions or if it is only an artifact of crystallization. Another study, performed in our laboratory, provided a strong evidence for the alternative binding of darunavir. Based on thermodynamic analysis, it was shown that two molecules of darunavir bind to the PR dimer. Surprisingly, this observation was not confirmed by the X-ray structure analysis since the inhibitor was bound only within the active site.

HIV-1 PR and Nuclear magnetic resonance (NMR). Multidimensional protein NMR method was chosen to prove the mechanism of inhibition of a mutated protease by darunavir. The experimental conditions for NMR measurement require, however, long-term protein stability at high sample concentration. Such measurements are quite difficult for HIV-1 PR since it is known to be poorly stable in higher concentrations and undergoes rapid autoproteolysis. To stabilize the protease and prevent it from degradation, three mutations at auto-cleavage sites (Q7K, L33I, L63I), two that prevent protease from thiol oxidation (C67A and C95A) and mutation D25N inactivating the enzyme, are typically introduced by mutagenesis. However, the mutated protease studied within this thesis contains ten mutations that decrease protease activity and stability by themselves. Therefore the introduction of additional mutations would probably change the protease properties. For this reason, only the mutation D25N was introduced by site-directed mutagenesis.

Preparation of HIV-1 proteases for NMR. Isotopically labeled mutated PR (MUT) and its inactive form (inMUT) as well as the inactive "wild-type" PR variant (inWT) were expressed in *E.coli* in minimal media containing $^{15}NH_4Cl$ as the only source of the nitrogen. All proteases were expressed in the form of insoluble inclusion bodies. Inactive variants were purified using gel permeation chromatography under denatured conditions. MUT protease was refolded and purified by cation exchange chromatography. The yield of purified active enzyme was slightly lower in comparison to that of the active one. The lower yields could be explained by the decreased level of recombinant protein expression of the protease in bacteria in the minimal media conditions. Only MUT and inMUT variants were prepared in concentrations that were sufficient for heteronuclear single-quantum correlation (HSQC) experiments, since it was not possible to concentrate the inWT PR. HSQC technique serves for the preliminary determination of the proper folding of the protein, before it is used for the NMR titration experiment including also the ligand. The organization of the experiment originally consisted of the titration of isotopically labeled protease with the inhibitor darunavir. The details of their interaction would have been further analysed by comparing of the changes in chemical shifts in the HSQC spectra of the darunavir-free and of the darunavir-bound protease and by subsequent determination of the residues that are close to the darunavir binding site. From the two-dimensional HSQC spectra for MUT and inMUT variants, it was obvious that both variants are present mostly in unfolded structures. sNegative effect of D25N mutation on the refolding process of inMUT variant and the auto-degradation of MUT protease variant during measurement may serve as a likely explanation. The autoprocessing of active MUT variant was also confirmed by SDS-PAGE. Consequently, these protease variants could not be used for further NMR titration studies.

HIV-1 protease and surface plasmon resonance (SPR). SPR technique was employed for investigation of the interaction kinetics between HIV-1 protease and its inhibitors by several authors. In that studies protease was immobilized to the surface of the sensor using amine coupling. Using the N- or C-terminally tag-fused protease variants that can be specifically attached to the surface of the sensor represents an alternative approach well aplicable for studying the inhibitory mechanisms of compounds that can bind to the sites outside of the protease active site. On the other hand the already published random immobilization of the protease through its free and

accessible amine groups could not be suitable for these purposes due to occupation of the alternative unexplored binding sites.

Preparation of tag-extended HIV-1 protease variants. The panel of eight tag-extended protease variants was expressed in *E.coli*: wild-type and mutated HIV-1 proteases with either N- and C-terminal His-tag or Avi-tag.

The purification of His-tagged WT and MUT variants using metal chelate affinity chromatography seemed to be effective, since the elution fraction contained relatively pure protease. However, the proteases were not active or they possessed very low activity when refolded after precipitation by 50% ammonium sulphate from solution containing 8M urea. That could be probably due to the ineffective refolding protocol or due to the intrinsic property of the tag-fused protease. To investigate the influence of the conditions of purification on their activity, refolded His-tagged proteases were purified by cation exchange chromatography. All His-tagged variants, except N-His MUT PR, were active after this purification procedure. Moreover, it was observed that these variants undergo autoproteolysis during the purification process.

Avi-tagged WT and MUT protease variants were co-expressed with BirA ligase in the presence of D-biotin in order to accomplish *in vivo* biotinylation of the target protein. The cultivation of bacteria ran at lower temperature in order to slow-down the production of the protease and to direct it preferably into soluble form and also to enable the biotinylation. However, avi-tagged WT and MUT variants were mostly present in insoluble incusion bodies. The western blotting analysis confirmed that a portion of the inclusion bodies contained also biotinylated protease. After the standard refolding procedure, only the C-terminally tagged proteases were active. Proteases were subsequently purified by affinity chromatography using mutein matrix. Even though the fractions prior and after purification as well as the eluted fractions contained relatively active protease, none of those, however, contained biotinylated variant. The refolded C-Avi MUT variant also contained some degradation product. Despite the fact that refolded C-Avi-tagged proteases contain mostly, if not only, the non-biotinylated form, they were used for their further enzymological characterization. The attempts to biotinylate these protease variants *in vitro* were unsuccessful as well. It was probably due to the low efficiency of biotin ligase under the conditions, where the protease is stable (data were not shown).

Influence of the tag-extension on the HIV-1 PR activity. Taken together with the His-tagged protease purification results, it is probable that N-terminal extension negatively affect the biological activity of HIV-1 protease (proteases were not active). The influence of C-terminal tag-extension on proteolytic activity was studied. The N-terminal sequencing of the degradation products of C- and N-His WT, C-His MUT and C-Avi MUT protease variants revealed that all of them, except of C-His WT, are cleaved between the amino acid residues Leu/Phe 33 and Glu 34. It is in good agreement with the data published in literature, which describe this site as one of the three major autoprocessing sites (Leu 5*Trp 6, Leu 33*Glu 34 and Leu 63*Ile 64) of the PR monomer. Cleavage site for C-His WT variant was not identified, since it was not possible to obtain the sufficient amount of the degradation product (about 2 kDa) that was necessary for the sequence analysis. The amino acid composition and length of the linker sequence probably do not affect the stability of tagged proteases, because C-Avi and C-His MUT variants comprising different linkers were both cleaved at the same position. Moreover, these data also indicate that C-terminal tag is not cleaved out. Furthermore, the truncated species are not active and, consequently, do not influence the kinetic analyses. Therefore, these variants could be further characterized.

Michaelis-Menten constants were determined using the spectrophotometric assay with chromogenic substrate. The most significant differences were observed for values obtained for non-biotinylated C-Avi-tagged variants, when compared with relevant values for WT and MUT proteases. The catalytic efficiency of C-Avi MUT variant decreased 20- times that was caused by the 2-fold increase of K_m value and even 10-fold decrease of k_{cat} value. Similar trend was observed for C-His tagged variants as well. It is obvious that the presence of the tag at the C-terminus of HIV-1 protease slightly decreases the affinity to the substrate (and probably also to the inhibitor) and it also negatively affects catalytic efficiency of the enzyme. It may happen due to the disruption of dimer formation or even by the blocking of the active site by the tag.

Since it is necessary to prepare stable sensor surface with protease for SPR, the stability of His-tag and Avi-tag-extended protease variants has to be optimized,. Several possibilities arise how to avoid the autodegradation, such as the further optimization of conditions for purification (changing the composition of the running buffers for chromatography- different pH, ionic strength, additives stabilizing the protease dimer). The refolding and purification in the presence of competitive inhibitor or preparation of

the protease with one of the autoproteolysis-protecting mutations that would stabilize the dimer may also lead to the stable, nondegraded tagged protease.

Mechanism of inhibition. The kinetics of binding between MUT PR and inhibitor darunavir were determined using double-reciprocal Lineweaver-Burk plot. Initial rates of substrate cleavage were measured at five different concentrations of darunavir. Since the curves did not intersect at any of the axis, the mixed-type of inhibitory mechanism was suggested for these conditions. It indicates indirectly that darunavir may also bind to the region different from that of the active site.

8. CONCLUSIONS

- To study the mechanism of the inhibitor darunavir binding to the highly mutated HIV-1 protease (L10I, L24I, L33F, M46L, I47A, I54V, L63P, A71V, V82A and I84V), nuclear magnetic resonance and surface plasmon resonance-based kinetic study were chosen. For this purpose, the panel of eleven recombinantly expressed HIV-1 protease variants was prepared within this thesis: ^{15}N labeled inactive (harboring mutation D25N) wild type (inWT) and mutated (inMUT) proteases, ^{15}N labeled and non-labeled forms of active mutated (MUT) protease, four C- and N-terminally His-tagged wild-type and mutated proteases (C-His WT and MUT, N-His WT and MUT) and four C- and N-terminally Avi-tagged proteases (C-Avi WT and MUT, N-Avi WT and MUT).

- Heteronuclear single-quantum correlation (HSQC) experiments provided the evidence for unfolded structures of ^{15}N labeled inMUT and MUT proteases. It is a consequence of the negative effect of D25N mutation on the stability of inMUT protease as well as the autoproteolysis of MUT protease during measurement.

- The influence of the tag-extension on the stability and activity of proteases was investigated. The autoprocessing site between residues Leu(Phe) 33 and Glu 34 of C-terminally tagged protease variants was identified using N-terminal sequence analysis of the degradation products. All four C-terminal tag-extended protease variants were kinetically characterized. The catalytic efficiency (k_{cat}/K_m) decreased in all cases.

- Using the spectrophotometric assay, the inhibitory mechanism for darunavir and mutated protease was interpreted as that of the mixed type, which is consistent with is consistent with an alternative binding site for the inhibitor outside the PR active site.

- This thesis represents a background for the analysis of various HIV-1 PR inhibitors binding to the regions outside protease active site

9. REFERENCES

1. Barré-Sinoussi, F., Chermann, J.C., Rey, F., Nugeyre, M.T., Chamaret, S., Gruest, J., Dauguet, C., Axler-Blin, C., Vézinet-Brun, F., Rouzioux, C., Rozenbaum, W., Montagnier, L. (1983) Isolation of a T-lymphotropic retrovirus from a patient at risk for acquired immune deficiency syndrome (AIDS). *Rev. Invest. Clin*. **56**, 126-129.
2. Gallo, R.C., Sarin, P.S., Gelmann, E.P., Robert-Guroff, M., Richardson, E., Kalyanaraman, V.S., Mann, D., Sidhu, G.D., Stahl, R.E., Zolla-Pazner, S., Leibowitch, J., Popovic, M. (1983) Isolation of human T-cell leukemia virus in acquired immune deficiency syndrome (AIDS). *Science*. **220**, 865-867.
3. UNAIDS and WHO AIDS epidemic update December 2009 URL: http://www.unaids.org/en/media/unaids/contentassets/dataimport/pub/report/2009/jc1700_epi_update_2009_en.pdf [Cited August 26, 2011].
4. Wain-Hobson, S., Sonigo, P., Danos, O., Cole, S., Alizon, M. (1985) Nucleotide sequence of the AIDS virus, LAV. *Cell*. **40**, 9-17.
5. Whittle, H., Morris, J., Todd, J., Corrah, T., Sabally, S., Bangali, J., Ngom, P.T., Rolfe, M., Wilkins, A. (1994) HIV-2-infected patients survive longer than HIV-1-infected patients. *AIDS*. **8**, 1617-1620.
6. McCutchan, F.E. (2000) Understanding the genetic diversity of HIV-1. *AIDS*. **14 Suppl 3**, S31-44.
7. Frankel, A.D., Young, J.A. (1998) HIV-1: fifteen proteins and an RNA. *Annu. Rev. Biochem*. **67**, 1-25.
8. ViralZone: Human immunodeficiency virus 1 URL: http://viralzone.expasy.org/all_by_protein/7.html [Cited August 26, 2011].
9. Alkhatib, G. (2009) The biology of CCR5 and CXCR4. *Curr Opin HIV AIDS*. **4**, 96-103.
10. Doms, R.W. (2000) Beyond receptor expression: the influence of receptor conformation, density, and affinity in HIV-1 infection. *Virology*. **276**, 229-237.
11. Tibotec BVBA 2010: HIV Life Cycle URL: http://www.tibotec.com/content/backgrounders/www.tibotec.com/hiv_lifecycle.html [Cited August 26, 2011].
12. Briggs, J.A.G., Riches, J.D., Glass, B., Bartonova, V., Zanetti, G., Kräusslich, H.-G. (2009) Structure and assembly of immature HIV. *Proc. Natl. Acad. Sci. U.S.A.* **106**, 11090-11095.
13. Saad, J.S., Miller, J., Tai, J., Kim, A., Ghanam, R.H., Summers, M.F. (2006) Structural basis for targeting HIV-1 Gag proteins to the plasma membrane for virus assembly. *Proc. Natl. Acad. Sci. U.S.A.* **103**, 11364-11369.
14. Hill, M., Tachedjian, G., Mak, J. (2005) The packaging and maturation of the HIV-1 Pol proteins. *Curr. HIV Res*. **3**, 73-85.
15. Sierra, S., Kupfer, B., Kaiser, R. (2005) Basics of the virology of HIV-1 and its replication. *J. Clin. Virol*. **34**, 233-244.
16. De Clercq, E. (2009) Anti-HIV drugs: 25 compounds approved within 25 years after the discovery of HIV. *Int. J. Antimicrob. Agents*. **33**, 307-320.

17. U.S. Food and Drug Administration: Antiretroviral drugs used in the treatment of HIV infection URL: http://www.fda.gov/ForConsumers/ByAudience/ForPatientAdvocates/HIVandAIDSActivities/ucm118915.htm [Cited August 26, 2011].
18. Cihlar, T., Ray, A.S. (2010) Nucleoside and nucleotide HIV reverse transcriptase inhibitors: 25 years after zidovudine. *Antiviral Res*. **85**, 39-58.
19. Wensing, A.M.J., van Maarseveen, N.M., Nijhuis, M. (2010) Fifteen years of HIV Protease Inhibitors: raising the barrier to resistance. *Antiviral Res*. **85**, 59-74.
20. Cervia, J.S., Smith, M.A. (2003) Enfuvirtide (T-20): a novel human immunodeficiency virus type 1 fusion inhibitor. *Clin. Infect. Dis*. **37**, 1102-1106.
21. Cocohoba, J., Dong, B.J. (2008) Raltegravir: the first HIV integrase inhibitor. *Clin Ther*. **30**, 1747-1765.
22. Tilton, J.C., Doms, R.W. (2010) Entry inhibitors in the treatment of HIV-1 infection. *Antiviral Res*. **85**, 91-100.
23. Adamson, C.S., Salzwedel, K., Freed, E.O. (2009) Virus maturation as a new HIV-1 therapeutic target. *Expert Opin. Ther. Targets*. **13**, 895-908.
24. Adamson, C.S., Freed, E.O. (2010) Novel approaches to inhibiting HIV-1 replication. *Antiviral Res*. **85**, 119-141.
25. Greene, W.C., Debyser, Z., Ikeda, Y., Freed, E.O., Stephens, E., Yonemoto, W., Buckheit, R.W., Esté, J.A., Cihlar, T. (2008) Novel targets for HIV therapy. *Antiviral Res*. **80**, 251-265.
26. Pettit, S.C., Lindquist, J.N., Kaplan, A.H., Swanstrom, R. (2005) Processing sites in the human immunodeficiency virus type 1 (HIV-1) Gag-Pro-Pol precursor are cleaved by the viral protease at different rates. *Retrovirology*. **2**, 66.
27. Szeltner, Z., Polgár, L. (1996) Rate-determining steps in HIV-1 protease catalysis. The hydrolysis of the most specific substrate. *J. Biol. Chem*. **271**, 32180-32184.
28. Huff, J.R. (1991) HIV protease: a novel chemotherapeutic target for AIDS. *J. Med. Chem*. **34**, 2305-2314.
29. Dunn, B.M., Goodenow, M.M., Gustchina, A., Wlodawer, A. (2002) Retroviral proteases. *Genome Biol*. **3**.
30. Wlodawer, A., Gustchina, A. (2000) Structural and biochemical studies of retroviral proteases. *Biochim. Biophys. Acta*. **1477**, 16-34.
31. Navia, M.A., Fitzgerald, P.M., McKeever, B.M., Leu, C.T., Heimbach, J.C., Herber, W.K., Sigal, I.S., Darke, P.L., Springer, J.P. (1989) Three-dimensional structure of aspartyl protease from human immunodeficiency virus HIV-1. *Nature*. **337**, 615-620.
32. Wlodawer, A., Miller, M., Jaskólski, M., Sathyanarayana, B.K., Baldwin, E., Weber, I.T., Selk, L.M., Clawson, L., Schneider, J., Kent, S.B. (1989) Conserved folding in retroviral proteases: crystal structure of a synthetic HIV-1 protease. *Science*. **245**, 616-621.

33. Strisovsky, K., Tessmer, U., Langner, J., Konvalinka, J., Kräusslich, H.G. (2000) Systematic mutational analysis of the active-site threonine of HIV-1 proteinase: rethinking the „fireman's grip" hypothesis. *Protein Sci*. **9**, 1631-1641.

34. Ingr, M., Uhlíková, T., Strísovský, K., Majerová, E., Konvalinka, J. (2003) Kinetics of the dimerization of retroviral proteases: the „fireman's grip" and dimerization. *Protein Sci*. **12**, 2173-2182.

35. Tie, Y., Boross, P.I., Wang, Y.-F., Gaddis, L., Liu, F., Chen, X., Tozser, J., Harrison, R.W., Weber, I.T. (2005) Molecular basis for substrate recognition and drug resistance from 1.1 to 1.6 angstroms resolution crystal structures of HIV-1 protease mutants with substrate analogs. *FEBS J*. **272**, 5265-5277.

36. Louis, J.M., Ishima, R., Torchia, D.A., Weber, I.T. (2007) HIV-1 protease: structure, dynamics, and inhibition. *Adv. Pharmacol*. **55**, 261-298.

37. Wlodawer, A., Vondrasek, J. (1998) Inhibitors of HIV-1 protease: a major success of structure-assisted drug design. *Annu Rev Biophys Biomol Struct*. **27**, 249-284.

38. Spinelli, S., Liu, Q.Z., Alzari, P.M., Hirel, P.H., Poljak, R.J. (1991) The three-dimensional structure of the aspartyl protease from the HIV-1 isolate BRU. *Biochimie*. **73**, 1391-1396.

39. Hornak, V., Simmerling, C. (2007) Targeting structural flexibility in HIV-1 protease inhibitor binding. *Drug Discov. Today*. **12**, 132-138.

40. Hornak, V., Okur, A., Rizzo, R.C., Simmerling, C. (2006) HIV-1 protease flaps spontaneously close to the correct structure in simulations following manual placement of an inhibitor into the open state. *J. Am. Chem. Soc*. **128**, 2812-2813.

41. Wondrak, E.M., Louis, J.M. (1996) Influence of flanking sequences on the dimer stability of human immunodeficiency virus type 1 protease. *Biochemistry*. **35**, 12957-12962.

42. Louis, J.M., Wondrak, E.M., Kimmel, A.R., Wingfield, P.T., Nashed, N.T. (1999) Proteolytic processing of HIV-1 protease precursor, kinetics and mechanism. *J. Biol. Chem*. **274**, 23437-23442.

43. Zybarth, G., Carter, C. (1995) Domains upstream of the protease (PR) in human immunodeficiency virus type 1 Gag-Pol influence PR autoprocessing. *J. Virol*. **69**, 3878-3884.

44. Zybarth, G., Kräusslich, H.G., Partin, K., Carter, C. (1994) Proteolytic activity of novel human immunodeficiency virus type 1 proteinase proteins from a precursor with a blocking mutation at the N terminus of the PR domain. *J. Virol*. **68**, 240-250.

45. Tessmer, U., Kräusslich, H.G. (1998) Cleavage of human immunodeficiency virus type 1 proteinase from the N-terminally adjacent p6* protein is essential for efficient Gag polyprotein processing and viral infectivity. *J. Virol*. **72**, 3459-3463.

46. Beck, Z.Q., Morris, G.M., Elder, J.H. (2002) Defining HIV-1 protease substrate selectivity. *Curr Drug Targets Infect Disord*. **2**, 37-50.

47. Prabu-Jeyabalan, M., Nalivaika, E., Schiffer, C.A. (2002) Substrate shape determines specificity of recognition for HIV-1 protease: analysis of crystal structures of six substrate complexes. *Structure*. **10**, 369-381.

48. Prabu-Jeyabalan, M., Nalivaika, E.A., Romano, K., Schiffer, C.A. (2006) Mechanism of substrate recognition by drug-resistant human immunodeficiency virus type 1 protease variants revealed by a novel structural intermediate. *J. Virol*. **80**, 3607-3616.

49. Henderson, L.E., Benveniste, R.E., Sowder, R., Copeland, T.D., Schultz, A.M., Oroszlan, S. (1988) Molecular characterization of gag proteins from simian immunodeficiency virus (SIVMne). *J. Virol*. **62**, 2587-2595.

50. Miller, M., Schneider, J., Sathyanarayana, B.K., Toth, M.V., Marshall, G.R., Clawson, L., Selk, L., Kent, S.B., Wlodawer, A. (1989) Structure of complex of synthetic HIV-1 protease with a substrate-based inhibitor at 2.3 A resolution. *Science*. **246**, 1149-1152.

51. Rose, R.B., Craik, C.S., Douglas, N.L., Stroud, R.M. (1996) Three-dimensional structures of HIV-1 and SIV protease product complexes. *Biochemistry*. **35**, 12933-12944.

52. Randolph, J.T., DeGoey, D.A. (2004) Peptidomimetic inhibitors of HIV protease. *Curr Top Med Chem*. **4**, 1079-1095.

53. Wlodawer, A., Erickson, J.W. (1993) Structure-based inhibitors of HIV-1 protease. *Annu. Rev. Biochem*. **62**, 543-585.

54. DeLano, W.L. (2002) *The PyMOL Molecular Graphics System, Delano Scientific, Palo Alto, CA, USA*.

55. Pokorná, J., Machala, L., Řezáčová, P., Konvalinka, J. (2009) Current and Novel Inhibitors of HIV Protease. *Viruses*. **1**, 1209-1239.

56. Jain, R.G., Furfine, E.S., Pedneault, L., White, A.J., Lenhard, J.M. (2001) Metabolic complications associated with antiretroviral therapy. *Antiviral Res*. **51**, 151-177.

57. Grantz-Šašková, K. (2010) *HIV-1 Protease: Insights into Drug Resistance Development* (Dissertation thesis, Charles University in Prague, Faculty of Science, Department of Biochemistry, Prague).

58. Menéndez-Arias, L. (2010) Molecular basis of human immunodeficiency virus drug resistance: an update. *Antiviral Res*. **85**, 210-231.

59. Shafer, R.W., Schapiro, J.M. (2008) HIV-1 drug resistance mutations: an updated framework for the second decade of HAART. *AIDS Rev*. **10**, 67-84.

60. Stanford University HIV Drug Resistance Database URL: http://hivdb.stanford.edu/cgi-bin/PIResiNote.cgi [Cited August 26, 2011].

61. Rhee, S.-Y., Taylor, J., Fessel, W.J., Kaufman, D., Towner, W., Troia, P., Ruane, P., Hellinger, J., Shirvani, V., Zolopa, A., Shafer, R.W. (2010) HIV-1 protease mutations and protease inhibitor cross-resistance. *Antimicrob. Agents Chemother*. **54**, 4253-4261.

62. Baldanti, F., Paolucci, S., Dossena, L., Gerna, G. (2004) Assays for determination of HIV resistance to antiviral drugs. *Curr. Drug Metab*. **5**, 317-319.

63. Ohtaka, H., Schön, A., Freire, E. (2003) Multidrug resistance to HIV-1 protease inhibition requires cooperative coupling between distal mutations. *Biochemistry*. **42**, 13659-13666.

64. Muzammil, S., Ross, P., Freire, E. (2003) A major role for a set of non-active site mutations in the development of HIV-1 protease drug resistance. *Biochemistry*. **42**, 631-638.

65. Clemente, J.C., Moose, R.E., Hemrajani, R., Whitford, L.R.S., Govindasamy, L., Reutzel, R., McKenna, R., Agbandje-McKenna, M., Goodenow, M.M., Dunn, B.M. (2004) Comparing the accumulation of active- and nonactive-site mutations in the HIV-1 protease. *Biochemistry*. **43**, 12141-12151.

66. Kozísek, M., Sasková, K.G., Rezácová, P., Brynda, J., van Maarseveen, N.M., De Jong, D., Boucher, C.A., Kagan, R.M., Nijhuis, M., Konvalinka, J. (2008) Ninety-nine is not enough: molecular characterization of inhibitor-resistant human immunodeficiency virus type 1 protease mutants with insertions in the flap region. *J. Virol*. **82**, 5869-5878.

67. Winters, M.A., Merigan, T.C. (2005) Insertions in the human immunodeficiency virus type 1 protease and reverse transcriptase genes: clinical impact and molecular mechanisms. *Antimicrob. Agents Chemother*. **49**, 2575-2582.

68. Kolli, M., Stawiski, E., Chappey, C., Schiffer, C.A. (2009) Human immunodeficiency virus type 1 protease-correlated cleavage site mutations enhance inhibitor resistance. *J. Virol*. **83**, 11027-11042.

69. Nijhuis, M., van Maarseveen, N.M., Lastere, S., Schipper, P., Coakley, E., Glass, B., Rovenska, M., de Jong, D., Chappey, C., Goedegebuure, I.W., Heilek-Snyder, G., Dulude, D., Cammack, N., Brakier-Gingras, L., Konvalinka, J., Parkin, N., Kräusslich, H.-G., Brun-Vezinet, F., Boucher, C.A.B. (2007) A novel substrate-based HIV-1 protease inhibitor drug resistance mechanism. *PLoS Med*. **4**, e36.

70. Dautin, N., Karimova, G., Ladant, D. (2003) Human immunodeficiency virus (HIV) type 1 transframe protein can restore activity to a dimerization-deficient HIV protease variant. *J. Virol*. **77**, 8216-8226.

71. Yin, P.D., Das, D., Mitsuya, H. (2006) Overcoming HIV drug resistance through rational drug design based on molecular, biochemical, and structural profiles of HIV resistance. *Cell. Mol. Life Sci*. **63**, 1706-1724.

72. Ghosh, A.K., Chapsal, B.D., Weber, I.T., Mitsuya, H. (2008) Design of HIV protease inhibitors targeting protein backbone: an effective strategy for combating drug resistance. *Acc. Chem. Res*. **41**, 78-86.

73. Velazquez-Campoy, A., Kiso, Y., Freire, E. (2001) The binding energetics of first- and second-generation HIV-1 protease inhibitors: implications for drug design. *Arch. Biochem. Biophys*. **390**, 169-175.

74. Velazquez-Campoy, A., Muzammil, S., Ohtaka, H., Schön, A., Vega, S., Freire, E. (2003) Structural and thermodynamic basis of resistance to HIV-1 protease inhibition: implications for inhibitor design. *Curr Drug Targets Infect Disord*. **3**, 311-328.

75. Markgren, P.-O., Schaal, W., Hämäläinen, M., Karlén, A., Hallberg, A., Samuelsson, B., Danielson, U.H. (2002) Relationships between structure and interaction kinetics for HIV-1 protease inhibitors. *J. Med. Chem*. **45**, 5430-5439.

76. Shuman, C.F., Hämäläinen, M.D., Danielson, U.H. (2004) Kinetic and thermodynamic characterization of HIV-1 protease inhibitors. *J. Mol. Recognit*. **17**, 106-119.

77. Markgren, P.O., Hämäläinen, M., Danielson, U.H. (1998) Screening of compounds interacting with HIV-1 proteinase using optical biosensor technology. *Anal. Biochem*. **265**, 340-350.

78. Shuman, C.F., Markgren, P.O., Hämäläinen, M., Danielson, U.H. (2003) Elucidation of HIV-1 protease resistance by characterization of interaction kinetics between inhibitors and enzyme variants. *Antiviral Res*. **58**, 235-242.

79. Molina, J.-M., Hill, A. (2007) Darunavir (TMC114): a new HIV-1 protease inhibitor. *Expert Opin Pharmacother*. **8**, 1951-1964.

80. McKeage, K., Perry, C.M., Keam, S.J. (2009) Darunavir: a review of its use in the management of HIV infection in adults. *Drugs*. **69**, 477-503.

81. Ghosh, A.K., Leshchenko, S., Noetzel, M. (2004) Stereoselective photochemical 1,3-dioxolane addition to 5-alkoxymethyl-2(5H)-furanone: synthesis of bis-tetrahydrofuranyl ligand for HIV protease inhibitor UIC-94017 (TMC-114). *J. Org. Chem*. **69**, 7822-7829.

82. Ghosh, A.K., Dawson, Z.L., Mitsuya, H. (2007) Darunavir, a conceptually new HIV-1 protease inhibitor for the treatment of drug-resistant HIV. *Bioorg. Med. Chem*. **15**, 7576-7580.

83. Ghosh, A.K., Ramu Sridhar, P., Kumaragurubaran, N., Koh, Y., Weber, I.T., Mitsuya, H. (2006) Bis-tetrahydrofuran: a privileged ligand for darunavir and a new generation of hiv protease inhibitors that combat drug resistance. *ChemMedChem*. **1**, 939-950.

84. Koh, Y., Nakata, H., Maeda, K., Ogata, H., Bilcer, G., Devasamudram, T., Kincaid, J.F., Boross, P., Wang, Y.-F., Tie, Y., Volarath, P., Gaddis, L., Harrison, R.W., Weber, I.T., Ghosh, A.K., Mitsuya, H. (2003) Novel bis-tetrahydrofuranylurethane-containing nonpeptidic protease inhibitor (PI) UIC-94017 (TMC114) with potent activity against multi-PI-resistant human immunodeficiency virus in vitro. *Antimicrob. Agents Chemother*. **47**, 3123-3129.

85. Surleraux, D.L.N.G., Tahri, A., Verschueren, W.G., Pille, G.M.E., de Kock, H.A., Jonckers, T.H.M., Peeters, A., De Meyer, S., Azijn, H., Pauwels, R., de Bethune, M.-P., King, N.M., Prabu-Jeyabalan, M., Schiffer, C.A., Wigerinck, P.B.T.P. (2005) Discovery and selection of TMC114, a next generation HIV-1 protease inhibitor. *J. Med. Chem*. **48**, 1813-1822.

86. De Meyer, S., Azijn, H., Surleraux, D., Jochmans, D., Tahri, A., Pauwels, R., Wigerinck, P., de Béthune, M.-P. (2005) TMC114, a novel human immunodeficiency virus type 1 protease inhibitor active against protease inhibitor-resistant viruses, including a broad range of clinical isolates. *Antimicrob. Agents Chemother*. **49**, 2314-2321.

87. King, N.M., Prabu-Jeyabalan, M., Nalivaika, E.A., Wigerinck, P., de Béthune, M.-P., Schiffer, C.A. (2004) Structural and thermodynamic basis for the binding of TMC114, a next-generation human immunodeficiency virus type 1 protease inhibitor. *J. Virol*. **78**, 12012-12021.

88. Chellappan, S., Kairys, V., Fernandes, M.X., Schiffer, C., Gilson, M.K. (2007) Evaluation of the substrate envelope hypothesis for inhibitors of HIV-1 protease. *Proteins*. **68**, 561-567.

89. Lefebvre, E., Schiffer, C.A. (2008) Resilience to resistance of HIV-1 protease inhibitors: profile of darunavir. *AIDS Rev*. **10**, 131-142.

90. Tie, Y., Boross, P.I., Wang, Y.-F., Gaddis, L., Hussain, A.K., Leshchenko, S., Ghosh, A.K., Louis, J.M., Harrison, R.W., Weber, I.T. (2004) High resolution crystal structures of HIV-1 protease with a potent non-peptide inhibitor (UIC-94017) active against multi-drug-resistant clinical strains. *J. Mol. Biol*. **338**, 341-352.

91. Dierynck, I., De Wit, M., Gustin, E., Keuleers, I., Vandersmissen, J., Hallenberger, S., Hertogs, K. (2007) Binding kinetics of darunavir to human immunodeficiency virus type 1 protease explain the potent antiviral activity and high genetic barrier. *J. Virol*. **81**, 13845-13851.

92. Kozísek, M., Bray, J., Rezácová, P., Sasková, K., Brynda, J., Pokorná, J., Mammano, F., Rulísek, L., Konvalinka, J. (2007) Molecular analysis of the HIV-1 resistance development: enzymatic activities, crystal structures, and thermodynamics of nelfinavir-resistant HIV protease mutants. *J. Mol. Biol*. **374**, 1005-1016.

93. Sasková, K.G., Kozísek, M., Lepsík, M., Brynda, J., Rezácová, P., Václavíková, J., Kagan, R.M., Machala, L., Konvalinka, J. (2008) Enzymatic and structural analysis of the I47A mutation contributing to the reduced susceptibility to HIV protease inhibitor lopinavir. *Protein Sci*. **17**, 1555-1564.

94. Kovalevsky, A.Y., Liu, F., Leshchenko, S., Ghosh, A.K., Louis, J.M., Harrison, R.W., Weber, I.T. (2006) Ultra-high resolution crystal structure of HIV-1 protease mutant reveals two binding sites for clinical inhibitor TMC114. *J. Mol. Biol*. **363**, 161-173.

95. Kovalevsky, A.Y., Tie, Y., Liu, F., Boross, P.I., Wang, Y.-F., Leshchenko, S., Ghosh, A.K., Harrison, R.W., Weber, I.T. (2006) Effectiveness of nonpeptide clinical inhibitor TMC-114 on HIV-1 protease with highly drug resistant mutations D30N, I50V, and L90M. *J. Med. Chem*. **49**, 1379-1387.

96. Liu, F., Kovalevsky, A.Y., Tie, Y., Ghosh, A.K., Harrison, R.W., Weber, I.T. (2008) Effect of flap mutations on structure of HIV-1 protease and inhibition by saquinavir and darunavir. *J. Mol. Biol*. **381**, 102-115.

97. Talbot, A., Grant, P., Taylor, J., Baril, J.-G., Liu, T.F., Charest, H., Brenner, B., Roger, M., Shafer, R., Cantin, R., Zolopa, A. (2010) Predicting tipranavir and darunavir resistance using genotypic, phenotypic, and virtual phenotypic resistance patterns: an independent cohort analysis of clinical isolates highly resistant to all other protease inhibitors. *Antimicrob. Agents Chemother*. **54**, 2473-2479.

98. De Meyer, S., Azijn, H., Fransen, E., De Baere, I., Van Ginderen, M., Maes, B., de Béthune, M-P. (2007) The pathway leading to TMC114 resistance is different for TMC114 compared with other protease inhibitors URL: http://www.tibotec.com/content/congresses/www.tibotec.com/DeMeyer_TMC114_Resistance.pdf [Cited August 26, 2011].

99. Koh, Y., Amano, M., Towata, T., Danish, M., Leshchenko-Yashchuk, S., Das, D., Nakayama, M., Tojo, Y., Ghosh, A.K., Mitsuya, H. (2010) In vitro selection of highly darunavir-resistant and replication-competent HIV-1 variants by using a mixture of clinical HIV-1 isolates resistant to multiple conventional protease inhibitors. *J. Virol*. **84**, 11961-11969.

100. Lambert-Niclot, S., Flandre, P., Canestri, A., Peytavin, G., Blanc, C., Agher, R., Soulié, C., Wirden, M., Katlama, C., Calvez, V., Marcelin, A.-G. (2008) Factors associated with the selection of mutations conferring resistance to protease inhibitors (PIs) in PI-experienced patients displaying treatment failure on darunavir. *Antimicrob. Agents Chemother*. **52**, 491-496.

101. Sasková, K.G., Kozísek, M., Rezácová, P., Brynda, J., Yashina, T., Kagan, R.M., Konvalinka, J. (2009) Molecular characterization of clinical isolates of human immunodeficiency virus resistant to the protease inhibitor darunavir. *J. Virol*. **83**, 8810-8818.

102. Lambert-Niclot, S., Flandre, P., Malet, I., Canestri, A., Soulié, C., Tubiana, R., Brunet, C., Wirden, M., Katlama, C., Calvez, V., Marcelin, A.-G. (2008) Impact of gag mutations on selection of darunavir resistance mutations in HIV-1 protease. *J. Antimicrob. Chemother*. **62**, 905-908.

103. Kovalevsky, A.Y., Ghosh, A.K., Weber, I.T. (2008) Solution kinetics measurements suggest HIV-1 protease has two binding sites for darunavir and amprenavir. *J. Med. Chem*. **51**, 6599-6603.

104. Copeland, R.A. (2000) *Enzymes: A Practical introduction to Structure, Mechanism and Data Analysis* (Wiley-VCH, Inc., New York). 2nd Ed.

105. Jackson, M.B., Allosteric Mechanisms in the Activation of Ligand-Gated Channels.URL:http://www.biophysics.org/Portals/1/PDFs/Education/JacksonM.pdf [Cited August 26, 2011].

106. Gunasekaran, K., Ma, B., Nussinov, R. (2004) Is allostery an intrinsic property of all dynamic proteins? *Proteins*. **57**, 433-443.

107. Congreve, M., Murray, C.W., Blundell, T.L. (2005) Structural biology and drug discovery. *Drug Discov. Today*. **10**, 895-907.

108. Perryman, A.L., Zhang, Q., Soutter, H.H., Rosenfeld, R., McRee, D.E., Olson, A.J., Elder, J.E., Stout, C.D. (2010) Fragment-based screen against HIV protease. *Chem Biol Drug Des*. **75**, 257-268.

109. Hubbard, R.E. (2008) Fragment approaches in structure-based drug discovery. *J Synchrotron Radiat*. **15**, 227-230.

110. Bobkova, E.V., Weber, M.J., Xu, Z., Zhang, Y.-L., Jung, J., Blume-Jensen, P., Northrup, A., Kunapuli, P., Andersen, J.N., Kariv, I. (2010) Discovery of PDK1 kinase inhibitors with a novel mechanism of action by ultrahigh throughput screening. *J. Biol. Chem*. **285**, 18838-18846.

111. Xu, Z., Nagashima, K., Sun, D., Rush, T., Northrup, A., Andersen, J.N., Kariv, I., Bobkova, E.V. (2009) Development of high-throughput TR-FRET and AlphaScreen assays for identification of potent inhibitors of PDK1. *J Biomol Screen*. **14**, 1257-1262.

112. Hardy, J.A., Wells, J.A. (2004) Searching for new allosteric sites in enzymes. *Curr. Opin. Struct. Biol*. **14**, 706-715.

113. Harris, T.K. (2003) PDK1 and PKB/Akt: ideal targets for development of new strategies to structure-based drug design. *IUBMB Life*. **55**, 117-126.

114. Klein, J.C., Burr, A.R., Svensson, B., Kennedy, D.J., Allingham, J., Titus, M.A., Rayment, I., Thomas, D.D. (2008) Actin-binding cleft closure in myosin II probed by site-directed spin labeling and pulsed EPR. *Proc. Natl. Acad. Sci. U.S.A.* **105**, 12867-12872.

115. Ganesan, R., Eigenbrot, C., Wu, Y., Liang, W.-C., Shia, S., Lipari, M.T., Kirchhofer, D. (2009) Unraveling the allosteric mechanism of serine protease inhibition by an antibody. *Structure*. **17**, 1614-1624.

116. Hajduk, P.J., Huth, J.R., Tse, C. (2005) Predicting protein druggability. *Drug Discov. Today*. **10**, 1675-1682.

117. Laskowski, R.A., Gerick, F., Thornton, J.M. (2009) The structural basis of allosteric regulation in proteins. *FEBS Lett*. **583**, 1692-1698.

118. Bock, P.E., Panizzi, P., Verhamme, I.M.A. (2007) Exosites in the substrate specificity of blood coagulation reactions. *J. Thromb. Haemost*. **5 Suppl 1**, 81-94.

119. Romney, G., Glick, M. (2009) An updated concept of coagulation with clinical implications. *J Am Dent Assoc*. **140**, 567-574.

120. Lechtenberg, B.C., Johnson, D.J.D., Freund, S.M.V., Huntington, J.A. (2010) NMR resonance assignments of thrombin reveal the conformational and dynamic effects of ligation. *Proc. Natl. Acad. Sci. U.S.A.* **107**, 14087-14092.

121. Li, W., Johnson, D.J.D., Esmon, C.T., Huntington, J.A. (2004) Structure of the antithrombin-thrombin-heparin ternary complex reveals the antithrombotic mechanism of heparin. *Nat. Struct. Mol. Biol*. **11**, 857-862.

122. Olson, S.T., Richard, B., Izaguirre, G., Schedin-Weiss, S., Gettins, P.G.W. (2010) Molecular mechanisms of antithrombin-heparin regulation of blood clotting proteinases. A paradigm for understanding proteinase regulation by serpin family protein proteinase inhibitors. *Biochimie*. **92**, 1587-1596.

123. Banner, D.W., D'Arcy, A., Chène, C., Winkler, F.K., Guha, A., Konigsberg, W.H., Nemerson, Y., Kirchhofer, D. (1996) The crystal structure of the complex of blood coagulation factor VIIa with soluble tissue factor. *Nature*. **380**, 41-46.

124. Dennis, M.S., Eigenbrot, C., Skelton, N.J., Ultsch, M.H., Santell, L., Dwyer, M.A., O'Connell, M.P., Lazarus, R.A. (2000) Peptide exosite inhibitors of factor VIIa as anticoagulants. *Nature*. **404**, 465-470.

125. Roberge, M., Santell, L., Dennis, M.S., Eigenbrot, C., Dwyer, M.A., Lazarus, R.A. (2001) A novel exosite on coagulation factor VIIa and its molecular interactions with a new class of peptide inhibitors. *Biochemistry*. **40**, 9522-9531.

126. Bode, W., Huber, R. (1976) Induction of the bovine trypsinogen-trypsin transition by peptides sequentially similar to the N-terminus of trypsin. *FEBS Lett*. **68**, 231-236.

127. Friedrich, R., Panizzi, P., Fuentes-Prior, P., Richter, K., Verhamme, I., Anderson, P.J., Kawabata, S.-I., Huber, R., Bode, W., Bock, P.E. (2003) Staphylocoagulase is a prototype for the mechanism of cofactor-induced zymogen activation. *Nature*. **425**, 535-539.

128. Shiozaki, E.N., Chai, J., Rigotti, D.J., Riedl, S.J., Li, P., Srinivasula, S.M., Alnemri, E.S., Fairman, R., Shi, Y. (2003) Mechanism of XIAP-mediated inhibition of caspase-9. *Mol. Cell*. **11**, 519-527.

129. Hardy, J.A., Lam, J., Nguyen, J.T., O'Brien, T., Wells, J.A. (2004) Discovery of an allosteric site in the caspases. *Proc. Natl. Acad. Sci. U.S.A.* **101**, 12461-12466.

130. Hadler-Olsen, E., Fadnes, B., Sylte, I., Uhlin-Hansen, L., Winberg, J.-O. (2011) Regulation of matrix metalloproteinase activity in health and disease. *FEBS J*. **278**, 28-45.

131. Engel, C.K., Pirard, B., Schimanski, S., Kirsch, R., Habermann, J., Klingler, O., Schlotte, V., Weithmann, K.U., Wendt, K.U. (2005) Structural basis for the highly selective inhibition of MMP-13. *Chem. Biol*. **12**, 181-189.

132. Gooljarsingh, L.T., Lakdawala, A., Coppo, F., Luo, L., Fields, G.B., Tummino, P.J., Gontarek, R.R. (2008) Characterization of an exosite binding inhibitor of matrix metalloproteinase 13. *Protein Sci*. **17**, 66-71.

133. Tokunaga, E., Oki, E., Egashira, A., Sadanaga, N., Morita, M., Kakeji, Y., Maehara, Y. (2008) Deregulation of the Akt pathway in human cancer. *Curr Cancer Drug Targets*. **8**, 27-36.

134. Chang, F., Lee, J.T., Navolanic, P.M., Steelman, L.S., Shelton, J.G., Blalock, W.L., Franklin, R.A., McCubrey, J.A. (2003) Involvement of PI3K/Akt pathway in cell cycle progression, apoptosis, and neoplastic transformation: a target for cancer chemotherapy. *Leukemia*. **17**, 590-603.

135. Wu, W.-I., Voegtli, W.C., Sturgis, H.L., Dizon, F.P., Vigers, G.P.A., Brandhuber, B.J. (2010) Crystal structure of human AKT1 with an allosteric inhibitor reveals a new mode of kinase inhibition. *PLoS ONE*. **5**, e12913.

136. Doublié, S., Sawaya, M.R., Ellenberger, T. (1999) An open and closed case for all polymerases. *Structure*. **7**, R31-35.

137. Freisz, S., Bec, G., Radi, M., Wolff, P., Crespan, E., Angeli, L., Dumas, P., Maga, G., Botta, M., Ennifar, E. (2010) Crystal structure of HIV-1 reverse transcriptase bound to a non-nucleoside inhibitor with a novel mechanism of action. *Angew. Chem. Int. Ed. Engl*. **49**, 1805-1808.

138. Sluis-Cremer, N., Tachedjian, G. (2008) Mechanisms of inhibition of HIV replication by non-nucleoside reverse transcriptase inhibitors. *Virus Res*. **134**, 147-156.

139. Watkins, W.J., Ray, A.S., Chong, L.S. (2010) HCV NS5B polymerase inhibitors. *Curr Opin Drug Discov Devel*. **13**, 441-465.

140. Broglia, R.A., Provasi, D., Vasile, F., Ottolina, G., Longhi, R., Tiana, G. (2006) A folding inhibitor of the HIV-1 protease. *Proteins*. **62**, 928-933.

141. Broglia, R.A., Tiana, G., Sutto, L., Provasi, D., Simona, F. (2005) Design of HIV-1-PR inhibitors that do not create resistance: blocking the folding of single monomers. *Protein Sci*. **14**, 2668-2681.

142. Brynda, J., Rezácová, P., Fábry, M., Horejsí, M., Stouracová, R., Soucek, M., Hradílek, M., Konvalinka, J., Sedlácek, J. (2004) Inhibitor binding at the protein interface in crystals of a HIV-1 protease complex. *Acta Crystallogr. D Biol. Crystallogr*. **60**, 1943-1948.

143. Zhang, Z.Y., Poorman, R.A., Maggiora, L.L., Heinrikson, R.L., Kézdy, F.J. (1991) Dissociative inhibition of dimeric enzymes. Kinetic characterization of the inhibition of HIV-1 protease by its COOH-terminal tetrapeptide. *J. Biol. Chem*. **266**, 15591-15594.

144. Koh, Y., Matsumi, S., Das, D., Amano, M., Davis, D.A., Li, J., Leschenko, S., Baldridge, A., Shioda, T., Yarchoan, R., Ghosh, A.K., Mitsuya, H. (2007) Potent inhibition of HIV-1 replication by novel non-peptidyl small molecule inhibitors of protease dimerization. *J. Biol. Chem*. **282**, 28709-28720.

145. Bartonová, V., Král, V., Sieglová, I., Brynda, J., Fábry, M., Horejsí, M., Kozísek, M., Sasková, K.G., Konvalinka, J., Sedlácek, J., Rezácová, P. (2008) Potent inhibition of drug-resistant HIV protease variants by monoclonal antibodies. *Antiviral Res*. **78**, 275-277.

146. Rezacova, P., Brynda, J., Fabry, M., Horejsi, M., Stouracova, R., Lescar, J., Chitarra, V., Riottot, M.M., Sedlacek, J., Bentley, G.A. (2002) Inhibition of HIV protease by monoclonal antibodies. *J. Mol. Recognit*. **15**, 272-276.

147. Freedberg, D.I., Ishima, R., Jacob, J., Wang, Y.-X., Kustanovich, I., Louis, J.M., Torchia, D.A. (2002) Rapid structural fluctuations of the free HIV protease flaps in solution: relationship to crystal structures and comparison with predictions of dynamics calculations. *Protein Sci*. **11**, 221-232.

148. Judd, D.A., Nettles, J.H., Nevins, N., Snyder, J.P., Liotta, D.C., Tang, J., Ermolieff, J., Schinazi, R.F., Hill, C.L. (2001) Polyoxometalate HIV-1 protease inhibitors. A new mode of protease inhibition. *J. Am. Chem. Soc*. **123**, 886-897.

149. Bradford, M.M. (1976) A rapid and sensitive method for the quantitation of microgram quantities of protein utilizing the principle of protein-dye binding. *Anal. Biochem*. **72**, 248-254.

150. Leatherbarrow, J. *GraFit 5.0.4, Erithacus Software: London, UK*.

151. Hazen, R., Harvey, R., Ferris, R., Craig, C., Yates, P., Griffin, P., Miller, J., Kaldor, I., Ray, J., Samano, V., Furfine, E., Spaltenstein, A., Hale, M., Tung, R., St Clair, M., Hanlon, M., Boone, L. (2007) In vitro antiviral activity of the novel, tyrosyl-based human immunodeficiency virus (HIV) type 1 protease inhibitor brecanavir (GW640385) in combination with other antiretrovirals and against a panel of protease inhibitor-resistant HIV. *Antimicrob. Agents Chemother*. **51**, 3147-3154.

152. Lineweaver, H., Burk, D. (1934) The Determination of Enzyme Dissociation Constants. *Journal of the American Chemical Society*. **56**, 658-666.

153. Nilsson, J., Ståhl, S., Lundeberg, J., Uhlén, M., Nygren, P.A. (1997) Affinity fusion strategies for detection, purification, and immobilization of recombinant proteins. *Protein Expr. Purif*. **11**, 1-16.

154. Tykvart, J. (2009) *One-step purification of recombinant glutamate carboxypeptidase II and its homolog* (Diploma thesis, Charles University in Prague, Faculty of Science, Department of Biochemistry, Prague).